UNIVERSITÀ DEGLI STUDI DI GENOVA

Dottorato in Neuroscienze XXXVI ciclo

EXPLORING THE INTERACTION BETWEEN FOCAL INFLAMMATION AND AXONAL INJURY IN MULTIPLE SCELROSIS: A NEW MECHANISM-DRIVEN FRAMEWORK TO MONITOR DISEASE ACTIVITY AND PROGRESSION

Supervisor: Prof. Matilde Inglese
PhD Candidate: Dr. Maria Cellerino

INDEX

1. INTRODUCTION

1.1. Multiple sclerosis: clinical characteristics and disease management

Multiple sclerosis (MS) is a chronic, inflammatory, demyelinating and neurodegenerative disease of the central nervous system (CNS). MS is heterogeneous, multifactorial, immune-mediated, and caused by complex gene–environment interactions. The distinctive feature of MS is the accumulation of demyelinating lesions that occur in the white matter and the grey matter of the brain and spinal cord [1,2].

Etiology

MS represents the primary cause of non-traumatic disability among young adults[2]. The typical age of onset is between the ages of 20 and 40, but in up to 10% of cases MS can also initiate during childhood or adolescence[3]. Worldwide, around 2.3 million individuals are affected with MS, contributing significantly to a substantial economic burden on society, a burden that has grown over time[1,4]. The prevalence of MS exhibits notable variations across countries. Prevalence figures range from 2 per 100,000 individuals in Asia to approximately 1 per 1,000 individuals in Western countries, with some nations reporting a prevalence of 1 per 400 individuals[1]. Notably, a higher latitude, particularly in Europe and North America, is often linked to an elevated prevalence and incidence of MS[2]. Genetic factors, especially the distribution of the HLA-DRB1 haplotype, may partially explain this latitudinal gradient[1]. However, while familiarity and regional differences emphasize a potential role of genetic predisposition, this genetic component alone cannot completely explain MS pathogenesis and the rapid increase in incidence rates observed over recent decades[1]. This epidemiological trend has risen questions about the influence of environmental factors in the development and progression of MS, suggesting that these factors might act together with genetic predisposition to trigger the disease. A multitude of environmental factors have been proposed as potential contributors to the development of MS. Among these, vitamin D levels, body mass index (BMI),

infections including Epstein-Barr virus (EBV), and smoking have emerged as prominent candidates[1]. These factors, diverse in their nature and mechanism, collectively emphasize the need for a holistic approach when investigating MS etiology. The investigation of environmental factors in MS is of paramount importance for several compelling reasons. First, it offers the opportunity to uncover key insights into the interplay between genes and the environment, shedding light on the mechanisms that underlie MS development. As genetic factors alone cannot account for the increasing prevalence of MS, understanding how environmental factors interact with genetic predisposition is crucial. This knowledge can facilitate the identification of at-risk populations and inform targeted preventive strategies. Secondly, some of these environmental factors are modifiable. For instance, lifestyle interventions that address factors like BMI and smoking habits hold the potential to mitigate MS risk. By identifying and understanding these modifiable risk factors, actionable strategies to reduce the incidence and burden of MS can be developed. Furthermore, an exploration of environmental factors may provide valuable insight into the mechanism underpinning MS pathogenesis. Each factors offers a unique window into the complex interplay between the immune system, the nervous system and the environment. As we delve deeper into the effects of these factors on MS susceptibility and progression, we may uncover new pathways and targets for therapeutic intervention.

Disease course and diagnosis

The clinical presentations and course of MS are heterogeneous. In the early stages of the disease, most patients experience temporary episodes of neurological deficits, referred to as relapses, which typically endure for days or weeks. This phase includes clinically isolated syndrome (CIS) and relapsing–remitting MS (RRMS). Over time, the development of lasting neurological deficits and the progression of clinical disability become prominent a stage referred to as secondary progressive MS (SPMS) [1,5] A small proportion of individuals experience a progressive disease trajectory from onset, which is referred to as primary progressive MS (PPMS)[1,5]; (Fig 1). Progressive patients can be categorized as active or inactive based on clinical assessments of relapse occurrence or the detection of lesion activity through MRI[5]. Furthermore,

individuals with PPMS or SPMS can be classified depending on whether disability has progressed over a specified period[5].

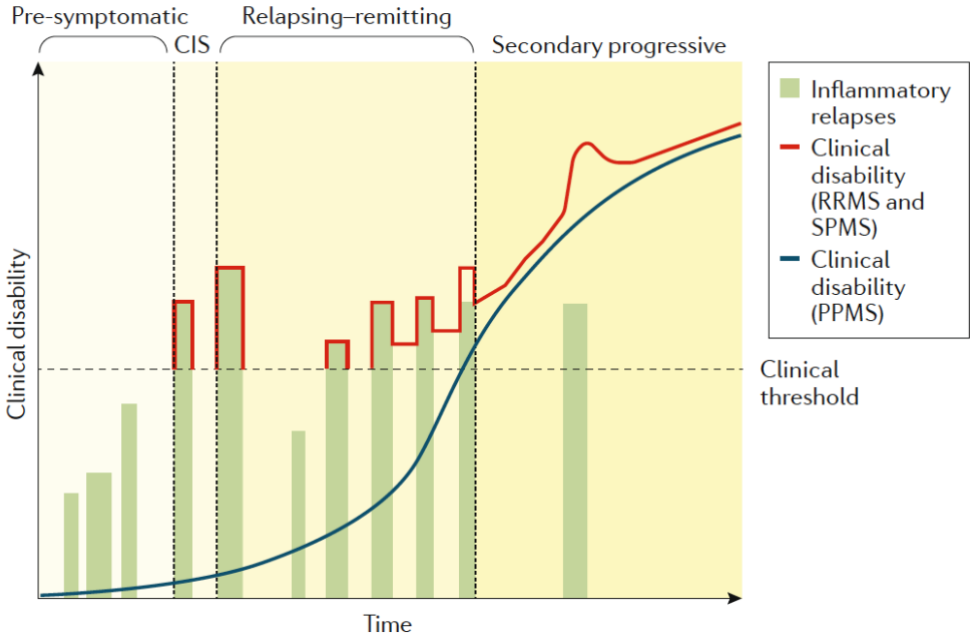

Fig 1: Clinical course of MS[1]

MS diagnosis is based on the demonstration of the dissemination of demyelinating lesions across different regions of the CNS (dissemination in space or DIS) and over time (dissemination in time or DIT). Clinical evaluation or paraclinical tools are utilized for this purpose once disorders mimicking MS have been ruled out. MRI, with its high sensitivity for detecting disease-related abnormalities, such as demyelinating lesions, has significantly transformed the diagnosis of MS. Additionally, MRI proves valuable for monitoring disease activity and the response to disease-modifying treatments (DMTs)(Thompson et al. 2018; Jakimovski et al. 2023).

Clinical presentation

The clinical presentation of MS is heterogeneous and is influenced by the location of demyelinating lesions within the central nervous system (CNS)[2]. While no clinical findings are exclusive to MS, some are highly indicative of the disease. Typically, MS onset involves an initial clinical attack (referred to as CIS) in approximately 85% of patients[6]. This attack manifests as an unpredictable episode of neurological dysfunction caused by demyelinating lesions in various CNS regions, including the optic nerve (resulting in optic neuritis), spinal cord (leading to myelitis), brainstem or cerebellum (resulting in brainstem and/or cerebellar

syndromes), or the cerebral hemispheres (causing cerebral hemispheric syndrome). Throughout the course of RRMS, additional clinical episodes, known as relapses, may occur. These episodes last for a minimum of 24 hours and occur in the absence of fever, infection, or clinical signs of encephalopathy (such as altered consciousness or epileptic seizures). Symptoms of a clinical attack typically exhibit an acute or sub-acute onset, worsen over days or weeks, peak in severity within 2–3 weeks, and then remit to varying degrees. Generally, resolution ranges from minimal improvement to complete recovery, typically occurring 2–4 weeks after reaching the maximum deficit[1].

Optic neuritis (ON) is the first neurological episode in ~20-25% of patients is associated with a transition to clinically definite MS in 34–75% of patients within 10 to 15 years after the clinical onset[7]. Approximately 70% of individuals with MS experience ON at some point during the course of the disease. ON is characterized by partial or total visual loss in one eye, along with a central scotoma (a blind spot in the visual field), dyschromatopsia (color vision deficiency), and orbit pain exacerbated by eye movement. During a fundus oculi examination using ophthalmoscopy, the optic nerve head appears normal if inflammation is confined to the retrobulbar portion of the nerve. However, around one-third of patients may exhibit inflammation of the optic disc (papillitis) and disc edema due to anterior ON[7].

In up to 43% of patients, sensory symptoms serve as the initial clinical manifestation, primarily attributed to myelitis or brainstem syndromes[1]. These sensory symptoms encompass paresthesia, often described as numbness, tingling, a pins-and-needles sensation, tightness, coldness, and/or swelling of the limbs or trunk. Additionally, patients may experience Lhermitte's sign, a transient symptom characterized by an electric shock sensation radiating down the spine or into the limbs during flexion of the neck. Other sensory impairments include disruptions in vibration and joint position sensation, as well as reduced perception of pain and light touch. These symptoms may exhibit temporary exacerbation with an increase in body temperature, a phenomenon known as the Uhthoff phenomenon[1].

Motor manifestations serve as the initial symptoms in 30–40% of patients, impacting nearly all individuals over the course of the disease. These motor symptoms are characterized by pyramidal signs, such as the Babinski sign,

heightened reflexes, and clonus, along with manifestations of paresis and spasticity. Brainstem and cerebellar symptoms are evident in up to 70% of MS patients[1]. These include impairments in ocular movements, such as nystagmus, oscillopsia, and diplopia. Other symptoms encompass ataxia and gait imbalance, dysmetria and decomposition of complex movements, slurred speech, and dysphagia. Sphincter and sexual dysfunction often parallel the degree of motor impairment in the lower extremities, becoming permanent late in the disease course and affecting 34–99% of patients. Urinary urgency is the most common symptom of bladder dysfunction, although hesitancy, frequency, and urge incontinence can also occur. Constipation is more prevalent than fecal incontinence, and men with MS frequently experience erectile dysfunction and impotence[1].

Other symptoms include cognitive impairment, fatigue and affective disturbance[1]. Cognitive impairment is present in 40–70% of patients, and can start since the early phases of the disease. These deficits can predict the conversion to clinically definite MS in patients with CIS, are more frequent in chronic progressive MS, worsen over time, and impact daily life activities[1,2]. Common cognitive symptoms involve difficulties in information processing speed, episodic memory, attention, efficiency of information processing, and executive function. Fatigue affects up to 95% of patients with MS and can have various causes. It may be associated with relapses, persist after the attack has subsided, or be a chronic feature lasting for years. Evidence suggests a central origin of MS-related fatigue due to dysfunction in cortico-subcortical circuits, particularly involving structural damage in fronto-parietal regions and the basal ganglia. Sleep disorders, such as insomnia, obstructive sleep apnea, and restless legs syndrome, are found in up to 54% of patients and may contribute to fatigue[8–10]. Affective disturbances occur in up to two-thirds of patients, with depression being the most common manifestation. Pain is reported in up to 43% of patients and can include trigeminal neuralgia, dysesthetic pain, back pain, visceral pain, and painful tonic spasms. Generally, the prevalence and severity of these clinical manifestations are higher in patients with PPMS and SPMS compared to those with RRMS[1,11].

Disability assessment

Several qualitative and semi-quantitative scales have been proposed to grade the clinical manifestations of MS[1]. Of these, the Expanded Disability Status Scale (EDSS)[12] is the most widely accepted measure of clinical disability. The EDSS is a scale that ranges from 0 (a completely normal neurological examination) to 10 (death owing to MS) and provides 8 subscale measurements (functional system scores) that include the main functional domains affected by MS, including pyramidal, cerebellar, brainstem, sensory, bowel and bladder, visual, mental and other domains (see Fig 2)[12].

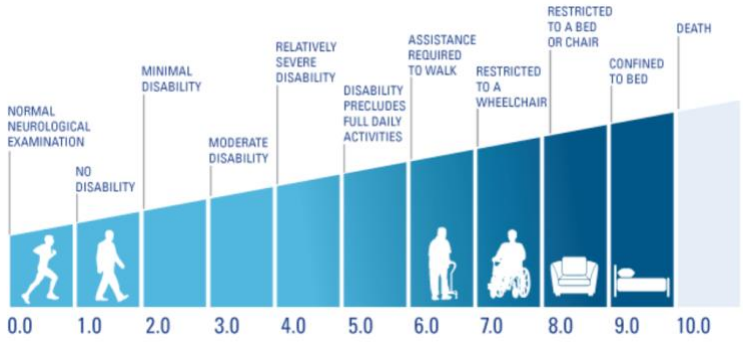

Fig 2 Expaneded Disability Status Scale[12]

https://www.researchgate.net/figure/The-Extended-Disability-Status-Scale-EDSS-Kurtzke-1983-Image-source

Biomarkers and prognostic factors

Several biomarkers and prognostic factors associated with transition from CIS to MS and disability progression in individuals with CIS and early RRMS have been recognized. These factors span environmental, genetic, clinical, laboratory, and MRI features (see BOX 2)[1]. In patients with CIS displaying brain lesions on MRI, even those with just one lesion, there is a greater than 80% likelihood of developing MS within 20 years. Predicting the long-term clinical outcomes in patients with MS, including the severity of disability, is more challenging than forecasting the conversion to MS in those with CIS. Nonetheless, several risk factors have been identified (see BOX 2). Predictors of unfavorable outcomes in PPMS include a progressive disease from the onset and a faster rate of disability accumulation in the initial 2–5 years.[1,13]

Factor	Association with conversion to MS	Association with disability progression
Environmental and lifestyle factors		
Smoking	Higher risk	Poor prognosis
Low vitamin D levels	Higher risk	Unknown
EBV infection	Higher risk	Unknown
Obesity (particularly in childhood and adolescence)	Higher risk	Poor prognosis
Genetic factors		
*HLA-DRB1*1501*	Higher risk	Unknown
Clinical factors		
Non-white ethnicity	Higher risk	Poor prognosis
Female sex	Higher risk	Good prognosis
Male sex	Lower risk	Poor prognosis
Older age	Lower risk	Poor prognosis
Younger age	Higher risk	Good prognosis
Onset with optic neuritis or somatosensory disturbances	Lower risk	Good prognosis
Onset affecting efferent pathways (for example, motor)	Higher risk	Poor prognosis
Monofocal onset[a]	Lower risk	Good prognosis
Multifocal onset[b]	Higher risk	Poor prognosis
Cognitive impairment	Higher risk	Poor prognosis
Higher relapse rate in the first 2–5 years from disease onset	NA	Poor prognosis
Incomplete recovery after a relapse		
Higher disability accumulation in the first 2–5 years from disease onset		
Shorter time to conversion to SPMS		
Laboratoristic factors		
Presence of cerebrospinal OCBs	Higher risk	Poor prognosis
High level of neurofilament light subunit	Higher risk	Poor prognosis
Neuroradiological factors		
Higher number and volume of T2-hyperintense lesions	Higher risk	Poor prognosis
Lesions in infratentorial regions	Higher risk	Poor prognosis
Spinal cord lesions	Higher risk	Poor prognosis
Presence of gadolinium-enhancing lesions	Higher risk	No data
New T2 lesions formation in the first 5 years	Higher risk	Poor prognosis
Optical coherence tomography factors		
Lower ganglion cell and inner plexiform layer thickness	Higher risk	No data

BOX 2: Features of CIS and early MS predicting conversion to definite MS and disability progression[1]

Disease management

The treatment of MS includes (i) DMTs that are used to reduce inflammatory disease activity and its long-term clinical consequences, (ii) the management of MS relapses, and (iii) symptomatic treatments used for short term amelioration of MS symptoms such as fatigue, pain and spasticity. Several DMTs are available for the treatment of RRMS, whereas only one DMT is approved for SPMS and

one for PPMS. Additional DMTs are now in clinical trials for RRMS, PPMS and SPMS, and intense efforts are being made to identify novel therapeutic targets.

Disease-modifying treatments for RRMS

A DMT should be prescribed as soon as a patient has been diagnosed with RRMS or CIS to reduce the risk of disease progression. Injectable DMTs, such as IFNβ or glatiramer acetate, have been the main first-line treatment options for two decades mainly because of their excellent safety profiles but also owing to their lower cost than newer drugs. However, although these therapies have very low risk of severe adverse drug reactions, they have only moderate clinical effectiveness and often poor tolerability owing to injection-related adverse effects, such as flu-like symptoms with IFNβ and injection site inflammation with both IFNβ and glatiramer acetate, which frequently prompt treatment switches[1]. The increasing number of approved DMTs improves the possibility of tailoring therapy to individual patient needs with regard to efficacy, safety aspects and patients' preferences. Although caution should be applied when comparing across studies owing to the heterogeneity of patient cohorts and the lack of reliable comparative studies among treatments, approximate measures of clinical efficacy can be deduced from some parameters typically evaluated in randomized clinical trials (RCTs), including the relative reduction in annual relapse frequency and the number of patients needed to treat (the number of patients you need to treat to prevent one additional bad outcome, typically a relapse or disability progression)[14,15].

The dominant current treatment strategy for RRMS, called escalation therapy[1], is endorsed by the European[15] and American[14] guidelines and is, in part, dictated by the label of different DMTs and public or insurance based regulations. The basis of escalation therapy is to start with a safe but moderately effective DMT, typically IFNβ, glatiramer acetate, teriflunomide or dimethyl fumarate, and switch to another first-line DMT in patients with intolerable adverse effects or to a more effective DMT (second-line or third-line therapies) in those with new relapses or MRI lesions. In patients with severe disease who do not respond to traditional DMTs, autologous haematopoietic stem cell transplantation might be effective[16]. However, owing to the availability of more effective DMTs, such treatment failures are increasingly rare, and in general, <1% of patients with RRMS are candidates for transplantation[16,17].

Another treatment strategy, known as induction therapy[1], has been introduced on the basis of the availability of more effective drugs and of the evolving concept of treating patients earlier with more effective drugs (such as alemtuzumab or ocrelizumab) to prevent the accumulation of irreversible CNS damage and clinical disability. Induction therapy refers to a strong immune-intervention that is started soon after a confirmed diagnosis in a patient with negative prognostic factors (that is, a higher disease activity (severe and frequent relapses and a higher number of lesions at MRI) and an accumulation of disability. This approach enables a rapid reduction in disease associated inflammation by removing T cells, B cells and myeloid cells and possibly shifting towards a more tolerogenic condition owing to a reset of the immune system, which can be followed by use of less aggressive therapies as maintenance if needed. One or more cycles of induction therapy can be performed, followed by a possible de-escalation therapy. However, when treatment with a high-efficacy drug is stopped, a careful evaluation of further treatment selection is needed; particularly for therapies that do not exert a substantial immune reset (such as natalizumab or fingolimod), another high-efficacy treatment should be started to prevent potential disease reactivation. However, despite the benefits of induction therapy, an important reason to restrict the use of more effective DMTs, such as second-line or third-line treatments, is their risk profile. Collectively, older injectable DMTs have the lowest risk of more serious adverse effects, although these therapies have more frequent but lessserious adverse effects that affect tolerability. By contrast, more recent DMTs typically have a better tolerability but are associated with increased risks of severe adverse effects, especially infections[1]. These effects include respiratory and urinary tract infections, herpesvirus reactivation and PML. Importantly, newer DMTs have substantial immunosuppressive activity, which has been suggested to increase risk of long-term malignancy, although the precise risk of this is still uncertain[1]. In addition, before starting a DMT, the teratogenic risks associated with the treatment must be considered in women planning pregnancy[15]. One of the limitations of data derived from RCTs is that trials include a selected group of mostly treatment naive patients who do not have substantial comorbidities and relevant DMT comparators, which means that we have an imprecise evidence base for tailoring DMT strategies in these patient groups. Therefore, careful monitoring of patients with MS is constantly needed. Also, carrying out an individualized

risk–benefit assessment for MS therapies is important, as the relative benefit of individual DMTs differs between patients and all DMTs are associated with adverse effects of varying severities. For example, younger age and a more active disease (in terms of relapse frequency and MRI activity) are associated with increased benefit regarding treatment associated long-term protection of neurological functions. As the risk–benefit ratio of therapy can change over time, studies addressing the contexts in which DMTs can safely be discontinued are also needed, even if current guidelines suggest continuing a DMT if a patient is stable and shows no safety or tolerability issues[14,15,18].

Disease-modifying treatments for progressive disease

DMTs that are used for the treatment for RRMS cannot prevent disease worsening in patients with PMS. Mitoxantrone, a cytostatic drug, was approved by the US FDA for SPMS in 2000, but its use is limited by cardiotoxic and mutagenic adverse effects. Fingolimod and natalizumab have been tested in patients with PPMS or SPMS, respectively, but did not demonstrate superiority over placebo[1]. More promising data emerged from a placebo-controlled study with rituximab in PPMS, in which the risk of disability progression was reduced in younger patients with signs of active inflammation on the baseline MRI scan[19]. A beneficial effect of anti-CD20 agents in PPMS was substantiated in a larger study with ocrelizumab, which significantly reduced the risk of disability progression compared with placebo and led to the first approval of a DMT for PPMS[20]. Notably, the patients in this study were young (mean 44.6 years of age), and 27% of patients had signs of active inflammation on baseline MRI, suggesting that earlier phases of the disease might be more responsive to treatment. Collectively, data indicate that DMTs that act mainly on the adaptive immune system have a reduced efficacy in progressive disease compared with in RRMS but that treatment with anti-CD20 DMTs such as ocrelizumab or rituximab should be considered, especially in patients with shorter disease duration and/or signs of active inflammation on MRI[1]. In line with this, siponimod - a sphingosine 1-phosphate receptor modulator – has been recently approved for active SMPM (aSPMS) in most countries[1,21].

Relapses

The most established treatment for the acute management of MS relapses is high-dose corticosteroids. These drugs are associated with a faster functional recovery and protect against the occurrence of more severe deficits in the first weeks after treatment but have unclear long-term benefits. Current protocols typically include 3–5 days of intravenous methylprednisolone with or without oral tapering with prednisone. Relapses that do not respond to corticosteroids can be treated with plasma exchange (3–5 courses) or intravenous immunoglobulin.

Symptomatic treatments

Several different pharmacological agents are used to treat the symptoms of MS, such as impaired walking capability, spasticity, pain, loss of bladder and bowel control and neuropsychiatric symptoms. However, for most therapies, the evidence base for clinical efficacy in patients with MS is weak. Only two symptomatic treatments have undergone more extensive testing in MS: nabiximols for the treatment of spasticity and dalfampridine for walking ability. Nabiximols can ameliorate spasticity in patients with MS, and empirical evidence supports the use of baclofen, dantrolene, tizanidine and botulinum toxin A injections for the treatment of spasticity in restricted muscle groups. Dalfampridine is a voltage-dependent potassium channel blocker that improves the transmission of nerve signals in demyelinated axons and improves the walking ability of people with MS. In addition to medical treatments, walking aids such as orthoses, crutches or walkers are important to improve ambulation capacity. Traditional or electrical wheel-chairs and other mobility devices constitute important means to preserve independence of movement among patients with more advanced disease. Damage to sensory nerve tracts in MS leads to chronic neuropathic pain conditions for which gabapentinoids (such as gabapentin and pregabalin), tricyclic antidepressants and serotonin noradrenaline reuptake inhib itors are first-line treatments. Opioids such as tramadol or codeine are second-line treatments for moderate to severe pain. In some countries, cannabinoids in the form of medical marijuana or synthetic drugs are recommended as a possible third-line option. The management of lower urinary tract symptoms consists of oral antimuscarinic drugs, administered alone or in combination with intermittent self- catheterization, and the use of botulinum toxin A bladder instillations,

neuromodulation, indwelling catheters and surgery in patients with more- severe symptoms.

Despite the high prevalence and clinical relevance of cognitive impairment in patients with MS, effective treatments options are still lacking. The effects of symptomatic therapies such as modafinil and donepezil are inconsistent; however, some DMTs in combination with cognitive rehabilitation might improve or at least stabilize cognitive performances, although data regarding the impact of specific DMTs in term of cognitive functions are still lacking. Fatigue and psychiatric comorbidities are important contributors to loss of working ability and social participation of patients with M. The off- label prescription of alertness improving drugs such as modafinil and amphetamine is common even though evidence supporting the efficacy of these therapies in MS is poor or absent. However, several smaller studies suggest that novel approaches to treat fatigue, including alfacalcidol (a vitamin D analogue), physical exercise, cognitive behavioral therapy, deep transcranial magnetic stimulation and fatigue management courses, give some clinical benefit.

Considering the high prevalence of sleep disorders in patients with MS, the treatment of an underlying sleep disorder (continuous positive airway pressure for obstructive sleep apnoea, drug therapy and cognitive behavioural therapy for insomnia and drug therapy for restless leg syndrome) significantly reduced fatigue and might exert positive effects on the quality of life (QOL) of patients with MS.

Anxiety and depression, as well as suicide, rates are elevated in MS, but studies addressing the efficacy of pharmaceutical and non-pharmaceutical interventions specifically in MS are rare, therefore, treatment guidelines largely rely on data from non-MS populations and include the use of selective serotonin or noradrenergic reuptake inhibitors and/or cognitive behavioural therapy.

As a whole, offering patients with MS comprehensive rehabilitation programs to address the wide range of MS - associated symptoms, with the aim of alleviating burdensome symptoms through increasing the levels of physical activity, is important[1].

1.2. Pathological insights and mechanisms of injury

The pathological hallmark shared by all phenotypes of MS is the presence of focal plaques, also known as lesions. These plaques are areas of demyelination typically situated around postcapillary venules and are characterized by the breakdown of the blood–brain barrier (BBB)[1,2]. The mechanisms leading to BBB breakdown are not fully understood but appear to involve the direct impact of pro-inflammatory cytokines and chemokines (such as TNF, IL-1β, and IL-6) produced by resident cells and endothelial cells[2]. Additionally, indirect cytokine-dependent and chemokine-dependent leukocyte-mediated injury contributes to this process. The dysregulation of the BBB enhances the trans-endothelial migration of activated leukocytes, including macrophages, T cells, and B cells, into the central nervous system (CNS). This migration results in further inflammation and demyelination, followed by oligodendrocyte loss, reactive gliosis, and neuro-axonal degeneration. Plaques are observed in both white matter and grey matter and are distributed throughout the CNS, including the brain, optic nerve, and spinal cord[1,2]. While the anatomical location of white matter lesions is linked to specific clinical manifestations of MS, the total volume of these lesions is only moderately correlated with overall clinical disability and cognitive impairment. This is due to the involvement of other pathophysiological mechanisms, such as the occurrence of grey matter lesions and damage to normal-appearing brain tissue, which affects both grey and white matter[22,23].

Immune-pathophysiology

Our comprehension of the immune-pathophysiology underlying MS has evolved, shifting from the traditional view of T cell-mediated relapses to a more complex understanding involving bidirectional interactions among various immune cell types. These include T cells, B cells, and myeloid cells in the periphery, as well as resident cells of the central nervous system (CNS) like microglia and astrocytes[23–25]. Both peripheral and CNS-resident cells release inflammatory mediators that recruit immune cells into the CNS, leading to neuronal demyelination and inflammation within the CNS parenchyma[24]. Additionally, inflammatory mechanisms are compartmentalized in both the peripheral and CNS regions, with CNS resident cells contributing to neurotoxic inflammatory

mediator production that sustains neuro-axonal damage and neurodegeneration in MS. Both helper (CD4+) and cytotoxic (CD8+) T cells are present in MS lesions, with CD4+ T cells concentrated in perivascular areas and CD8+ T cells widely distributed within the parenchyma[2,24]. Limiting T cell access to the CNS can reduce or eliminate new MS lesions. However, the proportion of T cells reactive to myelin antigens is similar in people with and without MS, suggesting potential dysfunction in MS or the involvement of other immune factors[2]. B cells have gained attention due to the success of B-cell–depleting antibodies in limiting MS lesion formation and clinical disease activity[22,26,27]. Unique antibodies (oligoclonal bands) produced within the CNS are found in the cerebrospinal fluid (CSF) of most MS patients[2]. The rapid clinical response to B-cell depletion suggests that functions other than antibody production, such as antigen presentation and cytokine production, may be more relevant. Innate immune system cells, particularly bloodborne macrophages and microglia, play crucial roles in MS pathogenesis. In active MS lesions, macrophages infiltrate to remove myelin debris and inflammatory by-products. The role of microglia, the primary endogenous phagocytes of the CNS, remains uncertain – whether pathogenic, protective, or both. Disturbances in the blood–brain barrier (BBB) are integral to white matter lesion development, with abnormal vascular permeability preceding inflammatory demyelination[2]. Overall, the intricate interactions among various immune cell types and CNS-resident cells contribute to the complex immune-pathophysiology of MS, providing potential avenues for targeted therapies and further research[24,25,28].

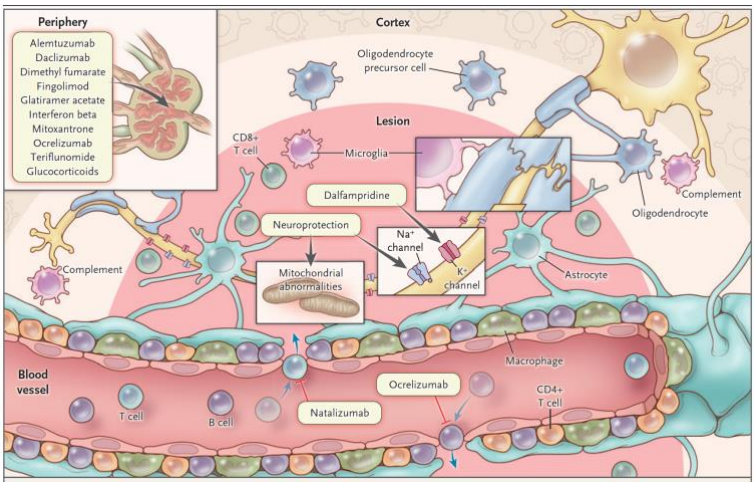

Fig 3: Cells, Molecules, and Therapies. Shown is a simplified schematic depiction of major cell types within white-matter multiple sclerosis lesions, along with several current and promising therapeutic targets in the central nervous system and in the periphery[24].

Active and non-resolving inflammation

As described above, focal inflammatory demyelination in the white matter follows a relatively stereotyped process characterized by perivenular inflammation involving both adaptive and innate immune cells, astrocytic and microglial reactions, and BBB opening[24]. This rapid wave of demyelination generally occurs over days to weeks (sometimes corresponding to clinical relapses) and is followed by a subsequent phase of tissue repair lasting weeks to months. Focal inflammation can be visualized as gadolinium enhancement on MRI, indicating "active" disease. Susceptibility-based MRI allows detection of the perivenular topography of focal inflammatory lesions. Approximately one quarter of lesions may "burn out" without adequate repair, leaving behind an astroglial scar. Residual effects can be observed in vivo through T2-weighted hyperintensity and T1-weighted hypointensity, indicative of neuropil loss ("black holes")[1,24]. The existence of an ongoing intrathecal immune response is demonstrated at the time of diagnosis by CNS-specific oligoclonal bands. In the acute phase, microglia activation, macrophage infiltration, and lymphocytic infiltrates accompany demyelination and plaque formation[24,28,29]. However, around 20% of lesions fail to resolve, leading to chronic tissue remodeling and damage. Mixed “active and inactive lesions" incorporate descriptions like "chronic active," "smouldering," and "slowly expanding" lesions. High-field MRI can identify these lesions due to iron-laden phagocytes at the lesion's white matter-bordering edge, known as the "paramagnetic rim sign." Inflammatory changes within these lesions may slowly enlarge into previously healthy perilesional tissue, contributing to disability accumulation[2,23]. Diffuse microglial activation and multifocal microglial nodules in the extralesional white matter are reported in MS autopsies, especially in progressive MS cases. The causes and consequences of this activation are not fully understood, and whether microglial nodules represent areas of incipient demyelination or reactions to local tissue perturbation remains unclear. Positron emission tomography (PET) studies using radioligands that bind to activated microglia and astrocytes provide in-vivo evidence for widespread microglial involvement, though cellular specificity is imperfect[2,23]. Non-resolving inflammation not only drives injury but may also hinder repair, raising questions about the need for inflammation resolution before tissue repair can commence. Developing noninvasive imaging markers and biomarkers for inflammation and

repair processes could shed light on these questions and evaluate the effects of DMTs on inflammation and progression in MS[23].

Neurodegeneration

Inflammation is closely linked to axonal and neuronal injury in MS[24]. Axonal damage can be evident since the earliest stages of lesions in MS, with neuronal loss becoming more apparent in patients with progressive disease. The release of neurofilament light chain (NfL), a cytoskeletal protein, into the interstitial space, CSF, and peripheral blood is associated with primarily axon damage. NfL concentration is directly linked to relapses and clinical progression, making it a potential prognostic biomarker for monitoring MS patients for progression, disease activity, and treatment efficacy[23]. At the molecular level, demyelination leads to ion channel dysfunction and abnormal distribution along axons. This results in intra-axonal calcium accumulation, potentially stimulating catabolism and triggering intra-axonal proteolytic degradation. Although altered ion channel distribution is challenging to detect clinically, some MRI studies in MS patients have shown elevated tissue sodium concentrations in acute and chronic lesions compared to extralesional white matter areas, indicating widespread or focal ion imbalance. Metabolically, myelin contributes to axon and neuron survival, with astrocytes transferring metabolites to oligodendrocytes to support neuroaxonal metabolism. Studying these metabolic changes involves techniques like MR spectroscopy and PET, but their application is currently limited to small samples in proof-of-concept studies, requiring standardization and improvements in signal-to-noise ratio for broader use. While measuring cellular, molecular, and metabolic mechanisms of neuroaxonal damage remains challenging, global and regional brain atrophy can be detected early in the disease course. This atrophy, associated with a higher risk of progressive disability accumulation, is particularly accelerated in cases of long-term disability progression independent of relapse activity, termed "silent progression." Atrophy indices have been employed as primary outcome measures in phase 2 clinical trials for progressive MS[2,23,24].

Molecular mechanisms of injury

Oxidative stress and mitochondrial dysfunction are proposed as key molecular mechanisms contributing to glial and neuronal injury, axonal energy failure, and

the loss of neuronal network function in MS progression[2,23,24]. Elevated levels of oxidative stress within the CNS, assessed through lipid peroxides, breakdown aldehydes, and oxidized DNA, can induce injury to axons, neurons, dendrites, and oligodendroglia in MS lesions. Excessive iron deposition in the CNS parenchyma is suggested to be a source of oxidative stress, with iron accumulation observed in deep grey matter nuclei through susceptibility-based MRI and in macrophages and microglia in the rim of mixed active and inactive lesions[23]. Mitochondrial dysfunction is evident in MS. Following demyelination, mitochondria migrate from the cell soma to the demyelinated axon. However, the peak of this potentially beneficial mitochondrial response is reached only after axonal degeneration has begun[23]. Chronic demyelination, iron accumulation, and oxidative injury may further lead to dysfunctional mitochondria, accumulating over the course of the disease. Dysfunctional mitochondria may fail to complete oxidative phosphorylation, resulting in energy failure, a state referred to as "virtual hypoxia." This condition amplifies oxidative injury through electron leakage in axons and neurons, potentially contributing to neuronal network failure and disease progression[23,24].

The role of vascular network

In this context, microvascular abnormalities within the CNS have been suggested as contributors to MS pathogenesis and as biomarker of the disease process. Global reductions in cerebral perfusion have been repeatedly illustrated in imaging studies of MS, which could simply be a sequelae of neurodegeneration or could be mediated by concomitant inflammatory vasculopathy[30–34]. Interstingly, findings from epidemiological studies suggest that patients with MS have a higher risk for ischaemic stroke than people who do not have MS. The underlying mechanism is unknown, but might involve endothelial dysfunction secondary to inflammatory disease activity and increased plasma homocysteine concentrations. It is also possible that the global cerebral hypoperfusion predispose MS patients to the development of ischaemic stroke[32]. Of note, smoking - known to be a cardio-vascular risk factor - has been repeatedly demonstrated as a risk factor for MS and has been linked to a faster disability progression and to higher risk of conversion from RRMS to SPMS[18]. On the other hand, emerging evidence support the beneficial effects induced by aerobic

exercise in MS, not only in terms of clinical improvement but also on fMRI parameters[35]. It has also been hypothesized that adaptations occurring during tissue repair might be initiated by acute/chronic increases in circulating growth factors (e.g. vascular endothelial growth factor, platlet-derived growth factor). The effects of MS at the level of the vascular and neuronal networks in the CNS have been the object of intensive investigation both in EAE and in humans[30,36]. Among the causes of neuroinflammation, there are recurrent and chronic infections accompanied by local innate immunity activation and consequent adaptive immune response, which in turn induces immune-thrombotic events[32,37–39]. Indeed, coagulation is activated during viral infections and plays multiple functions in the host immune system [37]. Several studies have suggested a viral etiology of multiple sclerosis and diverse viruses have been proposed as potential triggering agents [30,37]. In recent years, various MRI techniques have been developed to assess cerebral perfusion in multiple sclerosis, including dynamic susceptibility contrast-enhanced (DSC) perfusion MRI[40–42]. Using this technique, many cross-sectional studies have identified altered perfusion parameters with different combinations of either reduced cerebral blood flow (CBF) or reduced cerebral blood volume (CBV) and elevated mean transit time (MTT) in patients with MS sclerosis compared with controls in both normal appearing white matter (NAWM) and normal-appearing gray matter (NAGM)[43–45]. It is conceivable that the global hypoperfusion in GM and WM of MS patients may be determined by the overall deceleration of blood flow due to the inflammatory-thrombotic processes[44,45]. As already described, endothelial cell dysfunction, excessive platelet activation, evidence of oxidative stress, altered BBB permeability, vascular occlusion within demyelinating lesions, and hypoxia-like tissue injury have all been reported in people with MS[30,32]. However, to what extent vascular alterations, inflammation and neuronal loss interact remains to be elucidated.

Failure of compensatory mechanisms

Remyelination and repair of the neuronal damage are important mechanisms leading to recovery, although tissue repair is usually incomplete[23,46,47]. Remyelination is a spontaneous repair process in which new myelin sheaths are formed after a demyelinating event[23]. Repaired compared to native myelin is characterized by shorter and thinner myelin sheaths, resulting in slower action

potential conduction. Remyelination can occur in MS, but the extent of remyelination is very heterogeneous. The variability in remyelination depends on several factors, including patients' age, disease duration, lesion location, the presence of oligodendrocyte progenitor cells and axonal integrity; substantial remyelination is frequently observed during the earlier phases of MS and in younger individuals, whereas it is more sparse or absent in PPMS and SPMS[47,48]. A high proportion of remyelinated lesions is associated with slower disease progression[46]. MRI studies suggest that remyelination starts quickly after the onset of demyelination and continues over approximately six months. Whether remyelination continues beyond six months is uncertain but of tremendous interest[23]. Remyelination has not only been suggested as a mechanism of clinical recovery after a relapse, but could also represent a target for future therapies. As the remyelination era approaches, answering new questions regarding patient-specific factors (e.g., disease phase, age) that may influence the extent and optimal therapeutic window for remyelination appear essential.

Increasing evidence points at synaptic plasticity as an additional important mechanism for recovery, through adaptive changes of neuronal excitability[2349]. Evidence for reorganization of brain function underlying functional recovery comes from studies of focal ischemic brain damage, where systems-level reorganization reflects molecular, synaptic and cellular events and constitutes post-injury brain plasticity. The term "neuroplasticity" refers to the ability of the CNS to respond to intrinsic and extrinsic stimuli by reorganizing its structure, function, and connections, and it includes a variety of mechanisms that modify neurons and neural pathways, including the strength of synaptic transmission, the sprouting of novel synapses, changes to glial cell numbers and white matter fiber features (e.g., degree of myelination, membrane voltage-gated ion channel distribution, axonal diameter and fiber packing density), and the induction of angiogenesis and neurogenesis[49].

1.3. The visual pathways as a model to study MS

The visual pathway, from the optic nerve to the visual cortex, and including the optic tracts, lateral geniculate nuclei (LGN) and optic radiations (OR), provides a well-characterized neural system and unique setting to study MS related pathological processes in vivo. The anterior visual pathways consist of the retinal ganglion cells (neurons), whose somas are in the ganglion cell layer (GCL)[50–52]. Their axons form the retinal nerve fiber layer (RNFL) and are unmyelinated until they leave the eye. These axons form the optic nerve, which travels via the optic canal to the optic chiasm where the nasal fibers decussate and most of the fibers then go on to synapse at the LGN[53]. Since the retina reflects CNS tissue directly accessible to optical imaging, the anterior visual pathways represent a suitable model to study axonal damage. Optical coherence tomography (OCT) is a technique that uses near-infrared light. It is a fast, easy-to-use, non-invasive and cost-efficient imaging tool that can provide high-resolution and highly reproducible images of retinal layers[50,54–56]. The first OCT devices used time domain technology (TD-OCT), which could measure the thickness of the peripapillary RNFL (pRNFL). As such, this layer was the focus of most early research. However, with the advent of spectral domain OCT (SD-OCT) technology, came the ability to assess other retinal layers, including the macular RNFL (mRNFL), GCL, inner plexiform layer (IPL), inner nuclear layer (INL), outer plexiform layer (OPL) and outer nuclear layer (ONL)[56] (see Fig 4)

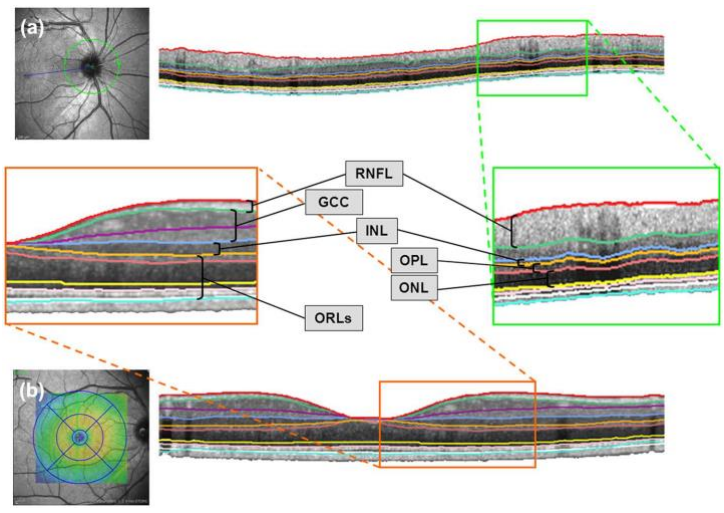

Fig 4: Segmentation protocol for the retinal OCT scan. Segmented layers of the peripapillary ring scan ((a), upper image) and macular volume scan ((b), bottom image)[57].

As described above, visual symptoms are common in MS. ON is the onset symptom in ~20-25%% of patients, but even patients who have not experienced ON, will most likely also have lesions in their visual pathways, as post-mortem studies show that this is the case for 90% of patients regardless of ON history[7]. The progressive thinning of RNFL and of the combined measure of GCL and IPL (GCIPL) have been proposed as valuable biomarkers of neurodegeneration in MS[56]. The pathological mechanism behind the reduction in RNFL and GCIPL thickness in MS patients both with and without prior ON is still in dispute. In patients with prior ON, the most likely explanation is loss of axons following the inflammation of the optic nerve. In patients without previous ON, the suggested explanations include axonal degeneration after a subclinical ON, presence of an asymptomatic lesion in the optic nerve, as well as presence of lesions in the optic radiation that may lead, via trans-synaptic degeneration, to loss of retinal ganglion cells and their axons[56,58,59]. More recently, increased thickening of the INL was found to be associated with signs of inflammation in MS, although mechanisms leading to this phenomenon remain unclear[56,60].

Association between OCT and MRI imaging

In 2007, the first study describing a high correlation between pRNFL and MRI-derived brain parenchymal fraction as marker of brain atrophy was published[61]. Since then, a plethora of studies combining different MRI and OCT measures replicated and specified these findings[51]. However, the data still remains inconsistent as to whether OCT measures are correlated primarily with white matter atrophy or gray matter changes. Also, INL seems to be inversely correlated with brain white matter volume[62,63]. However, it should be kept in mind that the correlation of retinal and brain atrophy is highly influenced by acute ON, as well as by afferent visual pathway lesions leading to trans-synaptic anterograde and retrograde axonal degeneration. The concept of bidirectional trans-synaptic degeneration in the afferent visual system is further supported by studies showing a significant correlation of lesion volume and optic radiation thinning with pRNFL reduction[53,64,65], as well as by multiple diffusion-weighted imaging (DTI)-based studies suggesting the correlation of axonal diffusivity, as potential marker of neuro-axonal damage in the optic nerve and optic radiation, with pRNFL and visual outcome after ON, as well as functional connectivity increase[66]. The

subsequent neuro-axonal thinning of pRNFL and GCIPL is not necessarily accompanied by widespread brain atrophy and thereby disrupts the association. Hence, the retina after ON episodes is primarily a marker of attack-dependent neuro-axonal retinal damage, whereas it can be seen as a mirror of brain atrophy and microstructural CNS changes in eyes without a history of ON. In line with these findings, pRNFL was also shown to be correlated with spinal cord MRI measures reflecting an ongoing widespread pathology and contribute to disability accrual. Nevertheless, ON is a common and severe interruption of these associations. OCT therefore rather adds complementary information to MRI and should be seen as a useful additional outcome instead of an alternative[56].

OCT findings according to disease subtype

OCT could potentially help differentiate between MS sub-types[67,68]. One multicentre study[67] looked at 571 eyes of MS patients without prior ON and they observed a lower RNFL thickness in patients with SPMS compared to RRMS. Furthermore, total macular volume was reduced in SPMS and PPMS eyes compared to RRMS eyes. There was no statistically significant difference between the RNFL thickness and total macular volume in patients with SPMS and PPMS. When the authors corrected for EDSS score in generalized estimation equation models, these differences disappeared. A similar trend could be detected in eyes with prior ON. In a group of MS patients with and without prior ON, Saidha et al[69]. observed lower GCIPL and RNFL values in SPMS compared to RRMS. However, after correcting for disease duration this was only significant with regards to the GCIPL. Overall, these findings suggest a prominent pRNFL/GCIPL thickening in patients with progressive disease course, although several factors including age, disease duration and EDSS seem to significantly impact the results.

Predicting and monitoring disease activity and progression in MS with OCT

OCT also showed to have a high value for the prognosis of progression and disability in patients with MS. Martínez-Lapiscina et al.[70] on behalf of the IMSVISUAL consortium showed in more than 800 patients with MS an association of thinned pRNFL ≤87 μm with disability accrual after 3 years measured by expanded disability status scale (EDSS). More recently, pRNFL[71] and total macular volume[72] have been shown to be predictive of disability

progression in smaller cohorts of patients with long-term follow-up. Regarding retinal segmantation, GCIPL thickness has been suggested as independent risk factor for disability worsening in RRMS[63,68]. Furthermore, thinner GCIPL values have been shown to be predictive for the violation of the NEDA3 criteria in patients with CIS[73] and higher risk of disability progression in patients with early MS[74]. Similarly, longitudinal thinning of pRNFL and GCIPL have been shown to predict disability progression after DMT initiation, thus suggesting that their longitudinal evaluation may be a useful and accessible biomarker of treatment failure in MS[75–78].

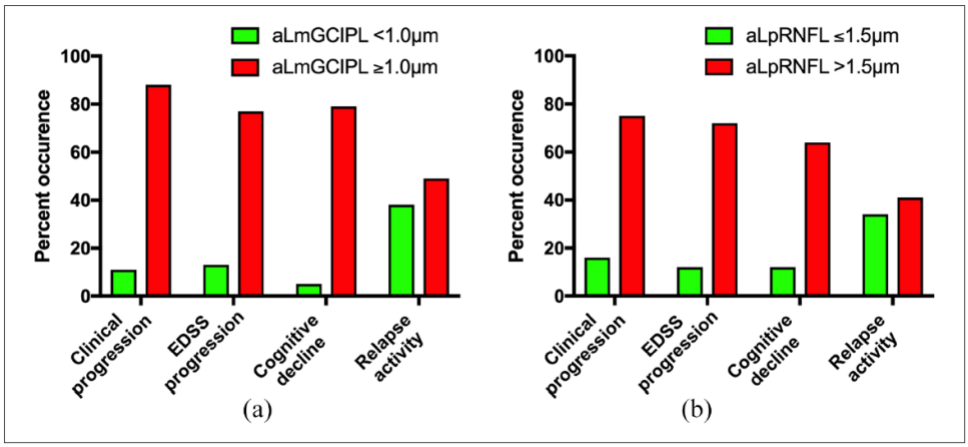

Fig 5: Occurrence of clinical progression, EDSS progression, cognitive decline and relapse activity depending on (a) annual loss of mGCIPL (aLmGCIPL) and (b) annual loss of of pRNFL (aLpRNFL)[77]

Interestingly, OCT parameters are not only related to axonal damage and neurodegeneration, but may also be able to capture early inflammatory activity. In particular, thickness of INL has been proposed as a measure of inflammatory activity within the CNS and thus as a potential marker for patients' stratification and therapy response monitoring[56,60,62,63]. Indeed, INL thickness has been shown to correlate with higher T2-FLAIR lesion volume and with the prospective increase in T2 lesion load, the number of gadolinium-enhancing lesions, annualized relapse rate (ARR), and progression in EDSS in MS[62]. On the contrary, longitudinal thinning of the INL was associated with reduced inflammatory activity, indicating efficient control of disease activity including NEDA[60,62]. An association of OCT parameters and disease course is highly relevant for the

clinical practice, since OCT would allow non-invasive frequent follow-up measurements and a fast adjustment of therapeutic regimes.

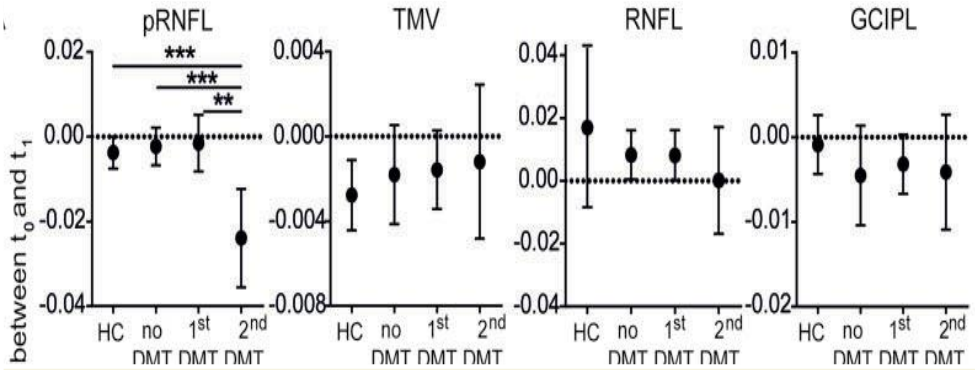

Fig 6: Time course of INL changes in patients treated with 1st line DMT (n = 11; 20 eyes) and 2nd line DMT (n = 9; 17 eyes) stratified according to NEDA-3 status[62].

However, large, homogeneous, and prospective studies assessing the OCT metrics trajectories over time and their correlation with response to specific treatments are still lacking.

2. THESIS PROJECT

2.1. Background and overarching aims

The progress toward a personalized and effective healthcare for MS is still hindered by an incomplete understanding of the biological processes underlying the disease, their interactions, and the heterogeneity between patients. Accordingly, there are several unsolved problems in MS management.

First, prognosticating MS remains challenging due to the high heterogeneity of the disease course, making it difficult to early identify patients who will develop an aggressive form of MS. Despite the identification of several clinico-demographic, immunologic, and radiologic risk factors for worse outcomes, long-term complete MS remission is still an elusive therapeutic goal[2]. Secondly, the question of whether treatment can fully prevent long-term clinical progression is controversial. The concept of "no-evidence-of-disease-activity" (NEDA-3), defined as the absence of inflammatory MRI activity, clinical relapses, and disability progression, has been proposed as a goal in MS patients treated with active DMTs[79]. However, real-world studies indicate that maintaining NEDA-3 status for longer than 2 years is challenging for most MS patients, even with the use of high-efficacy DMTs[80]. Longer-term follow-up studies reveal that over half of treated relapsing-remitting MS (RRMS) patients accumulate relevant disability over 10 years, questioning the utility of these metrics as outcome measures in clinical trials[81]. This highlights the need to explore new biomarkers for clinical practice, trials, and research to address the spectrum of MS pathology and clinical progression. Lastly, to date, no medication has convincingly demonstrated the ability to promote remyelination or neuronal plasticity, directly or indirectly reversing impaired neurologic functions in MS.

Altogether, these considerations suggest that clinical characterization and treatment selection should be guided by identification of the underlying disease-driving pathophysiological mechanisms rather than relying solely on traditional clinical descriptors. Adopting this approach has the potential to establish a consensus-based classification, transforming drug discovery and enhancing patient care[23]. In this context, understanding the role of focal inflammation - a treatable feature - on neuro-axonal injury as well as identification of early

biomarker able to predict future disease activity and the likelihood of good tissue repair are essential to better personalize the treatment approach.

Against this background, the overarching aims of this thesis project were to:
1) Characterize new pathophysiological mechanisms potentially involved in focal inflammation, local and diffuse neuro-axonal injury, and tissue repair
2) Assess the long-term outcomes of MS patients treated with highly active immunotherapies, investigating in vivo the role of different clinical and paraclinical biomarkers in the context of patients' stratification and monitoring.

For the first aim of this project, we performed two separate studies exploring (i) the contribution of pro-coagulative/vascular factors for MS pathogenesis and their correlation with brain hemodynamic abnormalities - possibly contributing to neuro-axonal loss and inhibition of remyelination - during the relapsing and the remitting phases of MS (ii) the role of multipotent neural stem cells' neurogenic and neuroprotective functions, thanks to an in-vivo characterization of the subventricular zone in MS patients with different disease course.

For the second aim, we performed a longitudinal, prospective, and real-life study evaluating the impact of ocrelizumab treatment on clinical and MRI outcomes in relapsing- and progressive-MS patients. Then, in order to explore the possible contribution of OCT metrics in detecting inflammatory and neurodegenerative processes within the CNS, we performed a "sub-study" focused on patients with a relapsing form of MS, combining MRI and OCT markers of inflammation and of axonal injury at both cerebral and retinal level and investigating their correlation with disease activity over follow-up (FU).

2.2. Aim 1: Characterizing pathological mechanisms potentially involved in in focal inflammation, local and diffuse neuro-axonal injury, and tissue repair

2.2.1 Potential coagulative/vascular markers in relapsing-remitting multiple sclerosis

Abstract

Objectives: Recent studies supported coagulation involvement in MS. The main objectives of this observational study were to identify the most specific pro-coagulative/vascular factors for MS pathogenesis and to correlate them with brain hemodynamic abnormalities.

Methods: We compared i) serum/plasma levels of complement(C)/coagulation/ vascular factors, viral/microbiological assays, fat-soluble vitamins and lymphocyte count among people with multiple sclerosis sampled in a clinical remission (n=30; 23F/7M, 40 ± 8.14 years) or a relapse (n=30; 24F/6M, age 41 ± 10.74 years) and age/sex-matched controls (n=30; 23F/7M, 40 ± 8.38 years); ii) brain hemodynamic metrics at dynamic susceptibility contrast-enhanced 3T- MRI during relapse and remission, and iii) laboratory data with MRI perfusion metrics and clinical features of people with multiple sclerosis. Two models by Partial Least Squares Discriminant Analysis were performed using two groups as input: (1) MS vs. controls, and (2) relapsing vs. remitting MS.

Results: Compared to controls, MS patients had a higher Body-Mass-Index (BMI), Protein-C and activated-C9; and a lower activated-C4. Levels of Tissue-Factor, Tie-2 and P-Selectin/CD62P were lower in relapse compared to remission and HC, whereas Angiopoietin-I was higher in relapsing vs. remitting multiple sclerosis. A lower number of total lymphocytes was found in relapsing MS vs. remitting MS and controls. Cerebral-Blood-Volume was lower in normal-appearing white matter and left caudatum while Cerebral-Blood-Flow was inferior in bilateral putamen in relapsing vs remitting MS. The mean-transit-time of gadolinium-enhancing lesions negatively correlated with Tissue-Factor. The top-5 discriminating variables for model (1) were: EBV-EBNA-1 IgG, BMI, Protein-C, activated-C4 and Tissue-Factor whereas for model (2) were: Tissue-Factor, Angiopoietin-I, MCHC, Vitamin A and T-CD3.

Conclusion: Tissue-factor was one of the top-5 variables in the models discriminating either MS from controls or MS relapse from remission and correlated with mean-transit-time of gadolinium- enhancing lesions. Tissue-factor appears a promising pro-coagulative/vascular biomarker and a possible therapeutic target in relapsing-remitting MS.

Scientific rational and study endpoints

As described in the previous paragraphs (see paragraph 1.2), accumulating evidence has pointed out the strong interplay between coagulation and inflammation with infections in the pathophysiology of MS, as well as its association with brain perfusion metrics, thus suggesting possible therapeutic targets that may integrate existing treatments. Thus, the primary endpoint of our study was the determination of potential differences in terms of serum/plasma concentrations of complement, pro-coagulative/vascular, and viral/microbiological markers among the participants' groups. Key secondary endpoints were: i) to assess the relative CBF, CBV and MTT, as well as the number and volume of enhancing lesions in relapsing- and remitting-multiple MS and to compare these parameters between the subgroups of patinets; ii) to explore the relationships between demographic/clinical features and laboratory data and MRI perfusion findings in the patient groups.

Study design

This is a multi-center, prospective, observational, controlled study that our group conducted in collaboration with two additional MS centers (the Multiple Sclerosis Center of the Sapienza University of Rome and the Multiple Sclerosis Center of the IRCCS Regina Elena National Cancer Institute). Individuals with MS were included if they fulfilled the following inclusion criteria: age 18–60 years; relapsing-remitting MS diagnosis according to the revised McDonald's criteria; being untreated or treated only with "first-line" immunomodulatory therapies (i.e., interferon, glatiramer acetate, teriflunomide, dimethyl-fumarate). Exclusion criteria were: ongoing pregnancy; co-existing neoplastic, hematologic, thyroid, metabolic, thrombotic, or autoimmune diseases; drug or alcohol addiction; therapy with immunosuppressive drugs, steroids, or any medication interfering with coagulation. Patients were defined as "relapsing" if, at the time of enrollment, they had ongoing symptoms suggesting a relapse (defined as a manifestation of

new or worsened neurological symptoms lasting for more than 24 hours) and "remitting" if no relapses occurred in the previous 2 months. Relapsing multiple sclerosis patients had to be enrolled before starting steroid therapy. Controls matched by age and sex with remitting patients were also included in the study (Fig 1 - 2.2.1).

Fig 1 - 2.2.1: Flow chart of the study.

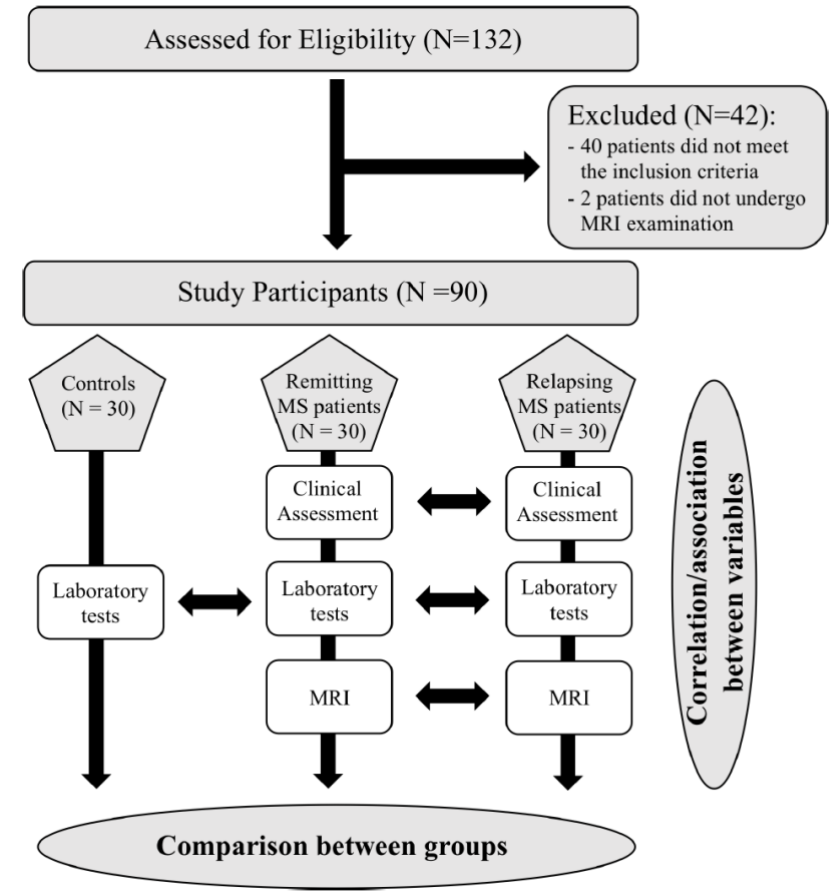

For each patient, at enrolment, data on demographics and clinical history and peripheral blood sample were collected and the assessment of physical disability using the EDSS and Multiple Sclerosis Functional Composite (MSFC) was carried out. DSC perfusion 3.0-T MRI (7) was performed within two weeks of enrolment. For the controls, only demographic data and laboratory markers were collected.

Statistical analysis

Overall, 90 subjects (30 for each group) were enrolled. By using the analysis of variance (ANOVA) test, this sample size allowed to detect effect size values [delta=(miA–miB)/sigma] equal to at least 0.71, with a statistical power of 80%, to a level of significance of 5%. In all analyses, potential confounding factors including treatment, sex, and age were controlled for. Descriptive statistics were used to summarize pertinent study information. Correlations between quantitative variables were assessed with Spearman's rho coefficient. The associations were analyzed by the Fisher exact test or Chi Square test for trends. Comparisons between disease subgroups and control group were carried out for different variables, using either Student's t-test or ANOVA. If the ANOVA showed a statistical difference between subgroups, a post-hoc analysis with Bonferroni-Holm correction for multiple comparisons was performed. For non-normally distributed data, non-parametric (Mann Whitney-U or Kruskal-Wallis-H) tests were used. In this study, missing data were identified to be Missing Completely at Random (MCAR), indicating that the missingness was not related to any measured or unmeasured variables. To deal with missing data, a pairwise deletion approach was employed when necessary. This approach removes cases with missing data pairwise, meaning that only the incomplete observations are excluded from the analyses, leaving the remaining complete data in the study. Given the MCAR assumption, this approach is an appropriate and bias-free way to handle missing data in the study. The level of significance was set at two-tailed $P \leq 0.05$ (SPSS version 20.0, SPSS Inc., Chicago, Illinois, USA). Partial Least Squares Discriminant Analysis (PLS-DA) was used in order to identify the variables that had a possible role in the identification of patients' groups[82]. The analysis was performed using the 'pls' package in R for classification and prediction of data. In order to define the variables responsible for the measured variance in PLS-DA prediction models, variable importance in projection (VIP) scores were calculated. A random forest classifier was built by hold-out analysis using the 'caret' package in R, in which the model was created using the top-5 VIP variables from the PLS-DA; the model was trained on 70% of the data and tested on the remaining 30% in order to prevent overfitting. To obtain more precise curves and assess the performance of the models on unseen data, we used a repeated 100-fold cross-validation that consisted of 100 train and test splits. The

cross-validation error curves and performances were averaged. The predictive value of each variable in the random forest models was calculated by Predictive Accuracy. The model's performance was further evaluated through the AUC on the test set using the 'pROC' R package.

Population characteristics

Demographic and clinical data of study groups are reported in Table 1-2.2.1. We observed a significantly higher body mass index (BMI) in both patient groups compared to controls. The mean (SD) number of total relapses, as well as relapses occurred within the previous 24 and 12 months, and baseline EDSS scores were significantly higher in relapsing-multiple sclerosis patients compared to those in remission. No differences between the two patient groups were observed in terms of the distribution of their ongoing treatments [untreated (U-), interferon (IFN-), other first line treatments (OT-)].

Table 1-2.2.1: Demographic and clinical variables in healthy controls, relapsing and remitting MS patients.

	Controls (n=30)	Remitting-MS (n=30)	Relapsing-MS (n=30)	*P-value**
Female; n (%)	23 (76%)	23 (76%)	24 (80%)	0.938
Age; mean (SD), y	40 (8.38)	40 (8.14)	41 (10.74)	0.920
Age at onset; mean (SD), y	–	28.8 (8.45)	29.3 (9.43)	0.807
BMI; mean (SD)	21.51 (2.78)	24.16 (4.07)	24.39 (4.25)	0.006[a]
Disease duration; mean (SD), y	–	15.56 (6.46)	15.33 (8.36)	0.900
Total relapses; n; median (IQR)	–	2 (1)	4 (3.75)	0.002
Relapses in the previous 24-months; n; median (IQR)	–	0 (0)	1 (2)	<0.001
Relapses in the previous 12-months; n; median (IQR)	–	0 (0)	1 (1)	<0.001
EDSS score at baseline; median (IQR)	–	1.5 (1.375)	3.25 (1.875)	<0.001
MSFC; mean (SD), consisted of: - 9-HPT, z score; mean (SD) - T25-FW, z score; mean (SD) - PASAT, z score; mean (SD)	–	0.06 (0.32) 0.03 (0.63) 0.26 (0.07) - 0.11 (0.53)	- 0.007 (0.44) - 0.24 (0.68) 0.26 (0.05) - 0.03 (0.80)	0.511 0.115 0.958 0.663
Therapy; n - U - IFN - OT	- - -	8 (26.7) 12 (40) 10 (33.3)	8 (26.7) 6 (20) 16 (53.3)	0.184

BMI, body mass index; EDSS, Expanded Disability Status Scale; 9-HPT, 9 Hole peg test; IFN, Interferon; IQR, interquartile range; MS, multiple sclerosis; MSFC, Multiple Sclerosis Functional Composite; OT, Other Therapy; PASAT, Paced Auditory Serial Addition Task; SD, standard deviation; T25-FW, Timed 25-Foot Walk; U, Untreated.
*Chi-square (sex, therapy), ANOVA (age, BMI), Mann-Whitney (age at onset, disease duration, total relapses, relapses previous. 24-months, relapses previous 12-months, EDSS), t-test (9-HPT, T25WT, PASAT, MSFC).
[a]Post-hoc analysis: controls vs relapsing-MS: p = 0.011; controls vs remitting-MS: p=0.021.

Differences in terms of laboratory biomarkers

Statistically significant differences between-groups in serum/plasma laboratory variables are reported in Table 2-2.2.1.

Compared to controls, patient groups exhibited: higher Protein C (PC) and

activated complement 9 (aC9) with a trend towards statistical significance for higher D-dimer levels (P=0.07); and lower aC4 levels with a trend for lower Protein S (p=0.06). Angiopoietin-I was higher in relapsing MS patients as compared to those in remission. Furthermore, levels of Tissue Factor (TF), Tie-2 and P-Selectin/CD62P were lower in the relapsing population as compared to both remitting patients and controls. Regarding vitamins, data were only available for 57 participants (22 controls, 18 remitting- and 17 relapsing-multiple sclerosis patients) and we found higher values of vitamins A and K in relapsing patients compared to both remitting patients and controls (see Table 2-2.2.1-A).

Differences in terms of viral/microbiological serological assays are reported in Table 2-2.2.1-B. EBVEBNA-1 IgG and InfluenzaA IgG were higher in the patient groups than in controls. InfluenzaA IgA levels were lower in relapsing compared to remitting MS patients; and Schistosoma IgG were lower in relapsing compared to both remitting-MS patients and controls.

Table 2 - 2.2.1: Statistically significant between-group differences in terms of laboratory biomarkers in controls and remitting- and relapsing MS patients. (A: Coagulation/complement biomarkers; B: serological viral/microbiological assey)

A - Coagulation/ complement biomarkers	Controls (n=30)		Remitting-MS (n=30)		Relapsing-MS (n=30)		
	Mean (SD)	Median (IQR)	Mean (SD)	Median (IQR)	Mean (SD)	Median (IQR)	*P*-value*
PC	99.13 (14.44)	97.5 (25.25)	110.66 (18.07)	116.5 (28.5)	116.86 (20.74)	117 (30)	0.001[a]
aC4	5.78 (5.21)	4.75 (1.725)	2.75 (1.43)	2.3 (1.125)	3.91 (3.13)	2.85 (2.107)	0.001[b]
aC9	3.38 (1.13)	3.4 (1.675)	4.91 (3.03)	4.3 (3.3)	5.42 (4.13)	4.4 (3.54)	0.019[c]
AngI	9.40 (4.04)	8.38 (4.34)	7.31 (2.96)	7.26 (2.84)	10.57 (4.83)	9.76 (5.75)	0.009[d]
TF	110.85 (56.31)	120.69 (101.11)	94.06 (55.83)	99.23 (104.22)	45.03 (37.66)	22.72 (58.67)	<0.001[e]
Tie-2	49.60 (17.58)	43.15 (10.775)	46.45 (17.36)	40.85 (22.425)	34.42 (19.94)	35.7 (25.3)	0.002[f]
P-Sel	245.85 (120.48)	197 (156)	216.26 (82.15)	216.5 (131)	169.41 (173.51)	160 (215.4)	0.020[g]
VitA°	40.75 (18.15)	32.68 (21.925)	43.15 (12.77)	41.63 (12.43)	105.18 (50.07)	100.8 (101.13)	<0.001[h]
VitK°	163.89 (110.80)	126.49 (119.56)	166.75 (107.20)	148.405 (167.115)	295.51 (64.84)	272.455 (299.222)	<0.001[i]
B - Serological viral/ microbiological assay	**Controls (n=30)**		**Remitting-MS (n=30)**		**Relapsing-MS (n=30)**		
	Mean (SD)	Median (IQR)	Mean (SD)	Median (IQR)	Mean (SD)	Median (IQR)	*P*-value*
EBV-EBNA IgG	26.81 (7.48)	27.65 (8.325)	31.05 (6.35)	32.15 (6.3)	31.89 (4.66)	32 (5.3)	0.014[l]
InfA IgA	2.49 (3.23)	1.45 (0.825)	2.91 (2.72)	2.1 (1.725)	1.71 (1.23)	1.35 (0.75)	0.029[n]

(Continued)

B - Serological viral/ microbiological assay	Controls (n=30)		Remitting-MS (n=30)		Relapsing-MS (n=30)		
	Mean (SD)	Median (IQR)	Mean (SD)	Median (IQR)	Mean (SD)	Median (IQR)	*P*-value*
InfA IgG	11.59 (7.61)	8.75 (9.275)	15.87 (7.49)	15.7 (12.375)	17.88 (11.98)	12.45 (21.45)	0.041[m]
Sch IgG	4.79 (1.74)	4.6 (2.225)	4.75 (2.28)	4.15 (2.25)	3.86 (1.41)	3.4 (0.65)	0.023°

IQR, interquartile range; MS, multiple sclerosis; SD, standard deviation.
°In the context of vitamin assessment, data were available in 57 subjects for Vit A and K (22 controls, 18 remitting- and 17 relapsing- MS patients).
*Kruskall-Wallis or ANOVA according to the variable distribution.
Significant differences are reported in bold; statistically significant post-hoc analysis details are described below:
aP=0.042 for controls vs Remitting-MS; p=0.001 for controls vs Relapsing-MS.
bP=0.002 for controls vs Remitting-MS; p=0.008 for controls vs Relapsing-MS; p=0.039 for Relapsing-MS vs Remitting-MS.
cP=0.022 for controls vs Remitting-MS; p=0.017 for controls vs Relapsing-MS.
dP=0.005 for Relapsing-MS vs Remitting-MS.
eP<0.001 for Relapsing-MS vs controls; p<0.001 for Relapsing-MS vs Remitting-MS.
fP<0.001 for Relapsing-MS vs controls; p=0.032 for Relapsing-MS vs Remitting-MS.
gP=0.013 for Relapsing-MS vs controls; p=0.032 for Relapsing-MS vs Remitting-MS.
hP<0.001 for Relapsing-MS vs controls; p<0.001 for Relapsing-MS vs Remitting-MS.
iP<0.001 for Relapsing-MS vs controls; p<0.001 for Relapsing-MS vs Remitting-MS.
lP=0.017 for controls vs Remitting-MS; p=0.011 for controls vs Relapsing-MS.
mP=0.037 for controls vs Remitting-MS; p=0.037 for controls vs Relapsing-MS.
nP=0.014 for Relapsing-MS vs Remitting-MS.
° P=0.014 for Relapsing-MS vs controls; p=0.038for Relapsing-MS vs Remitting-MS.

Differences in terms of MRI metrics

The mean (SD) number and volume of gadolinium-enhancing lesions were significantly higher in relapsing patients compared to those in remission [1.57 (2.54) vs 0.07 (0.26), and 0.18 (0.3) vs 0.009 (0.04) ml, respectively, P<0.001 for all]. Regarding perfusion metrics, data concerning CBV, CBF and MTT were evaluated in the context of gadolinium-enhancing lesions as well as in the NAWM and in the deep NAGM of MS patients. Given the very low number of active lesions in remitting patients, a comparison of the perfusion metrics between patient groups was not possible. The mean (SD) CBV of relapsing-multiple sclerosis patients was significantly lower compared to remitting-MS patients, either in NAWM (P=0.047) or the left caudatum (P=0.044). Similarly, a lower mean (SD) CBF in relapsing patients versus those in remission was found in both the left (P=0.028) and right putamen (P=0.037).

Relationships between demographic/clinical features, laboratory data, and MRI metrics

Relevant significant correlations between demographic/clinical/laboratory markers and MRI metrics emerged only for perfusion parameters of Gd-enhancing lesions (Table 3-2.2.1). Specifically, disease duration positively correlated with

the CBF of active lesions, while the number of relapses in the previous 12 months and Vitamin K showed a negative correlation with this MRI metric; the CBV of Gd-enhancing lesions positively correlated with either patients' age, PC or InfluenzaB IgA, and negatively correlated with Vitamin K. Notably, a negative correlation was found between MTT and TF, Vitamin K and P-Selectin\CD62P

Table 3-2.2.1: Relevant statistically significant correlations between demographic, clinical and radiological (MRI) markers in the relapsing- and remitting MS patients' groups.

Variable 1	Variable 2	Spearman's rho	*P*-value
EDSS	MSFC	-0.571	<0.0001
EDSS	9-HPT z-scores	-0.594	<0.0001
Number of relapses in the previous 24 months	Vitamin A	0.512	0.0004
Number of relapses in the previous 12 months	Vitamin A	0.540	0.0002
BMI	C3	0.592	<0.0001
Age	rCBV leakage* active (Gd+) lesions	0.704	0.0023
Disease duration	rCBF leakage* active (Gd+) lesions	0.761	0.0006
Number of relapses in the previous 12 months	rCBF leakage* active (Gd+) lesions	-0.734	0.0012
PC	rCBV leakage* active (Gd+) lesions	0.665	0.0049
TF	MTT leakage* active (Gd+) lesions	-0.746	0.0009
P-Selectin\CD62P	MTT leakage* active (Gd+) lesions	-0.645	0.007
Vit K	rCBV leakage* active (Gd+) lesions	-0.827	0.0017
Vit K	rCBF leakage* active (Gd+) lesions	-0.720	0.0125
Vit K	MTT leakage* active (Gd+) lesions	-0.70	0.0182
CMV IgM	MTT leakage* active (Gd+) lesions	0.828	0.0001
Inf B IgA	rCBV leakage* active (Gd+) lesions	0.777	0.0004

*A leakage correction analysis was also performed, in order to correct for contrast agent extravasation.
CMV IgM, Cytomegalovirus IgM; Gd+, gadolinium-enhancing lesions; Inf B IgA, Influenza B IgA; MTT, Mean Transit Time; rCBF, relative Cerebral Blood Flow; rCBV, relative Cerebral Blood Volume; TF, Coagulation Factor III/Tissue Factor; Vit K, vitamin K.

Data driven prediction of MS

The two PLS-DA analyses carried out for models (1) (controls vs. MS) and (2) (remitting vs. relapsing MS patients) to assess the variation in demographic/clinical, laboratory, and MRI features between groups. The results produced the Average Importance rankings of the variables, which are displayed in (Fig 2-2.2.1 A and B, respectively). The top-5 ranking variables were employed to construct the Random Forest classifiers. Specifically, for model (1), they were: EBV-EBNA-1 IgG, BMI, PC, aC4 and TF; and for model (2), they were: TF, Angiopoietin-I, MCHC, Vitamin A and CD3+ T-cells. The performance of the classifiers was evaluated in terms of sensitivity and specificity, and by the ROC curves. This resulted in an AUC of 0.853 (95% CI 0.730- 0.951) for discriminating controls from MS patients and an AUC of 0.942 (95% CI 0.84-1.0) for the discrimination of remitting MS patients from relapsing ones. Both models, using

a small number of variables, appeared to perform well in distinguishing the groups under exam with good accuracy.

Fig 2-2.2.1: Variables ranked by Average Importance score calculated by PLS-DA. (A) Model (1), controls vs. MS (remitting + relapsing); (B) Model (2), remitting MS vs. relapsing MS.

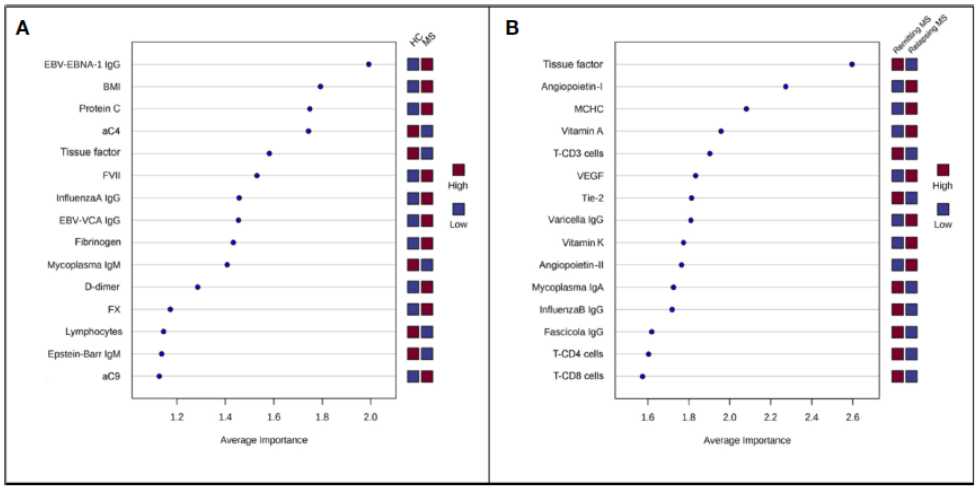

Discussion

In the past years, accumulating evidence has shed light on the role of the coagulation system in the pathogenesis of MS[36,83]. In this study, we have undertaken a large-scale controlled analysis, comprehensive of demographic, clinical, laboratory (including coagulation/complement and vascular factors, viral/microbiological assay, and fat-soluble vitamins) and radiological characteristics. Overall, we observed that blood and MRI alterations suggesting inflammatory-thrombotic processes occur in MS, especially during relapses, and can be influenced by demographic/clinical aspects and infectious status. We consequently built two predictive models to identify variables that played a possible role in distinguishing (1) controls vs. MS patients, and (2) remitting MS vs. relapsing MS patients. Among the top-5 ranking variables (EBV-EBNA-1 IgG, BMI, PC, aC4 and TF) in the first model, EBV-EBNA-1 IgG was found to be the best one to discriminate controls from MS patients supporting the increasing body of evidence that suggests a preceding infection by EBV as a leading cause of MS[84,85]. Other serological markers (InfluenzaA IgG and Mycoplasma IgM) expressing previous or ongoing infection also differed between controls and MS patients, although they seemed to play a less relevant role.

Furthermore, we found higher BMI in patients compared to controls, corroborating the growing evidence of a link between BMI and MS risk [86]. Obesity is known to generate, through adipokines, a subtle pro-inflammatory systemic state that increases BBB permeability and triggers neuroinflammation[86]. Indeed, we observed a positive association between BMI and C3, which in turn correlated with key coagulation factors such as fibrinogen and FX; this further supports the relationship between BMI and neuroinflammation/coagulation.

Several differences emerged not only between patients and controls, but also between relapsing and remitting-MS patients. Our predictive model (2) identified the following variables as the top-5 ranking ones: TF, Angiopoietin-I, MCHC, Vitamin A and T-cells. We observed lower levels of TF and Tie-2, as well as higher levels of Angiopoietin-I and VEGF in the relapsing-MS group. The Angiopoietin/Tie system controls endothelial cell survival and vascular maturation/ stabilization, acting as a vascular specific ligand/receptor system [87,88]. Altered Tie2 signaling has been linked to impairments in vascular function associated with many diseases, including cancer, cardiovascular diseases, and systemic inflammation[88]. Moreover, in endotoxemic mice, reduced Tie2 signaling preceded signs of overt disseminated intravascular coagulation[89]. Our findings suggest altered Angiopoietin-I/Tie2 signaling in the relapsing phase of MS patients which, to our knowledge, has not been yet investigated in MS and requires further in-depth studies. In our participants, the higher Vitamin A and K levels were found in relapsing- compared to either remitting patients or controls, and Vitamin K values negatively correlated with either CBV, CBF or MTT of active lesions while those of Vitamin A positively correlated with the number of relapses in previous 24- and 12 months. Moreover, within active gadolinium enhancing lesions, the CBV positively correlated with PC while the MTT negatively correlated with TF. Furthermore, the CBV of NAWM and caudatum, as well as the CBF of putamen, were significantly lower in relapsing- compared to remitting-MS patients, suggesting that the global hypoperfusion may correlate with the overall blood flow deceleration due to inflammatory-thrombotic processes. The observation of deep grey matter hypoperfusion in patients with MS confirms the findings of previous studies[40,42,44,90,91]. Some hypotheses have been proposed; hypoperfusion could be due to neuroaxonal loss as a consequence of demyelination processes, although in the majority of the studies no association

between perfusion and brain atrophy was found[92]. Other possible explanations could include a reduction in energy demand or metabolic consumption, primary ischemia, and cerebrovascular reactivity, and mitochondria alterations[40,44]. Hypoperfusion could be preliminary to the development of neurodegenerative processes leading to brain atrophy[92].

It is noteworthy to point out that, for both models, the TF is in the top-5 variables that have a major role in this successful discrimination. In our cohort, systemic levels of TF were lower in relapsing compared to remitting patients and in MS vs controls, likely indicating its free, unbound in complex, form. TF is the key trigger of the coagulation cascade and formation of the TF:FVIIa complex activates both FX and FIX, with consecutive thrombin generation, fibrin deposition and platelet activation[93]. Within the CNS, TF is predominantly expressed by astrocytes and mediates intracellular signaling via activation of protease-activated receptors (PARs) expressed in several cell types. BBB disruption, occurring in MS exposes both perivascular and astrocyte TF to circulating clotting factors, which trigger the coagulation cascade. Furthermore, hemostasis components like fibrinogen, which leak into the brain parenchyma due to increased BBB permeability, are incorporated by astrocytes, leading to the formation of extensive fibrin(ogen) deposition. Finally, fibrinogen seems to activate microglia, leading to subsequent chemokines and cytokines production, macrophage and lymphocyte T recruitment, autoimmunity and reactive oxygen species generation. Impaired fibrinolysis increases fibrin deposition. All these processes may lead to axonal damage, demyelination, and inhibition of remyelination[94]. PARs, also widely expressed by either immune or nonprofessional immune cells such as platelets, link the coagulation system with the inflammatory response, controlling the immune response to viral infection[37]. In particular, PAR-1 seems to induce proinflammatory and anti-inflammatory signaling under activation by thrombin or the anticoagulant activated PC (aPC), respectively[95]. However, the presence of TF and PC inhibitors in MS lesions suggests pro-inflammatory thrombin formation and suppression of the anti-inflammatory aPC pathways[94]. Given the above, it has been hypothesized that coagulation activation at the level of BBB and neurovascular unit might induce and sustain inflammatory processes underlying the pathophysiology of MS. Indeed, TF expression has been found to increase, along with extensive fibrin deposition, in MS lesions[94,95]. The findings

in EAE model also support the importance of vasculature damage and coagulation and their close relationship with neuroinflammation, neuroimmunology, and neurodegeneration[96,97].

It should be taken into account that the coagulation activation has also the role of limiting pathogen spreading. However, some viruses, such as Herpes-virus, use this system to coat virally infected cells with fibrin reducing their recognition and killing by NK cells and phagocytes[98]. In fact, TF expression is increased in HSV infected endothelial cells of mice that produce higher viral amount compared to TF-negative infected cells[98].

In conclusion, based on our two predictive models and the already recognized aspects of MS pathogenesis, we may assume that previous EBV infection, along with other conditions (obesity, altered gut microbiota, etc.), induces prolonged immune system dysfunction predisposing to the MS pathology. In this dis-immune state, MS exacerbations, accompanied by altered cerebral perfusion and inflammatory-thrombotic processes at both systemic and CNS level, could be determined by neurotropic infections together with consensual reactive immune responses. Circulating TF levels appear a promising pro-coagulative/vascular biomarker and a possible therapeutic target in relapsing-remitting MS.

2.2.2 In-vivo characterization of macro- and microstructural injury of the subventricular zone in relapsing-remitting and progressive multiple sclerosis patients

Abstract

Objectives: The subventricular zone (SVZ) represents one of the main adult brain neurogenesis niche. In-vivo imaging of SVZ is very challenging and little is known about MRI correlates of SVZ macro- and micro-structural injury in multiple sclerosis (MS) patients. The aim of the present study was to evaluate differences in terms of volume and microstructural changes [as assessed with the novel Spherical Mean Technique (SMT) model, evaluating: Neurite Signal fraction (INTRA); Extra-neurite transverse (EXTRATRANS) and mean diffusivity (EXTRAMD)] in SVZ between relapsing-remitting (RR) or progressive (P) MS patients and healthy controls (HC). We also wanted to explore whether SVZ microstructural injury correlate with caudate (a nucleus that is in the vicinity of the SVZ) or thalamus (another well-defined grey matter area which is further from SVZ than caudate) volume and clinical disability.

Methods: Clinical and brain MRI data were prospectively acquired from 20 HC, 101 RRMS, and 50 PMS patients. Structural and diffusion metrics inside the global SVZ, normal appearing (NA-) SVZ, caudate and thalamus were collected.

Results: We found a statistically significant difference between groups in terms of NA-SVZ EXTRAMD (PMS>RRMS>HC; $p=0.002$), EXTRATRANS (PMS>RRMS>HC; $p<0.0001$), and INTRA (HC>RRMS>PMS; $p=0.009$). Multivariable models showed that NA-SVZ metrics significantly predicted caudate ($R^2=0.21$, $p<0.0001$), but not thalamus, atrophy. A statistically significant correlation between EXTRAMD and EXTRATRANS of the NA-SVZ and EDSS ($r=0.25$, $p=0.003$ and $r=0.24$, $p=0.003$, respectively) was found. These findings were confirmed in analyses restricted to RRMS, but not to PMS patients.

Conclusions: In conclusion, the microstructural damage we observed within the NA-SVZ of MS patients – reflecting higher free water content (higher EXTRAMD), cytoarchitecture disruption and astrogliosis (higher EXTRATRANS and lower INTRA) - was more evident in the progressive as compared to the relapsing phases of MS. These abnormalities were significantly associated with a more pronounced caudate atrophy and higher clinical disability scores. Our findings may support the neuroprotective role of SVZ in MS patients.

Scientific rationale and study endpoints

The subventricular zone (SVZ), immediately beneath the ependymal layer on the lateral wall of the lateral ventricles, contains multipotent neural stem cells. Together with the subgranular zone in the hippocampal dentate gyrus, the SVZ represents one of the main adult brain neurogenesis niche[99,100]. Although data regarding SVZ functioning mostly derive from animal studies, data in humans suggest that the SVZ persists in the adult human brain[99], and SVZ astrocytes have been shown to retain the functions of neural stem cells in vitro [101,102]. Although the capacity of SVZ cells to proliferate and migrate in vivo is still a matter of debate[102], recent findings suggest that in normal conditions and after injury the adult human SVZ can generate mature astrocytes [103]. Importantly, neurogenesis in humans has been shown to rapidly decline with increased age, supposedly due to a loss of function of adult stem cell and progenitor cell populations[104,105]. In line with that, elderly individuals are more susceptible to neurodegenerative disease such as Parkinson's (PD) and Alzheimer's (AD) diseases [100]. Interestingly, post-mortem studies have identified mature and immature oligodendrocytes and oligodendrocyte precursor cells (OPCs) in some chronic MS lesions, suggesting a mobilization of SVZ-derived progenitors mainly to peri-ventricular lesions[101]. SVZ-derived cells have also been shown to contribute to remyelination through various mechanisms in murine models of MS [106–108]. At the same time, accumulating evidence showed that the SVZ might also exert non neurogenic functions via the secretion of soluble growth factors, the release of neuroprotective molecules and the modulation of microglia functions [109,110] . The objective of our study was to obtain an in-vivo characterization of SVZ in MS patients with advanced MRI techniques. Since the presence of MS lesions in the periventricular areas - hence possibly involving the SVZ - is a hallmark of MS, and considering that the widespread tissue damage worsens in the progressive phases of the disease, we predicted that microstructural alterations involving SVZ are present in MS patients and increase with the progression of the disease. We accordingly expected to observe a microstructural disruption in the SVZ – radiologically similar to that occurring in other MS lesions and in the NAWM - in MS patients, more evident in the progressive with respect to the relapsing–remitting stages of the disease. Assuming that this hypothesis held true, we sought to explore whether the microstructural injury found could impact the neuroprotective functions of

SVZ. To that end - as exploratory analyses – we investigated its correlations with caudate/thalamus nuclei volume (considering the SVZ position, we expected to find a stronger association with caudate rather than with thalamus volumes, since the first is closer to the SVZ, and we thus expected it could more easily benefit from its neuroprotective functions) and clinical disability. More specifically, the aims of our study were to:

(I) explore differences in terms of volume and microstructural characteristics in SVZ between RRMS patients, PMS patients and healthy controls (HC)

(II) investigate whether SVZ microstructural characteristics may help predict the volume of caudate nucleus - that is in the vicinity of the SVZ - and of thalamus - as representative of another well-defined grey matter area which is further from SVZ than caudate nucleus; we chose to conduct this analysis in order to exclude that the possible association between the damage of the SVZ and that of caudate nucleus was non-specific and driven by a global NAWM damage and/or a diffuse brain atrophy;

(III) investigate whether SVZ microstructural characteristics' correlate with patients' disability status.

Study design

Population

A total of 151 patients (101 RRMS, 50 PMS) and 20 sex- and age-matched HC were prospectively enrolled. The PMS population included both primary (n = 32) and secondary (n = 18) PMS patients. Inclusion criteria for patients were (I) age 18–70 years (II) MS diagnosis according to the 2017 revisions to McDonald's criteria[111] and (III) Expanded Disability Status Scale (EDSS)[12] score ≤ 7. For HC, only the criterion (I) was required. Exclusion criteria for all subjects were (I) other neurological comorbidities and (II) contraindications to MRI. All patients underwent neurological examination with the assessment of the EDSS score. On the same day, all subjects underwent brain MRI.

MRI acquisition

All patients underwent MRI on a Siemens Prisma 3 T scanner (Erlangen, Germany) with a 64-channel head and neck coil. The MRI protocol included: (i)

3D sagittal T2-FLAIR (176 slices, repetition time/inversion time/echo time (TR/TI/TE): 5,000/1,800/393 ms; resolution 0.4 × 0.4 × 1 mm3); (ii) 3D sagittal T1 MPRAGE (208 slices, TR/TI/TE: 2,300/919/2.96 ms; resolution 1 × 1 × 1 mm3;); (iii) twice-refocused spin echo echo-planar imaging sequence for multi-shell diffusion-weighted images (80 slices, TR/TE: 4,500/75 ms; distributed in 5 shells with b-value = 300, 700, 1,000, 2,000, 3,000 s/mm2 in 3, 7, 16, 29, 46 directions each, plus 7 b-value = 0 images acquired with both anterior–posterior and posterior–anterior phase encoding directions; spatial resolution 1.8 × 1.8 × 1.8 mm3).

MRI analysis

Lesions and SVZ segmentation: FLAIR and T1 lesions were manually segmented using Jim software (Jim 7.0, Xinapse System; http://www.xinapse.com), creating FLAIR and T1 lesion masks, respectively. Given the anatomical information provided in Cherubini et al.[112] we segmented a mask of SVZ on high-resolution T1-weighted images in a standard space (Montreal Neurological Institute space) and then non-linearly co-registered on native T1- and diffusion-weighted images through FSL non-linear registration tool [FNIRT[113]]. We then obtained the normal appearing SVZ tissue (NA-SVZ) by masking out the volume occupied by FLAIR lesions. Thalamus and Caudate subcortical structures were segmented using FIRST[114]. Finally, to avoid any overlap between the masks, all segmentations were then checked on native T1 of each subject. Total intracranial volume (TIV) and grey matter (GM) volume were obtained using CAT12, part of SPM.

Diffusion processing: Diffusion MR images were first denoised using the Marchenko-Pastur principal component analysis algorithm[115] available in MRtrix3[116]. Then they were corrected for movement artifacts and susceptibility induced distortions using eddy and top-up commands from FMRIB Software Library (FSL; [117–119]). As last step of pre-processing we also performed B1 field inhomogeneity correction to all the dMRI volumes[120]. To compute the microstructural maps derived from SMT model, we used the open-source code available at https://github.com/ekaden/smt. To improve the registration of structural masks in diffusion space, once the SMT maps were obtained we up-sampled them from original resolution of 1.8 × 1.8 × 1.8 mm3 to the higher T1 resolution (1x1x1 mm3); we simply regrid the SMT maps to match T1 resolution without interpolation to reduce registration errors. Then, diffusion weighted

images were rigidly registered on T1- weighted images using FLIRT with boundary-based registration[121], and the resulting transformations were inverted and applied to the masks to register them in the diffusion weighted image space. All the registrations were visually checked and eventually edited by a trained professional with more than 5 years of experience in neuroimaging to avoid mislabeling of clear CSF voxels. Finally, we extracted the mean values inside global SVZ, SVZ-NA, NAWM, caudate and thalamus of the following SMT metrics: the microstructural maps of neurite signal fraction (INTRA), extra-neurite transverse diffusivity (EXTRATRANS), and extra-neurite mean diffusivity (EXTRAMD) that describe the intracellular compartment, the anisotropic extra-neurite compartment including its transverse microscopic diffusivity and the mean diffusion outside the axons, respectively [122,123] .

Statistical analysis

Demographic differences between groups were analyzed using Chi-square, Mann–Whitney and independent samples t-test where appropriate. Differences in terms of MRI metrics between RRMS, PMS patients and HCs were assessed by analysis covariance (ANCOVA) adjusting for age and gender; for volumes comparison, total intracranial volume (TIV) was added to the covariates; for the comparison of each SMT metric within NA-SVZ between groups, analyses were also adjusted for the average microstructural damage in the NAWM. Bonferroni corrected post-hoc analyses (to adjust for multiple comparisons) were performed. Multivariable linear regression models adjusted for age and gender explored associations between normal appearing SVZ microstructural metrics and the ratio of caudate and thalamus volumes with total GM volume in the global MS population and in RRMS or PMS patients, separately, as well as in the HC group; analyses regarding patients were additionally adjusted for FLAIR lesion volume. In line with the literature (Chard et al., 2002), we chose to explore the association of NA-SVZ microstructural injury with caudate/GM and thalamus/GM ratio (calculated as the ratio between caudate and thalamus nuclei volume - respectively – and total GM volume) instead of the volume of the single nuclei to account for the relationship between total GM and the volumes of caudate and thalamus. Partial Spearman correlation models explored the association between SVZ microstructural characteristics and EDSS, adjusting for age and gender. All *p*-

values were two-sided and considered statistically significant when $p \leqslant 0.05$. *p*-values after Bonferroni correction are provided for the comparisons of MRI metrics between groups. Given their exploratory nature, other analyses were not adjusted for multiple comparisons. SPSS 22 (IBM; version 22.0) was used for computation.

Population characteristics

Demographic and clinical data are reported in Table 1-2.2.2. A total of 151 patients (101 RRMS and 50 PMS; 99 female; mean age 43 ± 11 years, mean disease duration 43 ± 9 years; median EDDS 2.5) and 20 HC (11 female; mean age 42 ± 13.6 years) were included. Although the global MS population and HC were matched in terms of age and gender, as expected gender composition and age differed between the three groups, as the PMS population had a higher percentage of male patients and older age as compared to other groups; these variables were consequently included as a covariate in all the analyses comparing groups. As expected, progressive patients presented higher EDSS scores than relapsing subjects ($p < 0.0001$). Disease duration was similar between the two groups of patients.

Table 1-2.2.2: Demographics and clinical characteristics.

	MS *N*=151	RRMS *N*=101	PMS *N*=50	HC *N* =20		
Demographics					*p*-values*	*p*-values**
Age, mean (SD), y	43 (11.6)	39 (10.5)	51 (8.6)	42 (13.6)	<0.0001	HC vs. RRMS: 0.748 HC vs. PMS: 0.001 RRMS vs. PMS: <0.001
Female, no (%)	99 (66%)	74 (73%)	25 (50%)	11 (55%)	0.01	HC vs. RRMS: 0.103 HC vs. PMS: 0.705 RRMS vs. PMS: 0.005
Clinical characteristics					*p*-values***	
Disease duration, mean (SD), y	11 (8.8)	10 (8.3)	12 (9.7)	-	0.2	-
EDSS score at baseline, median (range)	2.5 (0–7)	2 (0–6.5)	4.5 (1.5–7)	-	<0.0001	-

RRMS, relapsing–remitting multiple sclerosis; PMS, progressive multiple sclerosis; HC, healthy controls; SD, standard deviation; y, years; EDSS, expanded disability status scale.**p*-values for the RRMS vs. PMS vs. HC comparison; ANOVA (age), Chi-square (gender).
***p*-values for the single groups comparison; Bonferroni corrected post-hoc analyses of ANOVA (age), Chi-square (gender).
****p*-values for the RRMS vs. PMS comparison; Mann–Whitney (disease duration, EDSS).

MRI characteristics in HC, RRMS, and PMS patients

While no differences in global SVZ and SVZ-NA volumes between HC, RRMS and PMS emerged at ANCOVA analyses ($p = 0.188$ and $p = 0.145$, respectively), as expected caudate and thalamus nuclei volumes differed between HC, RRMS and PMS patients ($p = 0.016$ and $p < 0.0001$, respectively). Post-hoc analysis

showed statistically significantly smaller caudate and thalamus volumes in PMS ($p = 0.013$ and $p < 0.0001$, respectively) and smaller thalamus volume in RRMS ($p = 0.001$) patients with respect to HC. FLAIR lesion volumes were, as expected, higher in PMS than in RRMS patients; however, such difference did not reach statistical significance.

As per microstructural characteristics, we observed that EXTRAMD, EXTRATRANS and INTRA metrics within SVZ-NA were different among HC, RRMS and PMS patients ($p = 0.002$, $p < 0.0001$ and $p = 0.009$ respectively). At post-hoc analysis, EXTRAMD was higher in PMS with respect to RRMS and HC ($p = 0.017$ and $p = 0.003$ respectively), EXTRATRANS was higher in PMS with respect to RRMS and HC ($p = 0.005$ and $p = 0.001$ respectively), INTRA was lower in PMS with respect to HC ($p = 0.008$). When considering the total NAWM, EXTRATRANS and INTRA significantly differed between groups ($p = 0.017$ and $p = 0.015$, respectively), while EXTRAMD did not ($p = 0.124$); at post-hoc analysis only a statistically significant difference between RRMS and PMS patients in terms of INTRA ($p = 0.032$) emerged.

In the caudate, EXTRATRANS was the only SMT metric which differed between HC, RRMS and PMS patients ($p = 0.042$); no differences in EXTRAMD and INTRA metric were found ($p = 0.055$ and $p = 0.071$ respectively); no statistically significant differences emerged at post-hoc analysis. All SMT metrics in the thalamus significantly differed between groups (EXTRAMD $p = 0.012$; EXTRATRANS $p = 0.002$; INTRA $p < 0.0001$). Similarly to SVZ-NA, post-hoc analyses showed higher EXTRAMD and EXTRATRANS and lower INTRA in PMS patients as compared to HC ($p = 0.014$, $p = 0.001$ and $p < 0.0001$, respectively); INTRA was lower in PMS also with respect to RRMS ($p = 0.002$).

Figure 1-2.2.2: Selected examples of axial slice in a healthy control, a RRMS and a PMS patient. On the left ***(A)*** *a selected axial slices from T1-weighted image showing segmented masks of SVZ (yellow), caudate (red), and thalamus (light blue). On the right* ***(B)*** *representative axial slices of EXTRAMD (top; 10^{-3} mm2/ms), EXTRATRANS (center; $10^{-}3$ mm2/ms), and INTRA (bottom) maps in a HC, a RRMS and a PRS patient. *; **p-values referring to the analyses performed on the global population (*p < 0.05 and **p < 0.01).*

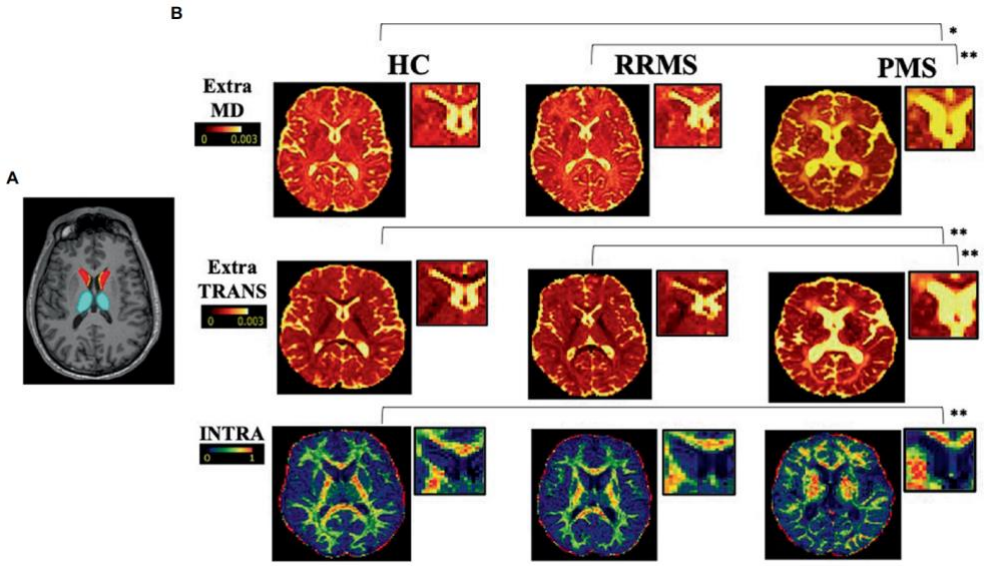

HC=healthy control; RRMS=relapsing–remitting multiple sclerosis; PMS=progressive multiple sclerosis;

Correlation of SVZ microstructural characteristics with caudate and thalamus nuclei volume

Given the difference observed in terms of SMT metrics between HC and different groups of patients, we sought to investigate whether such microstructural properties were associated with the volumes of caudate and thalamus nuclei (expressed as fractions between caudate/thalamus and total GM volume). Results of the analyses exploring this association are shown in Table 2-2.2.2.

Considering the global population, the multivariable model exploring NA-SVZ metrics as predictors of caudate/GM volumes' ratio was able to explain approximately 20% of the variance in the outcome (R2 0.21, $p < 0.0001$), being INTRA the only microstructural metric of the SVZ independently contributing to the model ($p = 0.035$). When analyses were restricted to RRMS patients the model remained statistically significant (R2 0.3, $p < 0.0001$), and we found that all the SMT metrics were significantly associated with the outcome (EXTRAMD $p = 0.025$, EXTRATRANS $p = 0.028$, INTRA $p = 0.015$). When analyses were restricted to PMS patients, the model was not statistically significant ($p = 0.448$). Applying the same multivariate models, none of the SMT metrics of the NA-SVZ

appeared to be significantly associated with thalamus/GM ratio in the global population, nor when analyzing RRMS and PMS patients separately. The same analyses performed in the HC population found no associations between SMT metrics of NA-SVZ and caudate/GM (p value of the model: 0.126) or thalamus/GM (p = 0.100) ratio volumes.

Table 2-2.2.2: Multivariate analyses exploring the association between NA-SVZ microstructural properties and caudate and thalamus GM ratio.

	Caudate/GM ratio		Thalamus/GM ratio	
HC (*n*=20)				
	B (95% CI)	*p* value	B (95% CI)	*p* value
EXTRAMD	−51838.31 (−134827.50–31150.88)	0.202	−108840.13 (−230249.9–12569.65)	0.075
EXTRATRANS	58918.21 (−32080.55–149916.98)	0.187	119826.76 (−13300.71–252954.35)	0.074
INTRA	55.82 (−24–26 – 135.91)	0.157	120.25 (3.09–237.42)	0.054
Total Cohort (*n*=151)				
	B (95% CI)	*p* value	B (95% CI)	*p* value
EXTRAMD	−15164.21 (−31409.17 – −1080.74)	0.067	−1834.49 (−29149.14–25840.15)	0.895
EXTRATRANS	16276.21 (−1315.43–33867.84)	0.070	371.84 (−29207.14–25480.83)	0.980
INTRA	17.23 (1.27–33.19)	0.035	5.84 (−20.00–32.68)	0.667
RRMS (*n*=101)				
	B (95% CI)	*p* value	B (95% CI)	*p* value
EXTRAMD	−21022.17 (−39363.11 – −2681.22)	**0.025**	4415.65 (−24877.48–33708.78)	0.765
EXTRATRANS	22578.48 (2512.08–42644.87)	**0.028**	−7426.52 (−39475.44–24622.39)	0.647
INTRA	22.41 (4.41–40.41)	**0.015**	−1.36 (−30–11 – 27.38)	0.925
PMS (*n*=50)				
	HR (95% CI)	*p* value	B (95% CI)	*p* value
EXTRAMD	3092.43 (−35574.22–41759.08)	0.873	19275.51 (−50362.36–76313.38)	0.682
EXTRATRANS	−2448.31 (−43604.95–38780.32)	0.905	−13475.68 (−80892.27–53940.91)	0.689
INTRA	2.94 (−34.51–40.40)	0.875	−1.87 (−62.23–59.49)	0.951

n = number; B = non standardized coefficient; 95% CI = confidence intervals; GM = grey matter; RRMS = relapsing–remitting multiple sclerosis; PMS = progressive multiple sclerosis; NA-SVZ = normal appearing sub-ventricular zone. Statistically significant *p*-values are reported in bold.

Correlations between SVZ microstructural characteristics and patients' disability status

Considering the global population, we observed a statistically significant correlation between EXTRAMD and EXTRATRANS of the NA-SVZ and EDSS (r = 0.25, p = 0.003 and r = 0.24, p = 0.003, respectively). The correlation between NA-SVZ EXTRAMD/EXTRATRANS and EDSS remained significant even when considering only RRMS patients (r = 0.20, p = 0.044 and r = 0.21, p = 0.039, respectively), but none of the microstructural characteristics of the SVZ significantly correlated with EDSS in PMS patients. A graphical representation of these correlations is reported in Figure 2-2.2.2.

Figure 2-2.2.2.: Scatter plot showing associations between (A) EXTRATRAMD of the NA-SVZ and EDSS; (B) EXTRATRANS of the NA-SVZ and EDSS; and (C) INTRA of the NA-SVZ and EDSS. EDSS = expanded disability status scale; RRMS = relapsing–remitting multiple sclerosis; PMS = progressive multiple sclerosis; NA-SVZ = normal appearing sub-ventricular zone Axes represent residuals. Linear fit and 95% confidence intervals are shown

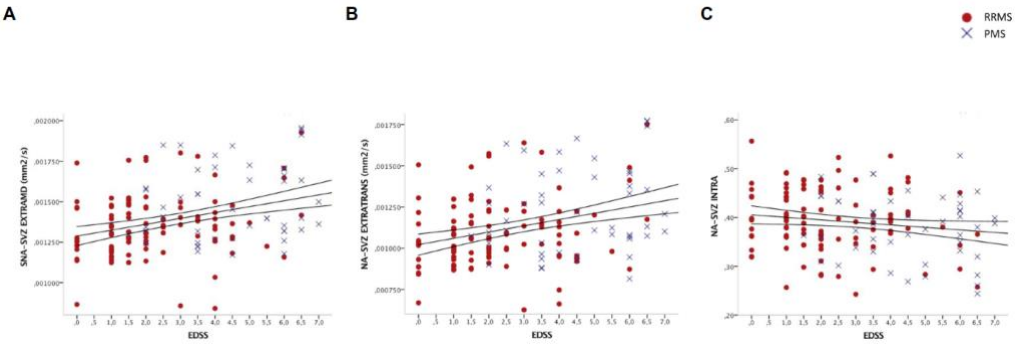

Discussion

In animal models, SVZ is recognized as an area that might contribute to CNS regeneration following tissue damage, exerting both neurogenic and neuroprotective functions through the proliferation, differentiation and maturation of neural cell precursors among which OPCs, the release of soluble molecules (neurotrophic cytokines/growth factors) that act on the survival of local oligodendrocytes, and by modulating microglia [109,110]. In humans, SVZ functions are known to decline during brain development and aging. Nevertheless, accumulating evidence suggest that adult human SVZ might represent a site of major modifications in response to neurological diseases, thanks to SVZ-derived precursor cells recruitment into remyelinating oligodendrocytes and SVZ-mediated secretion of soluble neuroprotective molecules. It suggests that SVZ impairment might have a role in neurodegenerative processes [124]. However, most data derive from animal studies or in-vitro characterization of SVZ. Indeed, in-vivo characterization of SVZ is very challenging, possibly due to the limited resolution of MRI images which prevents the possibility of isolating the small cellular layers such as those that compose the SVZ[112]. Against this background, in a recent paper Cherubini et al. were able to radiologically characterize the SVZ microstructural damage in patients with dementia, and more specifically reported a progressive increase of mean diffusivity, reflecting a defect in neurogenesis, in the SVZ of patients with mild cognitive impairment and AD[112]. Given the paucity of information available regarding MRI correlates of SVZ in MS, the main

objective of the present study was to obtain an in vivo-characterization of macro- (i.e. volume) and microstructural (i.e. SMT metrics) injury of the SVZ in MS patients and to explore the clinical implications of such damage. The hypotheses that (I) a microstructural disruption in the SVZ characterizes MS patients, (II) that these alterations are even more evident in the progressive stages and (III) that such microstructural injury correlate with caudate nucleus volume and clinical disability are supported by the results of our study. Indeed, we observed statistically significant differences in all SMT metrics when comparing HC, RRMS and PMS, and specifically we observed a continuous increase (HC<RRMS<PMS) in EXTRAMD and EXTRATRANS, and a decrease (HC>RRMS>PMS) for INTRA. In the healthy brain, the SVZ consists of an ependymal layer, a gap region and an astrocytic ribbon, and it is separated from the caudate nucleus and the striatum by a layer of myelin; it contains three different cell types (types A, B and C) that are organized in a specific pattern, with the type A cells closest to the ependymal layer, the type B cells forming the astrocytic ribbon and the type C cells located close to the myelin layer and the striatum [125]. An interconversion of cell types has been shown to occur in different neurodegenerative diseases [125], and an infiltration of T cells in the SVZ of aging human brains, both under non-pathological conditions and in neurodegenerative contexts (as it could be considered progressive MS) has been demonstrated [126]. The variations in terms of SMT metrics that we observed during the different phases of MS might reflect similar pathological processes, being suggestive of higher free water content (higher EXTRAMD, indirectly reflecting ongoing inflammatory processes), cytoarchitecture disruption and astrogliosis (higher EXTRATRANS and lower INTRA, indirectly reflecting a higher degree of cellular damage and fiber disruption). The choice to use SMT to investigate the possible pathological substrate of SVZ injury in different phases of MS relied on its interesting basic assumptions and its encouraging recent results in MS [122,127,128]. Overcoming the issue represented by the fixed intrinsic diffusivity of other multicompartment models [128], SMT considers WM as a two-compartment (intra- and extra-axonal) tissue and provides signal fraction and diffusion metrics per axon without confounds from fiber direction, crossing, or dispersion [122]. This model provided validation against axonal histology in the tuberous sclerosis animal model, which is more suitable for detecting CNS axonal injury than the

MS animal model because it is free from the inflammatory component. Importantly, SMT has been shown to reliably quantify axonal content without artifactual effects from fiber-crossing and orientation dispersion. Since such model is applicable to any condition affecting myelin and axonal integrity, SMT has been already applied in vivo in different studies focusing on the brain [129]and spinal cord (By et al., 2018) of MS patients, demonstrating to be helpful in differentiating MS lesions damage from the NAWM as well as the NAWM of MS patients from that of healthy subjects [128] and in characterizing pathological features within MS lesions [130]. Overall, our findings showed a certain degree of tissue disruption characterizing the SVZ region of MS patients, and a more evident damage in the progressive as compared to the relapsing phases of MS. Interestingly, in the caudate and thalamus nuclei a similar microstructural damage together with reduced volumes (HC>RRMS>PMS) were both observed. However, similarly to Cherubini et al [112], we found no significant change in the volume of SVZ between the groups of patients. Although the mis-segmentation of the periventricular white matter could be one of the possible explanations (due to the previously mentioned limited resolution of MRI), considering our results we could also speculate that microstructural alterations reflecting tissue dysfunction within the SVZ might precede its atrophy. Although older age in PMS patients could be a possible confounding factor, since neurogenesis in humans is known to decline with increased age, it is worth noting that all our analyses were adjusted for age. Moreover, the two groups of patients did not differ in terms of disease duration. Thus, although still preliminary, our findings seem to indicate that microstructural SVZ involvement is related to disease stage. This is in line with recent results of Bodini et al [46] who found a borderline impact of age on dynamic remyelination as assessed with positron emission tomography (PET) and no significant effect for disease duration. Our results contribute to an ongoing debate regarding the relationship between neuro-repair potential, age and disease duration [46,47,131,132]. Once we characterized the microstructural alterations of SVZ, we sought to investigate whether they were associated with lower volumes of other deep nuclei. Indeed - in normal conditions - SVZ heterogeneous cells are maintained in an environment that is permissive to gliogenesis with neuroprotective potentialities, and responds to neurodegenerative insults in adjacent brain regions by increasing progenitor cell proliferation in an attempt to

limit the process of neurodegeneration [125]. The capacity of SVZ progenitor cells to proliferate, migrate and exert their neurogenic effect in favour of the caudate nucleus has been demonstrated in only animal models of Huntington's disease [125]. In humans, and particularly in an MS context, the SVZ response to nearby occurring insults is potentially restricted to gliogenesis and production of neurotrophic factors. We thus speculated that the microstructural damage that we observed in MS patients could impact SVZ protective functions. Considering the SVZ position, we expected to find a stronger association with caudate rather than with thalamus volumes, since the first is closer to the SVZ. Our findings confirmed the hypothesis and pointed at INTRA as the SMT metric with the strongest association with caudate volume. Indeed, lower INTRA values within the NA-SVZ - indirectly reflecting an abnormal cytoarchitecture and astrogliosis – was significantly associated with lower caudate volumes. These findings were confirmed in analyses restricted to RRMS but not to PMS patients, suggesting that a more severe microstructural damage (as we observed in PMS vs RRMS patients) might account for a loss of SVZ capability to enhance neuroprotection.

In parallel to its neuroprotective functions, SVZ in supposed to have a role in remyelination [131,133]. Accordingly, we speculated that the SVZ tissue damage could be one of the processes that affect remyelination efficiency in MS, especially in its progressive phases. Remyelination failure necessarily contribute to the progressive disability that characterizes the later stage of MS. Accordingly, we sought to investigate the correlation between SVZ microstructural characteristics and global disability. We decided to use EDSS as it represents the most widely used measure to assess clinical disability, thus indirectly reflecting the capacity of patients to recover from relapses. In a recently published paper [46], Pittsburgh compound B ([11C]PiB) PET was shown to allow quantification of myelin dynamics in MS and to enable stratification of patients depending on their individual remyelination potential. Importantly, authors showed that the index of dynamic remyelination was strongly associated with EDSS scores in relapsing MS patients, suggesting that an efficient remyelination process is one of the discriminating factors in determining a better prognosis in MS. In line with this hypothesis, we observed a significant correlation between SVZ microstructural properties and patients' disability status (higher EXTRAMD and EXTRATRANS - indirectly reflecting more inflammation and cell disruption - positively

correlated with EDSS scores), which was maintained in RRMS but not in PMS patients. Our findings are in line with the observations of Rasmussen et al [134], who showed that in a relapsing model of experimental autoimmune encephalomyelitis (EAE), the neural stem cells (NCS) became activated and initiated regeneration during the acute disease phase, but lost this ability during the chronic phase [134]. Various mechanisms have been proposed to enhance NSCs proliferation and mobilization, and consequently promote tissue repair [107,135,136] in murine model of MS. However, when it comes to patients, enhancing neuroprotection and neurorepair remains an important, but still elusive, therapeutic goal.

The main limitation of our study is that, given the cross-sectional nature of the study, we cannot exclude the SVZ alterations are a single epiphenomenon of the diffuse damage of the NAWM and that they do not actually reflect a greater/lesser ability to remyelinate. However, the microstructural alterations we found in the area of SVZ were stronger as compared to those observed in the global NAWM, suggesting that our results could be just partly explained by a non-specific global NAWM damage and/or a diffuse brain atrophy. Another important limitation represented by the risk of erroneous identification of SVZ due to its small size and location on MRI images, as an effect of partial volume. In fact, even if we up-sampled the diffusion weighted images to avoid mislabeling due to registration, the original resolution at which the maps were computed was 1.8 mm isotropic so some voxels might still be affected by partial volume. Other limitations of our study are the lack of spinal cord images, which could strongly affect the disability status, and the relatively small sample size. Lastly, the evidence for neurogenesis in the SVZ beyond infancy in humans remains limited, although some data suggesting the capacity of the adult human SVZ to generate mature astrocytes are reported in the literature [103]. Our findings need to be confirmed by larger analyses, which should include longitudinal data. Assessing the correlation between SVZ measures and lesion characteristics (number, volume and distribution) would be also of added value to further elucidate the role of SVZ in MS patients.

Although there are limitations to our analyses, our data suggest that the SVZ injury as assessed with MRI is evident in all phases of MS and becomes even more evident with disease progression. Moreover, based on our exploratory and still preliminary findings, we might speculate that such microstructural injury reflects

a loss of SVZ function resulting in compromised neuroprotection and neurorepair, possibly contributing to disease progression.

In conclusion, despite the reported limitations, we believe that our results may contribute to elucidate mechanisms underlying neuroprotection and tissue repair. The advent of new therapeutical strategies with the potential to promote remyelination requires the identification of patient-specific factors that may influence the response and the optimal therapeutic window for neurorepair. The advanced diffusion MRI modeling used in the present study might not only provide novel insight for understanding the pathophysiology of MS, but possibly also enable stratification and monitoring of patients based on their neurorepair potential for current and experimental treatments choice.

2.3. Aim 2: Assessing the role of different clinical and paraclinical biomarkers in the context of treatment response

2.3.1 Predictors of Ocrelizumab Effectiveness in Patients with Multiple Sclerosis

Abstract

Objectives: The aim of our study was to provide effectiveness and safety data of ocrelizumab treatment in patients with relapsing–remitting (RR-) and progressive MS (PMS) and to evaluate clinical and immunological predictors of early treatment response.

Methods: In this single center prospective observational study, we investigated effectiveness outcomes (time-to-confirmed disability worsening, time-to-first relapse, time-to-first evidence of MRI activity and time-to-first evidence of disease activity), and clinical and immunological predictors of early treatment response.

Results: One hundred and fifty-three subjects were included (93 RRMS; 84 females). Median follow-up was 1.9 (1.3–2.7). At 2-year follow-up (FU), disability worsening-free survival were 90.5%, 64.7%, and 68.8% for RRMS, primary-progressive MS (PPMS), and secondary-progressive MS (SPMS) patients, respectively. At 2-year FU, 67.1%, 72.7%, and 81.3% of patients with RRMS, PPMS, and SPMS were free of MRI activity, with NEDA3 percentages of 62.1%, 54.6%, and 55.1%, respectively. Lower baseline EDSS was independently associated with a reduced risk of disability worsening [HR (95%CI) = 1.45 (1.05–2.00), p = 0.024] and previous treatment exposure was independently associated with increased probability of radiological activity [HR (95%CI) = 2.53 (1.05–6.10), p = 0.039]. At 6-month FU, CD8 + cell decrease was less pronounced in patients with inflammatory activity (p = 0.022).

Conclusions: Our findings suggest that ocrelizumab is an effective treatment in real-world patients with RRMS and PMS. Better outcomes were observed in treatment-naïve patients and in patients with a low baseline disability level. Depletion of CD8 + cells could underlie early therapeutic effects of ocrelizumab.

Scientific rationale and study endpoints

Post-marketing studies exploring the onset of efficacy after treatment commencement and the clinical and immunological variables associated with outcomes are warranted, especially for patients with highly active forms of MS and advanced progressive MS. Providing these data can be particularly relevant in order to identify "biological-based" biomarker that can help in patients' clinical characterization and future treatment selection.

Ocrelizumab is a B-cell depleting drug recently approved for the treatment of MS. Phase III clinical trials have shown significant benefits of ocrelizumab use in terms of clinical and MRI outcomes in relapsing–remitting (RR)[137] and primary-progressive (PP) MS[20], along with a manageable safety profile. However, data regarding its use in the post-marketing setting are still sparse. Complementing the results of phase III clinical trials with observational data referring to an "unselected cohort" is critical in order to achieve information that could be transferred to real-life scenarios.

Accordingly, the primary objective of our study was to determine time-to-first relapse, time-to-confirmed disability worsening, time-to-first evidence of MRI activity, and time-to-first evidence of disease activity (according to the NEDA3 definition) in real-life patients treated with ocrelizumab.

Secondary outcomes were to (i) assess efficacy outcomes in patients with recent high disease activity and those with a relatively high disability at ocrelizumab commencement, and (ii) assess clinical and immunological predictors of early inflammatory activity based on flow-cytometry immune subsets characterization during ocrelizumab therapy.

Study design

This is an observational prospective single-center cohort study conducted at the MS Center of the University of Genoa, IRCCS Ospedale Policlinico San Martino, evaluating effectiveness and safety of ocrelizumab therapy for the treatment of RRMS and PMS. Ocrelizumab was prescribed and administered by the treating physician to relapsing forms of MS and early PPMS according to regulatory policies. From March to June 2020, due to coronavirus disease 2019 (COVID19) pandemic, ocrelizumab was administered following a tailored approach evaluating the profile risk of each, according to international indications. All

patients were clinically evaluated every 3 months for assessment of effectiveness and safety. One-hundred forty-five patients (95%) underwent baseline and follow-up MRI scans at our institution with a standardized 3-T MRI protocol (Siemens PRISMA). A subset of patients (n = 73) underwent serial blood samples at our institution every 6 months, before ocrelizumab infusion, for lymphocyte profiling and immunoglobulin concentration.

Baseline brain MRI (acquired within 3 months before ocrelizumab start) was the pre-treatment reference scan for assessment of treatment failure. As exploratory analyses, re-baseline of MRI activity was performed 100 and 180 days after ocrelizumab start. Recent highly active MS was defined, based on the criteria proposed by Rush et al.[138], as the presence of MRI activity and at least one relapse in the year before ocrelizumab start in patients with accelerated accrual of disability (EDSS $\geq$ 4.0). Early inflammatory activity was defined as the occurrence of MRI inflammatory activity or a relapse within the first 12 months of treatment. All the analyses were performed on the global cohort of patients and, as sensitivity analyses, in the cohort of patients with RRMS and PMS separately.

Statistical analyses

Descriptive results were reported as mean with standard deviation (SD) or median with interquartile range (IQR). The probability of disability worsening-free survival, relapse-free-survival, MRI activity-free-survival, and NEDA-3 status was calculated with the Kaplan–Meier estimator. Univariate and multivariate analyses assessing the association of demographic- and disease-related characteristics with survival endpoints were performed using Cox proportional hazards regression analysis models. Variables significantly associated with each outcome event on univariate analysis were included as covariates in the multivariate model. Differences in lymphocyte subpopulations at different timepoints were assessed with analysis of covariance, adjusting for age, sex, MS phenotype, and last DMT before ocrelizumab initiation. Correction was made for multiple comparisons (Bonferroni-p = 0.0028). Univariate and multivariate binary logistic regression analyses were used to explore the predictive role of clinical and immunological variables in terms of early inflammatory activity. A time*early treatment response group interaction was included into a linear mixed model with random intercept and random slope to test differences on lymphocyte subset

values time trend between patients with and without early inflammatory activity. A two-sided $p < 0.05$ was used for statistical significance. SPSS 23 (IBM; version 23.0) and R software (version 4.0.3) were used for computation.

Population characteristics

One hundred and fifty-three consecutive MS patients (93 RRMS, 43 PPMS and 17 relapsing, secondary-progressive (SP) MS) initiated treatment with ocrelizumab at the MS Center of the University of Genoa, IRCCS Osepdale Policlinico San Martino, from July 2017 to July 2020. Demographic- and disease-related characteristics at ocrelizumab start are reported in Table 1-2.3.1.

Table 1-2.3.1: Demographic and clinical characteristics

	Total cohort (*n* = 153)	**RRMS** (*n* = 93)	**Progressive-MS**		
			PPMS (*n* = 43)	**SPMS** (*n* = 17)	**Total PMS** (*n* = 60)
Females, *n* (%)	84 (54.9)	60 (64.5)	20 (46.5)	4 (23.5)	24 (40.0)
Age, mean (SD), y	41.9 (11.4)	36.9 (10.2)	49.2 (8.6)	50.6 (8.2)	49.6 (8.4)
Disease duration, mean (SD), y	10.3 (9.9)	9.3 (9.2)	8.4 (6.5)	20.8 (14.7)	11.9 (11.0)
EDSS, median (IQR)	3.5 (2–5.5)	2 (2–3.5)	5.5 (3.5–6.5)	6 (5–6.5)	6 (3.5–6.5)
Number of relapses in previous 12 months, mean (SD)	0.5 (0.7)	0.8 (0.7)	-	0.2 (0.4)	0.1 (0.2)
MRI activity at ocrelizumab start, *n* (%)	91 (59.5%)	75 (81.5)	9 (21.4)	7 (41.2)	16 (27.1)
Number of previous treatment, median (IQR)	1 (0–2)	1 (0–3)	1 (0–1)	1 (1–3)	1 (0–2)
Naïve patients, *n* (%)	46 (30.1)	25 (26.9)	18 (41.9)	3 (17.6)	21 (35.0)
Previous exposure to high efficacy DMT, *n* (%)	58 (54.2)	44 (64.7)	7 (28.0)	7 (50.0)	14 (35.9)
Last DMT, *n* (%)					
Interferon	12 (7.8)	7 (7.5)	4 (9.3)	1 (5.9)	5 (8.3)
Glatiramer acetate	10 (6.5)	4 (4.3)	3 (7.0)	3 (17.6)	6 (10.0)
Fingolimod	26 (17)	24 (25.8)	1 (2.3)	1 (5.9)	2 (3.3)
Dimethyl fumarate	13 (8.5)	6 (6.5)	5 (11.6)	2 (11.8)	7 (11.7)
Teriflunomide	4 (2.6)	4 (4.3)	0 (0)	0 (0)	0 (0)
Natalizumab	9 (5.9)	6 (6.5)	0 (0)	3 (17.6)	3 (5.0)
Alemtuzumab	11 (7.2)	10 (10.8)	0 (0)	1 (5.9)	1 (1.7)
Cladribine	2 (1.3)	2 (2.2)	0 (0)	0 (0)	0 (0)
Other	20 (13.1)	5 (5.4)	12 (27.9)	3 (17.6)	15 (25)
Time from DMT discontinuation to ocrelizumab start, median (IQR), d	68 (30–501)	60 (25–112)	335 (81–1157)	859 (132–2158)	452 (99–1228)
Highly active MS, *n* (%)	17 (11.1)	14 (15.1)	-	3 (17.6)	3 (5.0)
Advanced MS, *n* (%)	66 (43.1)	22 (23.7)	30 (69.8)	14 (82.4)	44 (73.3)
Follow-up, median (IQR), y	1.9 (1.3–2.7)	1.6 (1.11–2.03)	2.5 (2.0–3.0)	2.0 (1.2–2.7)	2.3 (1.8–2.99)

RRMS relapsing–remitting multiple sclerosis, *PPMS* primary-progressive multiple sclerosis, *SPMS* secondary progressive multiple sclerosis, *PMS* progressive multiple sclerosis, *n* number, *SD* standard deviation, *IQR* interquartile range, *EDSS* expanded disability status scale, *DMT* disease-modifying therapy

Outcomes

Fig 1-2.3.1 (panel A–F) reports the results of the primary outcome.

At 2-year FU, 90.5% of patients with RRMS, 64.7% of patients with PPMS, and 68.8% of patients with SPMS were free of disability worsening. Two out of five patients with RRMS who experienced disability worsening had highly active MS and 5/5 experienced progression independent of relapse activity.

A total of 95.1% patients with RRMS were free of relapses at 2-year FU. Four patients had a single relapse at + 27, + 72, + 103, and + 520 days, respectively. In the RRMS cohort, pre-treatment annualized relapse rate (ARR) was 0.78 (0.70), 1-year FU ARR was 0.04 (0.18), and 2-year FU ARR was 0.04 (0.21).

At 2-year FU, 67.1% RRMS patients, 81.3% PPMS patients, and 72.7% SPMS patients were free of MRI evidence of disease activity. After a 100-day re-baseline of MRI activity, percentages of patients without MRI activity increased to 82.1%, 83.8%, and 72.7% for RRMS, PPMS, and SPMS patients respectively. After a 180-day re-baseline, percentages increased to 92.1%, 88.4%, and 83.1%.

Male sex, RRMS phenotype, previous exposure to DMT, and baseline active MRI were associated with an increased risk of MRI activity during ocrelizumab therapy. At multivariate analysis, patients previously treated with a DMT had an increased risk of MRI activity (HR (95%CI) = 2.53 (1.05–6.10), p = 0.039). Among 21 patients who experienced MRI inflammatory activity within 180 days, only 1 patient had further MRI activity at + 520 days.

At 2-year FU, NEDA-3 percentages were 62.1%, 54.6%, and 55.1% for RRMS, PPMS, and SPMS respectively. After a 100-day re-baseline of MRI activity, NEDA-3 percentages increased to 71.9%, 71.4%, and 57.9% respectively. NEDA-3 rates after a 180-day rebaseline were 77.1%, 71.9%, and 67.3% for RRMS, PPMS, and SPMS respectively. Naïve patients had a higher probability of achieving NEDA-3 status (HR 0.48 (0.25–0.94), p = 0.032) (Fig 1-2.3.1, panel H).

Patients with Baseline EDSS ≥ 4 and with Highly Active MS

Patients with baseline EDSS ≥ 4 at ocrelizumab start had a higher risk of disability worsening (disability worsening-free survival 60.1% vs 94.1%, HR = 8.16 (2.81–23.7), p < 0.0001) and lower NEDA-3 rates (43.4% vs 70.1%, HR = 1.90 (1.11–3.24), p = 0.019) compared to patients with baseline EDSS < 4 (Fig 1-2.3.1, panel G).

Patients with highly active MS had a higher risk of persistent MRI inflammatory activity (MRI-free survival 58.3% vs 75.5%, HR = 0.35 (0.15–0.82), p = 0.015) and tended to have lower NEDA-3 rates (NEDA-3 percentage of 38.9% vs 60.1, HR = 0.48 (0.22–1.02), p = 0.056) compared to patients without the same baseline

characteristics.

Figure 1 – 2.3.1. NEDA-3 status and individual components during ocrelizumab therapy in relapsing-remitting and progressive MS

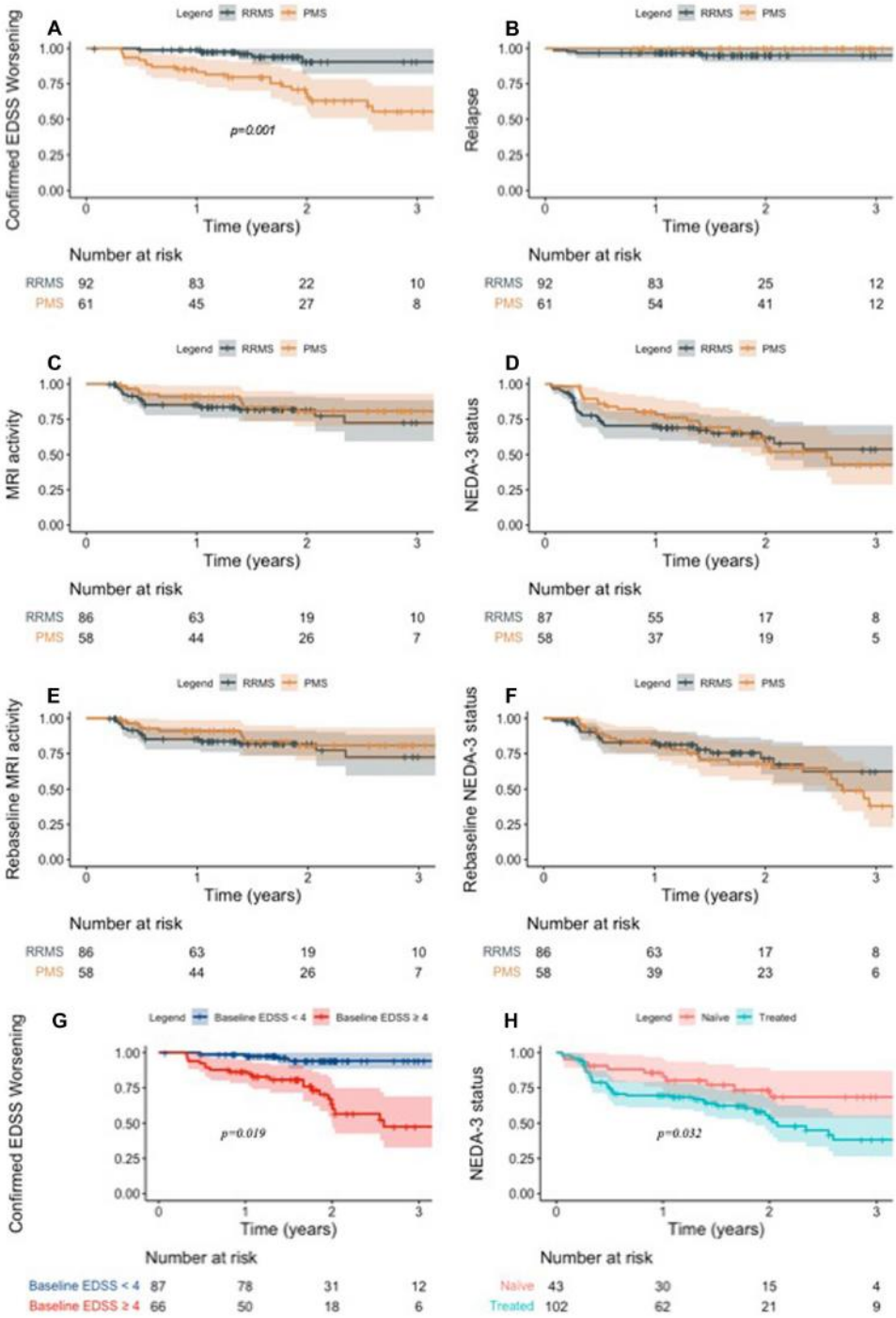

Predictors of Early Inflammatory Activity

Out of 145 patients, 30 (20.7%) had early inflammatory activity in the first year of treatment. The RRMS phenotype (OR 3.19 (1.21–8.39), p = 0.019) and MRI

activity at baseline (OR 0.21 (0.07–0.59), p = 0.003) were associated with an increased risk of early inflammatory activity. Leukocyte, total lymphocyte, CD4+, CD8+, and CD19+ cell counts during the first year of ocrelizumab therapy are reported in Table 2-2.3.1.

Table 2-2.3.1: Lymphocyte subsets during the first year of treatment

	Total cohort	Treated	Treatment-naive	Treated vs naive *p* value^	With early inflammatory activity	Without early inflammatory activity	With vs without early inflammatory activity *p* value°
Baseline							
Available, *n*	73	55	18		17	56	
Leukocytes, N/mm^3	6273 (2262)	6064 (2208)	6913 (2368)	0.254	6501 (3232)	6205 (1908)	0.522
Lymphocyte, N/mm^3	1793 (771)	1680 (801)	2139 (557)	0.050	2030 (1188)	1721 (587)	0.088
CD3+, N/mm^3	1259 (602)	1158 (624)	1568 (404)	0.022*	1452 (879)	1201 (484)	0.085
CD4+, N/mm^3	807 (446)	742 (463)	1006 (323)	0.047*	922 (641)	772 (367)	0.172
CD8+, N/mm^3	439 (214)	411 (224)	526 (153)	0.088	515 (263)	416 (193)	0.064
CD19+, N/mm^3	291 (257)	289 (244)	299 (303)	0.960	334 (366)	279 (217)	0.407
6 months							
Available, *n*	73	55	18		17	56	
Leukocytes, N/mm^3	5712 (1666)	5681 (1737)	5806 (1469)	0.870	5991 (1386)	5627 (1745)	0.209
Lymphocyte, N/mm^3	1388 (547)	1306 (554)	1639 (451)	0.036*	1564 (666)	1335 (501)	0.049*
CD3+, N/mm^3	1122 (505)	1042 (508)	1367 (419)	0.027*	1327 (617)	1060 (454)	0.014*
CD4+, N/mm^3	714 (367)	652 (366)	903 (309)	0.016*	824 (446)	680 (338)	0.046*
CD8+, N/mm^3	369 (192)	352 (196)	421 (176)	0.305	484 (214)	334 (173)	0.001**
CD19+, N/mm^3	19 (32)	23 (36)	7 (11)	0.084	29 (46)	17 (27)	0.495
12 months							
Available, *n*	61	45	16		11	50	
Leukocytes, N/mm^3	6306 (2704)	6296 (3055)	6334 (1314)	0.912	5432 (1499)	6532 (2926)	0.482
Lymphocyte, N/mm^3	1488 (655)	1359 (669)	1868 (476)	0.022*	1513 (561)	1528 (661)	0.584
CD3+, N/mm^3	1204 (524)	1091 (496)	1525 (476)	0.012*	1233 (493)	1211 (533)	0.469
CD4+, N/mm^3	780 (356)	695 (328)	1020 (330)	0.003*	760 (320)	794 (365)	0.759
CD8+, N/mm^3	397 (224)	370 (228)	471 (199)	0.251	456 (314)	387 (201)	0.199
CD19+, N/mm^3	25 (70)	32 (81)	5 (7)	0.267	11 (14)	28 (78)	0.314

^Multivariate ANCOVA corrected for age, sex, MS phenotype

°Multivariate ANCOVA corrected for age, sex, MS phenotype, and last DMT before ocrelizumab initiation

* Uncorrected $p < 0.05$

** Bonferroni $p < 0.0028$

While no significant differences in cell count were present at baseline, at 6-month FU, patients with early inflammatory activity had higher total lymphocytes, CD3+, CD4+, and CD8+ cell counts compared with stable patients. Only difference in CD8+ cell count survived Bonferroni correction for multiple comparisons. Using linear mixed model, CD8+ cell decrease at 6-month FU was

less pronounced in patients with early inflammatory activity (p = 0.022), while no significant differences were noted in the dynamics of CD4 + and CD19 + counts. When including CD4+, CD8+, and CD19 + cell counts to MS phenotype and MRI baseline activity in a logistic regression model predicting early inflammatory activity, CD8+ count was the only independent variable associated with outcome (OR 1.005 (1.001–1.009), p = 0.019).

Discussion

We herein provide single-center effectiveness data about ocrelizumab treatment in relapsing–remitting and progressive MS patients, prospectively followed in a real-world setting for a median follow-up of almost 2 years. Our cohort consisted of a heterogeneous group of patients with a large variety in terms of age, disease activity, phenotype, treatment history, and comorbidities, and included a relatively high number of patients with recent high disease activity.

In the RRMS population we observed that, at 2-year FU, 95.1% patients were free of relapses, 90.5% patients free of disability worsening, and 67.1% patients free of MRI activity, with an overall percentage of patients reaching NEDA3 of 62.1%. The ARR decreased from 0.78 to 0.04 (at 1- and 2-year FU), which is in line with the relapse rate at 2-year FU reported in the OPERA I and II studies (0.16)[139]. Despite such encouraging results, we observed some evidence of persistent MRI activity in the first year of treatment, both in RRMS and PMS patients (MRI activity-free-survival at 2 years of 67.1%, 81.3%, and 72.7% for RRMS, PPMS, and SPMS patients, respectively). The post hoc analysis pooling results of phase II and III trials suggested that ocrelizumab efficacy in terms of MRI outcome is evident as early as 4 weeks, and nearly complete by week 8[140]. We performed a re-baseline of MRI activity at 100 and 180 days after ocrelizumab start and observed that percentages of MRI activity free patients increased to 73– 82% and to 83–92%, respectively. Accordingly, NEDA3 percentages after 180 days of treatment increased to 77.1%, 71.9%, and 67.3% for RRMS, PPMS, and SPMS respectively. These results are in line with the post hoc analysis of the OPERA trial, in which the proportion of patients reaching NEDA3 status was 72.2% after a 24-week re-baseline. In RRMS patients, the presence of inflammatory activity at baseline MRI and a previous DMT exposure were associated with an increased risk of MRI activity during ocrelizumab treatment, with previous DMT exposure being the only independent variable associated with worse outcome at the

multivariate analysis. These results are in line with those from an independent cohort of patients treated with ocrelizumab, in which lower baseline EDSS and higher previous relapse rate were associated with an increased risk of early inflammatory activity during ocrelizumab treatment[141].

As per the progressive cohort, we observed a percentage of patients free of disability worsening at 2-year FU of 64.7% and 68.8% in PPMS and SPMS, respectively. ORATORIO study was the first clinical trial to demonstrate a benefit on disability progression in PPMS patients treated with ocrelizumab, showing a percentage of disability worsening-free patients of 67.1%[20]. Our results show a sustained beneficial effect of ocrelizumab treatment in progressive patients over a period of 2 years in a real-world setting.

When analyzing potential predictors of treatment response, lower baseline EDSS was independently associated with a reduced risk of disability worsening, especially in the PMS cohort. In line with this finding, we observed that patients with baseline EDSS ≥ 4 had a higher risk of disability worsening and lower NEDA-3 rates at 2-year FU. We also observed significantly lower rates of MRI activity free survival (58.3%) in the subgroup of patients with highly active MS, compared to the total cohort of patients. Since a rapid effect in controlling MRI activity is critical to minimize brain damage and prevent accumulation of disability in aggressive MS, these results suggest that in patients in whom immediate and complete disease control is warranted, DMTs with more rapid immune-ablative action should be considered[80].

It is generally believed that the impairment of the antigen presenting capacity of B cells is one of the major mechanisms underlying the therapeutic efficacy of ocrelizumab. However, a subset of T cells, mainly CD8+, also expresses CD20 and represents a highly activated cell population CD20+ T cells have been found to be increased in MS patients, representing almost 20% of all CD20+ expressing cells[142]. It has been recently showed that ocrelizumab reduces CD20+ T cells after 6 months of treatment, in line with similar findings found during treatment with rituximab [143]. We showed that patients with persistent early inflammatory activity during the first year of treatment had higher levels of CD8 + cells at 6-month FU as compared with stable patients. Although our evidence is limited, we cautiously speculate that the decrease in CD8 + cells is driven, at least partially, by the reduction of CD20 + T cells induced by ocrelizumab. Indeed, a transient reduction

in CD8 + cells has been reported in phase III trials and in real-life patients [144] , but to date no evidence exists on the possible therapeutic effect of this cellular subset reduction. Since these findings are based on immunophenotyping data collected in clinical practice, we could not validate them with double staining analyses and thus provide a mechanistic explanation for our observations. Larger studies exploring the effect of ocrelizumab treatment on CD20 + CD8 + cells and its possible association with clinical outcomes are needed to confirm our findings. Our study has several limitations, including the lack of spine MRI, patients' BMI, and a relatively short follow-up. In addition, flow cytometry immune subset characterization was available only for a subgroup of patients. Finally, pre-treatment brain MRI were acquired within 3 months of ocrelizumab start and not just before treatment commencement; thus, we cannot rule out whether part of the persistent MRI activity we observed during the first months of treatment occurred before treatment start.

Taken together our results - in parallel with the recent literature[145–147] - suggest that early commencement of a highly efficacy DMT such as ocrelizumab is associated with better clinical outcomes. Indeed, low disability status and being treatment-naïve patients at the time of treatment initiation were associated with lower risk of disease activity and disability accrual over the subsequent follow-up. Depletion of CD8 + cells could account for early therapeutic effects of anti-CD20 therapy.

2.3.2 Effect of ocrelizumab on retinal atrophy: the role of OCT in monitoring treatment response

Abstract

Objectives: The aim of our study was to provide first experience data regarding (i) the predictive role of OCT-derived metrics in terms of response to ocrelizumab treatment, (ii) the effect of the therapy on retinal thinning in patients with relapsing-remitting (RR) MS, and (iii) investigate whether rates of macular layers' atrophy differ according to response to treatment over a follow-up (FU) period of 2 years.

Methods: RRMS patients starting ocrelizumab at the MS Center of the University of Genoa underwent SD-OCT scans at baseline and at 2-years FU. Demographic/clinical characteristics and effectiveness outcomes throughout FU were collected. Pearson bivariate correlation and linear regression models explored the association between baseline OCT metrics and subsequent disability, while analysis of covariance adjusted for possible confounding covariates was applied to explore atrophy rates of pRNFL, GCIPL, and INL at different timepoints and their differences according to clinical outcomes over FU.

Results: A total of 63 RRMS patients entered the final analyses [females: 73%; mean age and disease duration: 38.5+9.9 and 7.5+7.8 years; median (range) EDSS: 2 (0-7)]. A statistically significant correlation between baseline pRNFL/GCIPL thickness and EDSS scores at 24-months FU (r =-0.34, p=0.006/r =-0.25, p=0.046, respectively) was found, and baseline pRNFL thickness appeared to be an independent predictor of subsequent disability (0.02 increase in EDSS for each 1-μm decrease in the baseline pRNFL, 95%CI: 0.038 - 0.001; p=0.042). No significant differences were observed between baseline and FU pRNFL, GCIPL, and INL thickness when considering the global population. However, a more evident INL swelling over FU was found in patients with vs those without persistent MRI activity and in patients loosing vs those maintaining NEDA3 status during the first 12-months after treatment start (+0.51±2.07 vs -0.42±1.64, p=0.031 and +0.39±1.90 vs -0.45±1.67, p=0.042, respectively). No differences between groups were found in terms of pRNFL and GCIPL thinning throughout FU. In patients with baseline EDSS>3, a pRNFL thinning ≤ 2 μm (lowest tertile) was associated with significantly higher risk of disability progression (p=0.02).

Conclusions: Our findings confirm and strengthen the role of OCT in predicting disability accrual. The overall stability of pRNFL and GCIPL thickness over 2-years FU suggests a neuroprotective effect of ocrelizumab treatment in RRMS, even in patients with persistent early inflammatory activity. Our data point at INL as the macular layer whose dynamic better reflects inflammatory processes within the CNS. Early treatment commencement – when disability status is still low - may yield significant benefits even in terms of retinal atrophy prevention.

Scientific rationale and study endpoints

Given the easily accessible and cost-efficient use of OCT in clinical practice, and its capabilities of capturing both neurodegenerative and inflammatory processes within the CNS (see paragraph 1.3), studies exploring the potential of retinal layers' thickness as a biomarker for predicting and monitoring treatment response/failure in MS are of paramount importance. With this study, we wanted to explore the interaction between markers of inflammation and of axonal injury at both cerebral and retinal level and to investigate their correlation with disease activity over follow-up (FU) in a group MS patients starting an "highly-efficacy" treatment with ocrelizumab, in order to explore whether the eye can predict and reflect mechanisms involved in tissue injury and to deepen our knowledge into mechanisms leading to INL thickening during CNS inflammation.

The specific aims were:

(i) To explore the predictive role of baseline OCT metrics in terms of clinical outcomes (in particular disability progression)

(ii) To investigate changes in terms pRNFL, GCIPL, and INL thickness in a homogenous and "highly-active" group of RRMS patients treated with ocrelizumab over a follow-up (FU) period of 2 years

(iii) To assess whether rates of OCT metrics atrophy differ according to NEDA3 status (and separately: progression, relapses, MRI activity) over FU

Study design

In this single-center longitudinal observational study, we prospectively included 70 RRMS patients starting ocrelizumab treatment at the MS Center of the University of Genoa, IRCCS Ospedale Policlinico San Martino. Inclusion criteria

were: (I) age 18-70 years (II) RRMS diagnosis according to the 2017 McDonald's criteria[111] (III) EDSS[12] score $\leq$ 7 (III) commencement of ocrelizumab treatment within 15 days distance from baseline OCT. Exclusion criteria were: (I) other neurological comorbidities, (II) contraindications to MRI, (III) substantial ophthalmological pathologies (including iatrogenic optic neuropathy/diabetes/uncontrolled hypertension), (IV) refractive errors +/− 6-diopters.

Demographic and clinical characteristic were collected at baseline. In order to assess the "no evidence of disease activity" (NEDA3)[79] criteria during follow-up, information regarding occurrence of clinical relapses, radiological activity, and EDSS scores at baseline, at 12-months, and at 24-motnhs follow-up were collected. Relapses, MRI activity, and disability progression were defined "early" in they occurred during the first 12-months after treatment commencement.

All subjects enrolled underwent spectral domain (SD)-OCT (Spectralis, Heidelberg-Engineering) at baseline and after 24-months FU, performed and processed by a single certified neurologist, in accordance with the APOSTEL recommendations[148]. In line with our previous analyses[68,149], pRNFL was obtained with a 360° RNFL-B circle scan located at 3.4 cm from the center of the optic nerve head; peripapillary measurements were averaged from 100 images and macular estimations from 15 ART. Macular volumetric scans consisting of at least 25 single horizontal axial B-scans were acquired in a rectangular section centered over the macula and segmented automatically into different layers using the Heidelberg Eye Explorer mapping software version 6.0.9.0. Segmented layers were checked and manually corrected, if necessary.). The thickness of GCIPL and INL were measured. Scans violating international-consensus quality-control criteria (OSCAR-IB)[150] were excluded (n=2 patients excluded due to poor OCT quality). Patients with previous bilateral ON were excluded (n=4). In patients with previous unilateral ON (n=25, none occurring during the previous 12-months), only the non-affected eye was analyzed. In patients without history of ON, OCT metrics were averaged over the two eyes. One patient was excluded from the analyses because refused to undergo the FU evaluation. Accordingly, n=63 patients entered the final analyses.

Statistical analyses

Descriptive results were reported as mean with standard deviation (SD) or median with range. Baseline OCT-derived metrics relationships with 12-months and 24-months FU EDSS were assessed with Spearman correlation models. In order to investigate the ability of OCT-derived measures to predict disability accrual, univariate linear regression models adjusted for sex, age, disease duration, number of previous treatments and baseline EDSS explored associations between baseline pRNFL/GCIPL thickness and 24-months EDSS. In line with literature [68,72], we chose to use this approach as analyzing the changes in EDSS over a specific period of time could be partly influenced by the baseline EDSS score (i.e. more likely for patients with lower baseline EDSS to experience a sustained change in EDSS over time). Differences between baseline and FU pRNFL, GCIPL, and INL thickness were assessed by repeated-measure analysis covariance (ANCOVA) adjusted for sex, age, disease duration, number of previous treatments and baseline EDSS; ANCOVA adjusted for the same variables listed above was used also to explore differences in terms of OCT-derived metrics atrophy rates over FU between patients who maintained and those who lost NEDA3 over FU (also considering disability progression, relapses, and MRI separately). Lastly, atrophy rates of pRNFL, GCIPL, and INL over FU were divided in tertiles, and the distribution of these tertiles in the groups of patients who showed (i) disability progression, (ii) inflammatory activity (either relapses or MRI activity), and (iii) NEDA3 over FU was assessed with Chi-square test in the global population and in the single groups of patients with baseline EDSS ≤ 3 and those with baseline EDSS > 3. SPSS (v26.0) software (IBM) was used for computation. All p-values were two-sided and considered statistically significant when $p \leqslant 0.05$.

Population characteristics

Demographic and clinical characteristics of patients at baseline and during FU are reported in Table 1-2.3.2.

In line with our prior analysis in RRMS patients (see paragraph 2.3.1), we found an overall percentage of patients reaching NEDA3 at 24-months FU of 60.3%. Only n=3 patients experienced a relapse (all occurring during the first 12-months after treatment commencement, none of them being an ON), while n=10 showed disability progression (n=2 occurring “early”, n=8 observed during the second

year of treatment) and n=14 patients had MRI activity (of which n=12 occurring during the first 12-months of ocrelizumab treatment) during FU.

Table 1-2.3.2: Demographic and clinical characteristics

POPULATION CHARACTERISTICS	RRMS patients (n=63)
Female, no (%)	46 (73)
Age, mean (SD), y	38.5 (9.9)
Disease duration, mean (SD), y	7.5 (7.8)
Median (range) baseline EDSS score	2 (0 – 7)
Naive patients, n (%)	23 (36.5)
Mean (range) number of previous DMTs	1.32 (0 - 6)
CLINICAL DATA OVER 24-MONTHS FU	
Median (range) 1° year EDSS score	2 (1 - 7)
Median (range) 2° year EDSS score	2 (1 - 7)
Relapses, n (%)	3 (4.8)
Disease progression, n (%)	10 (15.9)
MRI activity, n (%)	14 (22.2)
NEDA3, n (%)	38 (60.3)

Relationship between baseline OCT-derived metrics and disability worsening over FU

In order to explore the association between baseline OCT metrics and subsequent EDSS scores, we initially performed bivariate correlation models. As expected, we observed a statistically significant association between baseline pRNFL/GCIPL thickness and EDSS scores at 12-months FU (r =-0.36, p=0.004 / r =-0.28, p0.025, respectively) and 24-months FU (r = -0.34, p=0.006 / r =-0.25, p=0.046, respectively). No statistically significant associations were found between baseline INL thickness and EDSS scores at 12-months and 24-months FU.

Once pRNFL and GCIPL were identified as the only OCT metrics with a significant correlation with FU EDSS, we applied univariate linear regression models to explore the predictive role of baseline pRNFL and GCIPL thickness in terms EDSS scores at 24-months FU adjusting for all possible confounding

covariates (sex, age, disease duration, number of previous treatments and baseline EDSS). Both models were statistically significant (p<0.001). However, only pRNFL appeared to be an independent predictor of subsequent disability (0.02 increase in EDSS for each 1-µm decrease in the baseline pRNFL, 95% CI: 0.038 - 0.001; p = 0.042).

Associations between baseline pRNFL and GCIPL thickness and 24-months FU EDSS score are shown in Fig. 1-2.3.2.

Fig 1-2.3.2: Scatter plots showing the association between baseline pRNFL (A) and GCIPL (B) thickness and EDSS score at 24-months FU

A

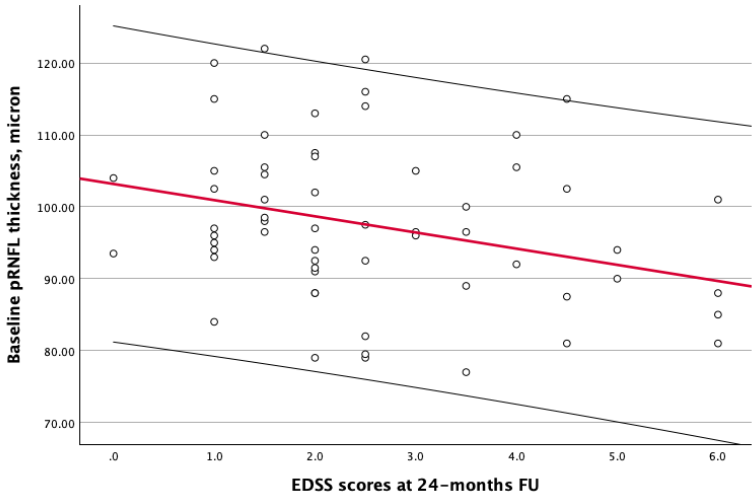

B

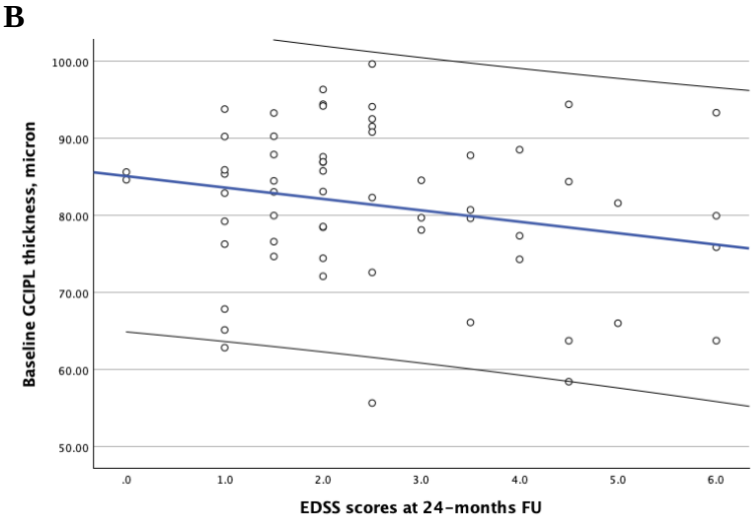

OCT metrics dynamics over 24-months FU in the global population and according to clinical outcomes

Initially, repeated measure ANCOVA accounting for possible confounding covariates was applied to explore the OCT metrics changes over FU in the global population. As shown in Table 2-2.3.2, no significant differences were found between baseline and FU thickness of pRNFL, GCIPL and INL.

Table 2-2.3.2: Changes in terms pRNFL, GCIPL and INL thickness at different timepoints in ocrelizumab treated patients

	Baseliene thickness, μm (n=63)	**24-months FU thickness, μm (n=63)**	***p-values****
pRNFL	97.0 (11.3)	95.5 (11.5)	0.108
GCPL	81.0 (10.41	79.0 (10.29)	0.407
INL	36.6 (3.5)	36.3 (3.4)	0.851

Afterwards, the rates of retinal atrophy according to NEDA3 status over FU (relapses, disability progression and MRI activity during the 1st year and during the whole observation period, separately) were explored. Since patients experiencing a relapse during FU were only 3, all occurring during the first 12-months, and patients with "early" disability progression were only 2, statistical analyses were not performed according to these events. Results of performed analyses are reported in Table 3-2.3.2.

Interestingly, while pRNFL and GCIPL thinning throughout follow-up was similar between groups, the swelling of INL was more evident in patients with "early" MRI activity vs those without MRI activity and in patients loosing vs those maintaining NEDA3 status during the first 12-months after treatment start (+0.51±2.07 vs -0.42±1.64, p=0.031 and +0.39±1.90 vs -0.45±1.67, p=0.042, respectively).

Table 3-2.3.2: Differences in terms pRNFL, GCIPL and INL thinning according to clinical outcomes over FU in ocrelizumab treated patients

	Disability progression during FU (n=10)	**No disability progression during FU (n=53)**	***p-value****
Delta pRNFL thickness, baseline-24months FU, µm	-2.15 (2.04)	-1.35 (2.94)	0.48
Delta GCIPL thickness, baseline-24months FU, µm	- 1.98 (4.59)	-2.01 (5.39)	0.94
Delta INL thickness, baseline-24months FU, µm	- 0.37 (0.99)	- 0.22 (1.87)	0.97
	MRI activity during FU (n=14)	**No MRI activity during FU (n=49)**	***p-value****
Delta pRNFL thickness, baseline-24months FU, µm	- 0.93 (2.26)	- 1.65 (2.96)	0.55
Delta GCIPL thickness, baseline-24months FU, µm	- 2.82 (4.07)	- 1.77 (5.54)	0.48
Delta INL thickness, baseline-24months FU, µm	+ 0.32 (2.08)	- 0.41 (1.64)	0.07
	MRI activity during the first 12-months (n=12)	**No MRI activity during the first 12-months (n=51)**	***p-value****
Delta pRNFL thickness, baseline-24months FU, µm	- 0.83 (2.43)	- 1.63 (2.91)	0.58
Delta GCIPL thickness, baseline-24months FU, µm	-3.14 (4.33)	-1.74 (5.43)	0.36
Delta INL thickness, baseline-24months FU, µm	+ 0.51 (2.07)	- 0.42 (1.64)	***0.03***
	NEDA3 loss during FU (n=25)	**NEDA3 maintenance during FU (n=38)**	***p-value****
Delta pRNFL thickness, baseline-24months FU, µm	-1.38 (2.22)	-1.55 (3.18)	0.85
Delta GCIPL thickness, baseline-24months FU, µm	- 2.37 (4.16)	-1.77 (5.88)	0.69
Delta INL thickness, baseline-24months FU, µm	+ 0.08 (1.69)	- 0.46 (1.78)	0.18
	NEDA3 loss during the first 12-months (n=15)	**NEDA3 maintenance during the first 12-months (n=48)**	***p-value****
Delta pRNFL thickness, baseline-24months FU, µm	- 0.70 (2.25)	- 1.73 (2.95)	0.44
Delta GCIPL thickness, baseline-24months FU, µm	- 2.73 (3.99)	- 1.78 (5.59)	0.43
Delta INL thickness, baseline-24months FU, µm	+ 0.39 (1.90)	- 0.45 (1.67)	***0.04***

**ANCOVA adjusted sex, age, disease duration, number of previous treatments and baseline EDSS*

FU: follow-up; pRNFL: peripapillary retinal nerve fiber layer; GCIPL: ganglion cell + inner plexiform layer; INL: inner nuclear layer

Statistically significant p-values are reported in bold

Distribution of OCT metrics thinning tertiles according to clinical outcomes

Lastly, patients were grouped according to: (i) evidence disability progression, without inflammatory activity over FU (n=9) (ii) evidence of inflammatory activity, either relapses or MRI activity (n=16), and (iii) NEDA3 status maintenance (n=38) over 24-months FU. OCT-metrics trajectories according to this classification are shown in Fig 2-2.3.2.

Fig 2-2.3.2: OCT metrics trajectories in patients maintaining NEDA and those experiencing EDSS progression or inflammatory activity (MRI activity and/or relapses) over FU

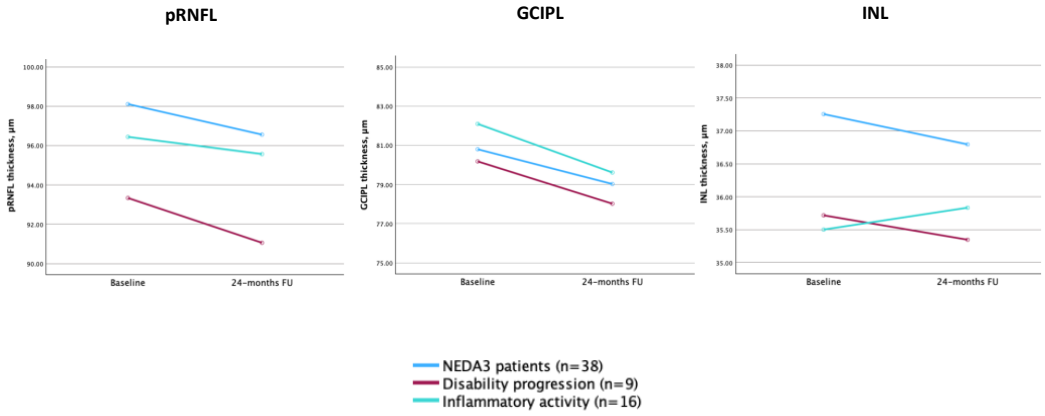

The atrophy rates of pRNFL, GCIPL, and INL over FU were divided in tertiles, and the distribution of these tertiles in the three sub-groups of patients described above were calculated in the global population and in patients with baseline EDSS ≤ 3 and those with baseline EDSS > 3, separately. Results of this analysis are shown in Fig 3-2.3.2. Interestingly, while no differences in terms of atrophy rates tertiles' distribution were found in the global population and in patients with baseline EDSS ≤ 3, when analyses were restricted to patients who started ocrelizumab treatment with baseline EDSS > 3 a pRNFL thinning ≤ 2 µm (lowest tertile) was associated with a statistically significant higher risk of disability progression (p=0.02).

Fig 3-2.3.2: Distribution of OCT metrics thinning tertiles according to clinical outcomes

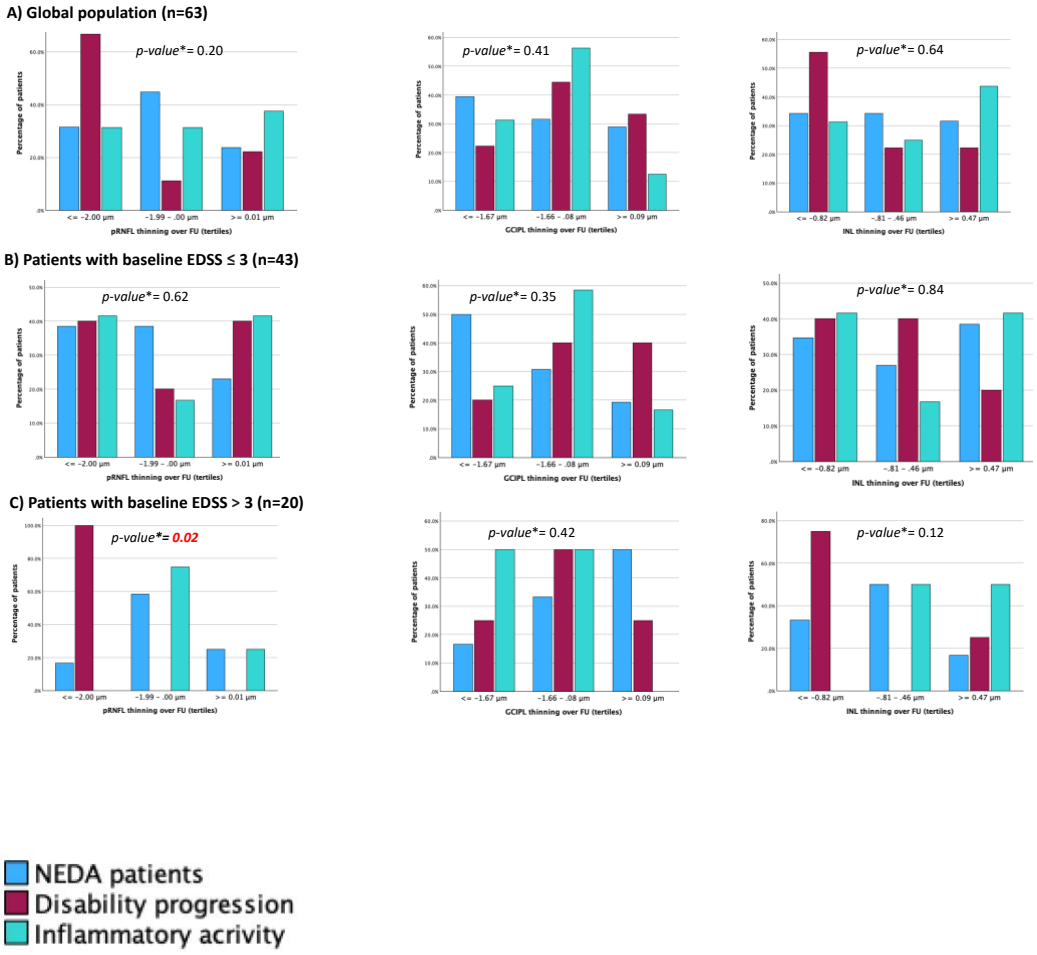

Discussion

Although accumulating evidence point at neuro-retinal changes - in eyes without acute ON - as a possible biomarker able to reflect both inflammatory and neurodegenerative processes within the CNS[56], data regarding longitudinal retinal layers' thickness trajectories in relation to treatment response are still sparse. We herein provide first-experience data regarding atrophy rates of different macular layers in a quite homogeneous group of ocrelizumab-treated RRMS patients, who underwent OCT at the time of treatment start and were followed over a follow-up of 24-months. We report an overall stability of pRNFL and GCIPL thickness, suggesting a neuroprotective effect of ocrelizumab treatment in RRMS, together with a swelling of INL in patients with persistent early inflammatory activity, pointing at this layer as the one whose dynamic better reflects CNS inflammatory

processes.

OCT is gaining increasing relevance in the assessment of patients with MS, thanks to its capability of (i) reflecting biological mechanisms underlying MS pathology and (ii) predicting and monitoring MS-related clinical outcomes. Indeed, literature reports that pRNFL and GCIPL thinning are faster in RRMS patients exhibiting clinical or radiological signs of disease activity[75,77,78], mirror brain atrophy evolution [151], and can be influenced by the use of DMTs [152]. In parallel, INL volume has been shown to increase following relapses other than ON (Balk 2019), while effective treatment with DMTs has been described in MS patients with a sustained reduction in INL volume in the absence of ON [153]. However, previous studies exploring longitudinal trajectories of retinal layers' thickness according to disease outcomes are limited by the heterogeneity of the population studied, often including patients with both relapsing-remitting and progressive disease course, undergoing a mix of DMTs throughout the study duration, and with OCT scans performed at different timeframes since treatment start and at variable intervals, leading to differences in median gap times among participants in different cohorts[55,60,63,153]. These aspects preclude a reliable assessment of the effects of single DMTs on retinal atrophy rates and their correlation with treatment response. Thus, our study significantly differs from the previous ones, since it specifically assessed the effect of ocrelizumab in a quite homogeneous population of RRMS patients who underwent the first OCT assessment at the time of treatment start. Implementing the present literature with studies including more uniformly treated MS subgroups has the potential to provide a more precise evaluation of the effects of DMTs on retinal thinning. This valuable information could prove instrumental in shaping future clinical trial designs that incorporate OCT as a key outcome measure.

In the first part of our study, we explored the association between baseline OCT-metrics and patients' disability status at FU. As expected, we observed an association between baseline pRNFL and GCIPL thickness and EDSS scores at FU, which confirms and strengthen the role of OCT metrics in predicting subsequent disability. Even accounting for possible confounding variables – including age, disease duration, and baseline EDSS scores - linear regression models confirmed the capability of pRNFL to independently predict subsequent disability. This observation further underscores the potential prognostic value of

OCT examination even in the context of patients treated with a single DMT. It opens the possibility of establishing specific cut-off for various macula-derived measures to use in clinical practice, aiding in the identification of patients with a higher likelihood of responding positively to treatment.

When analyzing OCT metrics longitudinally, we did not find any statistically significant difference between baseline and FU thickness of pRNFL and GCIPL. Literature suggest that thinning of these layers mirror concomitant global neurodegeneration and brain atrophy in MS[151]. Brain atrophy is considered a surrogate marker of neurodegeneration and one of the major pathological substrates of disability in MS, and therefore it has been incorporated as an endpoint in several recent clinical trials. Data from randomized control trials of RRMS patients report significant differences in the percentage brain volume change from week 24 to week 96 between the ocrelizumab and the interferon β-1a treated patients[139]. Moreover, recent studies proved that ocrelizumab significantly lowers brain atrophy in RRMS patients as compared to interferon β-1a [154] or fingolimod [155], with global and regional brain volume loss rates approaching that of healthy controls [156]. Being brain atrophy an estimation of tissue loss, these findings suggest that ocrelizumab not only promotes the reduction of inflammation, but prevents also the progression of neurodegeneration. In parallel, while data regarding the impact of ocrelizumab treatment in terms of retinal thinning in RRMS patients are still lacking, retinal atrophy in RRMS has been shown to be modulated by rituximab, another anti-CD20 treatment used for the treatment of MS[55]. In this context, the association observed between pRNFL and GCIPL thickness with EDSS in our population, together with the overall stability of their thickness throughout FU, support the neuroprotective effect of ocrelizumab treatment in RRMS, even in patients with persistent early inflammatory activity. Neurodegeneration in MS may be initially triggered by inflammation and subsequently sustained by persistent compartmentalized inflammation, especially if there is limited drug access to the neuronal compartment after the restoration of BBB integrity[2]. Additionally, various studies have highlighted the pivotal role of B-cell immunity in the biological mechanisms underlying cortical pathology [26]. Therefore, ocrelizumab, which targets the CD20 marker on B lymphocytes and restricts the circulation of immune cells from blood to the CNS, could play a crucial role in limiting the

establishment of intrathecal inflammation and, consequently, neurodegenerative processes [155]. This effect might be more pronounced when the drug is administered in the earliest phases of the disease. In line with this, although literature reports a more evident pRNFL and GCIPL thinning in patients loosing NEDA3 during FU, in our ocrelizumab-treated population we could observe this trend only in patients with baseline EDSS > 3. Taken together, our findings suggest that early treatment commencement – when disability status is still low - may yield significant benefits in terms of neuronal loss prevention.

An important finding of this study is that we observed a more prominent INL thickening during 24-months FU among patients with persistent inflammatory activity during the first 12-months of treatment as compared to stable ones. Conversely, the difference between baseline and FU INL thickness did not statistically differ when comparing stable patients to those exhibiting disease activity during the whole observation period (including the second year of treatment). Over the past years, accumulating evidence corroborated the usefulness of INL as a marker of inflammation, showing that it thickens after a clinical relapse and eventually returns to baseline values when the inflammatory activity ceases [60,62,157,158]. Different possible mechanisms involved in INL thickening in MS have been proposed, including presence of microcystic macular edema, non-inflammation-related traction following RNFL/GCIPL atrophy, inflammation-related dynamic fluid shifts due to a failure in the water-buffering function of Muller cells (also known as the "glymphatic hypothesis")[159]. According to this latter hypothesis, an increase in vascular permeability occurs within the retina due to acute inflammatory processes or to a primary injury of Muller cells[157,159]. This hypothesis may explain the transient nature of INL thickening and its association with disease activity, which has been showed by this and other prior studies [60,62,157,158]. Interstingly, Pisa et al[158] found that this phenomenon was counteracted by steroid treatment, further supporting an inflammatory etiology. Similarly to our findings, Balk et al[60] observed that the occurrence of clinical relapses was not related to change in INL within the same period, but was significantly associated with an increase in INL volume in the subsequent FU, suggesting that inflammatory activity precedes INL thickening. Overall, in line with the most recent evidence[60,158] our observations seem to suggest that INL thickens in a post-acute phase after an inflammatory event. Our

data, in parallel with those reported by Knier et al. [62] (who found that effective treatment with DMT in patients with MS is associated with a sustained reduction in INL volume), point at INL as the macular layer whose dynamic better reflects inflammatory processes within the CNS, and suggest that INL volume may be a response marker for successful treatment of inflammation in RRMS patients.
Our study is not without limitations, including the absence of a control group, the limited number of patients enrolled and the relatively short follow-up. However, we would like to underline that we studied a quite homogeneous group of patients in single-center cohort, with well-standardized techniques and methodologies. Moreover, a two-year clinical follow-up is in line with typical length of randomized controlled trials. Finally, this study did not include MRI-derived brain atrophy data, which would help to further corroborate our findings and to confirm that the effects of ocrelizumab on retinal atrophy similarly reflect its effects on brain atrophy. Further studies combining these two outcome measures in the context of ocrelizumab treatment response are warranted.

In conclusion, results of this study provide support that thinning of the RNFL and GCIP mirror concomitant global neurodegeneration in MS, thereby further validating the potential utility of OCT, an inexpensive, noninvasive, and well-tolerated imaging technique for the purpose of tracking MS patients overtime. Finally, we confirm and strengthen the hypothesis that INL volumes reflect a post-acute response of the retina to inflammatory activity in persons with MS. Altogether, our data support the use of OCT as a window into neurodegenerative and inflammatory mechanisms within the CNS, and – as such – as a potential biomarker for patients' stratification and monitoring for current and experimental treatments choice.

2.4 Conclusions

Despite significant progress in comprehending the pathophysiology of MS and the availability of treatments to prevent relapses, the challenges of halting and reversing disease progression persist. In this context, three prominent themes have shaped MS research in recent years: (1) viewing the disease as a continuum, where inflammation and neurodegeneration coexist from onset, requiring a thorough understanding of their interaction over time; (2) early disease identification and patients' stratification, with implications for very early treatment; and (3) the quest for new biomarkers to define, monitor, or predict the disease course.

Indeed, it is crucial to develop and validate tools that consistently assess and monitor relevant disease biology in clinical settings. Evidence suggests that disability progression in MS results from a combination of various mechanisms that exhibit distinct patterns among patients and even within individual patients over time. Different pathological mechanisms can independently manifest or combine within the same individual throughout the disease course. These processes, coupled with the failure of compensatory mechanisms and the effects of aging, determine the clinical presentation of the disease over time. To effectively address the persisting challenges, a shift from a clinical to a biologically oriented MS management is required[23].

To achieve this objective, the field must create methods to identify and quantify mechanisms of injury at the patient level in a minimally invasive manner and integrate the relevant measures into both clinical trials and everyday clinical practice. With the present PhD project, we conducted different and independent studies combining clinical-radiological-serum biomarker, which involved individuals with diverse rates of disease progression, irrespective of relapses and active lesions on MRI, to deepen our knowledge into mechanisms potentially involved tissue damage and disease-related clinical course over time.

Overall, our studies helped to deepen our knowledge into mechanism involved in focal inflammation, neuronal injury, and tissue repair, thanks to the application of advanced imaging techniques which not only may provide novel insight for understanding the pathophysiology of MS, but possibly also enable stratification and monitoring of patients. In particular, our findings support the concepts that (i)

coagulation activation at the level of BBB and neurovascular unit might induce and sustain inflammatory processes underlying the pathophysiology of MS, and that (ii) microstructural injury of the subventricular zone - occurring in the context of a diffuse brain tissue damage which characterize MS progression and patients' aging - reflects a loss of multipotent neural stem cells' neurogenic and neuroprotective functions, possibly contributing to disease progression.

In parallel, the results of our longitudinal, prospective, and real-life studies - correlating imaging and other paraclinical tools with clinical outcomes - underline the importance of early treatment commencement in order to prevent disease activity and disability accrual, and support the use of OCT as a biomarker to capture both inflammatory and neurodegenerative phenomena occurring within the CNS.

3. PUBBLCATIONS

Articles published during PhD (From 01/11/2020 to 1/1/2024):

1. Andorra M, Freire A, Zubizarreta I, de Rosbo NK, Bos SD, Rinas M, Høgestøl EA, de Rodez Benavent SA, Berge T, Brune-Ingebretse S, Ivaldi F, **Cellerino M**, Pardini M, Vila G, Pulido-Valdeolivas I, Martinez-Lapiscina EH, Llufriu S, Saiz A, Blanco Y, Martinez-Heras E, Solana E, Bäcker-Koduah P, Behrens J, Kuchling J, Asseyer S, Scheel M, Chien C, Zimmermann H, Motamedi S, Kauer-Bonin J, Brandt A, Saez-Rodriguez J, Alexopoulos LG, Paul F, Harbo HF, Shams H, Oksenberg J, Uccelli A, Baeza-Yates R, Villoslada P. *Predicting disease severity in multiple sclerosis using multimodal data and machine learning*. J Neurol. 2023 Dec 22. doi: 10.1007/s00415-023-12132-z. Epub ahead of print. PMID: 38133801.

2. Tazza F, Schiavi S, Leveraro E, **Cellerino M**, Boffa G, Ballerini S, Dighero M, Uccelli A, Sbragia E, Aluan K, Inglese M, Lapucci C. *Clinical and radiological correlates of apathy in multiple sclerosis.* Mult Scler. 2023 Dec 14:13524585231217918. doi: 10.1177/13524585231217918. Epub ahead of print. PMID: 38095151.

3. Lapucci C, Boccia VD, Sirito T, **Cellerino M**, Mikulska M, Sticchi L, Inglese M. *Safety of anti-varicella zoster virus vaccination in patients with multiple sclerosis treated with natalizumab: A case series.* Mult Scler. 2023 Oct;29(11-12):1514-1517. doi: 10.1177/13524585231204121. Epub 2023 Oct 3. PMID: 37786976.

4. Petracca M, Carotenuto A, Scandurra C, Moccia M, Rosa L, Arena S, Ianniello A, Nozzolillo A, Turrini M, Streito LM, Abbadessa G, **Cellerino M,** Bucello S, Ferraro E, Mattioli M, Chiodi A, Inglese M, Bonavita S, Clerico M, Cordioli C, Moiola L, Patti F, Lavorgna L, Filippi M, Borriello G, D'Amico E, Pozzilli C, Brescia Morra V, Lanzillo R. *Sexual dysfunction in multiple sclerosis: The impact of different MSISQ-19 cut-offs on prevalence and associated risk factors.* Mult Scler Relat Disord. 2023 Oct;78:104907. doi: 10.1016/j.msard.2023.104907. Epub 2023 Jul 26. PMID: 37523809.

5. Koudriavtseva T, Lorenzano S, **Cellerino M,** Truglio M, Fiorelli M, Lapucci C, D'Agosto G, Conti L, Stefanile A, Zannino S, Filippi MM, Cortese A, Piantadosi C, Maschio M, Maialetti A, Galiè E, Salvetti M, Inglese M. *Tissue factor as a potential coagulative/vascular marker in relapsing-remitting multiple sclerosis*. Front Immunol. 2023 Jul 31;14:1226616. doi: 10.3389/fimmu.2023.1226616. PMID: 37583699; PMCID: PMC10424925.

6. **Cellerino M**, Schiavi S, Lapucci C, Sbragia E, Boffa G, Rolla-Bigliani C, Tonelli S, Boccia D, Bruschi N, Tazza F, Franciotta D, Inglese M. *In-vivo characterization of macro- and microstructural injury of the subventricular zone in relapsing-remitting and progressive multiple sclerosis.* Front Neurosci. 2023 Apr 11;17:1112199. doi: 10.3389/fnins.2023.1112199. PMID: 37113155; PMCID: PMC10126477.

7. Lapucci C, Tazza F, Rebella S, Boffa G, Sbragia E, Bruschi N, Mancuso E, Mavilio N, Signori A, Roccatagliata L, **Cellerino M,** Schiavi S, Inglese M. *Central vein sign and diffusion MRI differentiate microstructural features*

within white matter lesions of multiple sclerosis patients with comorbidities. Front Neurol. 2023 Mar 8;14:1084661. doi: 10.3389/fneur.2023.1084661. PMID: 36970546; PMCID: PMC10030505.

8. Schiavetti I, Barcellini L, Lapucci C, Tazza F, **Cellerino M**, Capello E, Franciotta D, Inglese M, Sormani MP, Uccelli A, Laroni A. *CD19+ B cell values predict the increase of anti-SARS CoV2 antibodies in fingolimod-treated and COVID-19-vaccinated patients with multiple sclerosis.* Mult Scler Relat Disord. 2022 Dec 30;70:104494. doi: 10.1016/j.msard.2022.104494. Epub ahead of print. PMID: 36603292; PMCID: PMC9800324.

9. Boccia VD, Lapucci C, **Cellerino M**, Tazza F, Rossi A, Schiavi S, Mancardi MM, Inglese M. *Evaluating the central vein sign in paediatric-onset multiple sclerosis: A case series study.* Mult Scler. 2022 Dec 13:13524585221142319. doi: 10.1177/13524585221142319. Epub ahead of print. PMID: 36514274.

10. Zanghì A, Avolio C, Signoriello E, Abbadessa G, **Cellerino M**, Ferraro D, Messina C, Barone S, Callari G, Tsantes E, Sola P, Valentino P, Granella F, Patti F, Lus G, Bonavita S, Inglese M, D'Amico E. *Is It Time for Ocrelizumab Extended Interval Dosing in Relapsing Remitting MS? Evidence from An Italian Multicenter Experience During the COVID-19 Pandemic*. Neurotherapeutics. 2022 Sep;19(5):1535-1545. doi: 10.1007/s13311-022-01289-6. Epub 2022 Aug 29. PMID: 36036858; PMCID: PMC9422942.

11. Landi D, Bovis F, Grimaldi A, Annovazzi PO, Bertolotto A, Bianchi A, Borriello G, Brescia Morra V, Bucello S, Buscarinu MC, Caleri F, Capobianco M, Capra R, **Cellerino M**, Centonze D, Cerqua R, Chisari CG, Clerico M, Cocco E, Cola G, Cordioli C, Curti E, d'Ambrosio A, D'Amico E, De Luca G, Di Filippo M, Di Lemme S, Fantozzi R, Ferraro D, Ferraro E, Gallo A, Gasperini C, Granella F, Inglese M, Lanzillo R, Lorefice L, Lus G, Malucchi S, Margoni M, Mataluni G, Mirabella M, Moiola L, Nicoletti CG, Nociti V, Patti F, Pinardi F, Portaccio E, Pozzilli C, Ragonese P, Rasia S, Salemi G, Signoriello E, Vitetta F, Totaro R, Sormani MP, Amato MP, Marfia GA. *Exposure to natalizumab throughout pregnancy: effectiveness and safety in an Italian cohort of women with multiple sclerosis.* J Neurol Neurosurg Psychiatry. 2022 Sep 30:jnnp-2022-329657. doi: 10.1136/jnnp-2022-329657. Epub ahead of print. PMID: 36180219.

12. Sbragia E, Olobardi D, Novi G, Lapucci C, **Cellerino M**, Boffa G, Laroni A, Mikulska M, Sticchi L, Inglese M. *Vaccinations in patients with multiple sclerosis: a real-world, single-center experience.* Hum Vaccin Immunother. 2022 Jul 21:2099171. doi: 10.1080/21645515.2022.2099171. Epub ahead of print. PMID: 35863064.

13. Stefanile A, **Cellerino M**, Koudriavtseva T. *Elevated risk of thrombotic manifestations of SARS-CoV-2 infection in cancer patients: A literature review*. EXCLI J. 2022 Jun 30;21:906-920. doi: 10.17179/excli2022-5073. PMID: 36172074; PMCID: PMC9489888.

14. Rise HH, Brune S, Chien C, Berge T, Bos SD, Andorrà M, Valdeolivas IP, Beyer MK, Sowa P, Scheel M, Brandt AU, Asseyer S, Blennow K, Pedersen

ML, Zetterberg H, de Schotten MT, **Cellerino M**, Uccelli A, Paul F, Villoslada P, Harbo HF, Westlye LT, Høgestøl EA. *Brain disconnectome mapping derived from white matter lesions and serum neurofilament light levels in multiple sclerosis: A longitudinal multicenter study*. Neuroimage Clin. 2022 Jun 25;35:103099. doi: 10.1016/j.nicl.2022.103099. Epub ahead of print. PMID: 35772194; PMCID: PMC9253471.

15. Lapucci C, Schiavi S, Signori A, Sbragia E, Bommarito G, **Cellerino M**, Uccelli A, Inglese M, Roccatagliata L, Pardini M. *The role of disconnection in explaining disability in multiple sclerosis*. Eur Radiol Exp. 2022 Jun 8;6(1):23. doi: 10.1186/s41747-022-00277-x. PMID: 35672589; PMCID: PMC9174414.

16. Masala A, Mola ID, **Cellerino M**, Pera V, Vagge A, Uccelli A, Christian C, Traverso CE, Iester M. *Choroidal Thickness in Multiple Sclerosis: An Optical Coherence Tomography Study.* J Clin Neurol. 2022 May;18(3):334-342. doi: 10.3988/jcn.2022.18.3.334. PMID: 35589321; PMCID: PMC9163936.

17. Magnè F*, **Cellerino M*,** Balletto E, Aluan K, Inglese M, Mikulska M, Bassetti M. *Anti-SARS-CoV-2 monoclonal antibodies for the treatment of active COVID-19 in multiple sclerosis: An observational study.* Mult Scler. 2022 Jun 28:13524585221103787. doi: 10.1177/13524585221103787. Epub ahead of print. PMID: 35762136.

18. Landi D, Grimaldi A, Bovis F, Ponzano M, Fantozzi R, Buttari F, Signoriello E, Lus G, Lucchini M, Mirabella M, **Cellerino M**, Inglese M, Cola G, Nicoletti CG, Mataluni G, Centonze D, Marfia GA. *Influence of Previous Disease-Modifying Drug Exposure on T-Lymphocyte Dynamic in Patients With Multiple Sclerosis Treated With Ocrelizuma*b. Neurol Neuroimmunol Neuroinflamm. 2022 Mar 10;9(3):e1157. doi: 10.1212/NXI.0000000000001157. PMID: 35273036; PMCID: PMC9005049.

19. **Cellerino M***, Boffa G*, Lapucci C, Tazza F, Sbragia E, Mancuso E, Bruschi N, Minguzzi S, Ivaldi F, Poirè I, Laroni A, Mancardi G, Capello E, Uccelli A, Novi G, Inglese M. *Predictors of Ocrelizumab Effectiveness in Patients with Multiple Sclerosis*. Neurotherapeutics. 2021 Sep 22. doi: 10.1007/s13311-021-01104-8. Epub ahead of print. PMID: 34553320.

20. Baroncini D, Simone M, Iaffaldano P, Brescia Morra V, Lanzillo R, Filippi M, Romeo M, Patti F, Chisari CG, Cocco E, Fenu G, Salemi G, Ragonese P, Inglese M, **Cellerino M**, Margari L, Comi G, Zaffaroni M, Ghezzi A; Italian MS registry. *Risk of Persistent Disability in Patients With Pediatric-Onset Multiple Sclerosis.* JAMA Neurol. 2021 Jun 1;78(6):726-735. doi: 10.1001/jamaneurol.2021.1008. PMID: 33938921; PMCID: PMC8094039.

21. Landi D, Signori A, **Cellerino M**, Fenu G, Nicoletti CG, Ponzano M, Mancuso E, Fronza M, Ricchiuto ME, Boffa G, Inglese M, Marfia GA, Cocco E, Frau J. *What happens after fingolimod discontinuation? A multicentre real-life experience.* J Neurol. 2021 Jun 16. doi: 10.1007/s00415-021-10658-8. Epub ahead of print. PMID: 34136943.

22. Ferraro D, Iaffaldano P, Guerra T, Inglese M, Capobianco M, Brescia Morra V, Zaffaroni M, Mirabella M, Lus G, Patti F, Cavalla P, **Cellerino M**, Malucchi S, Pisano E, Vitetta F, Paolicelli D, Sola P, Trojano M; Italian MS Register. *Risk of multiple sclerosis relapses when switching from fingolimod to cell-depleting agents: the role of washout duration.* J Neurol. 2021 Jul 22. doi: 10.1007/s00415-021-10708-1. Epub ahead of print. PMID: 34292396.

23. Tazza F, Lapucci C, **Cellerino M**, Boffa G, Novi G, Poire I, Mancuso E, Bruschi N, Sbragia E, Laroni A, Capello E, Inglese M. *Personalizing ocrelizumab treatment in Multiple Sclerosis: What can we learn from Sars-Cov2 pandemic?* J Neurol Sci. 2021 Aug 15;427:117501. doi: 10.1016/j.jns.2021.117501. Epub 2021 May 20. PMID: 34044238; PMCID: PMC8133824.

24. Costabile T, Carotenuto A, Lavorgna L, Borriello G, Moiola L, Inglese M, Petruzzo M, Trojsi F, Ianniello A, Nozzolillo A, **Cellerino M**, Boffa G, Rosa L, Servillo G, Moccia M, Bonavita S, Filippi M, Lanzillo R, Brescia Morra V, Petracca M. *COVID-19 pandemic and mental distress in multiple sclerosis: Implications for clinical management.* Eur J Neurol. 2021 Oct;28(10):3375-3383. doi: 10.1111/ene.14580. Epub 2020 Nov 3. PMID: 33043560; PMCID: PMC7675416

25. Sbragia E, Colombo E, Pollio C, **Cellerino M**, Lapucci C, Inglese M, Mancardi G, Boffa G. *Embracing resilience in multiple sclerosis: a new perspective from COVID-19 pandemic.* Psychol Health Med. 2021 Apr 25:1-9. doi: 10.1080/13548506.2021.1916964. Epub ahead of print. PMID: 33899615.

26. Carotenuto A, Scandurra C, Costabile T, Lavorgna L, Borriello G, Moiola L, Inglese M, Trojsi F, Petruzzo M, Ianniello A, Nozzolillo A, **Cellerino M**, Boffa G, Rosa L, Chiodi A, Servillo G, Moccia M, Bonavita S, Filippi M, Petracca M, Brescia Morra V, Lanzillo R. *Physical Exercise Moderates the Effects of Disability on Depression in People with Multiple Sclerosis during the COVID-19 Outbreak*. J Clin Med. 2021 Mar 16;10(6):1234. doi: 10.3390/jcm10061234. PMID: 33809698; PMCID: PMC8002261.

27. **Cellerino M**, Priano L, Bruschi N, Boffa G, Petracca M, Novi G, Lapucci C, Sbragia E, Uccelli A, Inglese M. *Relationship Between Retinal Layer Thickness and Disability Worsening in Relapsing-Remitting and Progressive Multiple Sclerosis*. J Neuroophthalmol. 2021 Sep 1;41(3):329-334. doi: 10.1097/WNO.0000000000001165. PMID: 33399416.

28. Carmisciano L, Signori A, Pardini M, Novi G, Lapucci C, Nesi L, Gallo E, Laroni A**, Cellerino M**, Meli R, Sbragia E, Filippi L, Uccelli A, Inglese M, Sormani MP. *Assessing upper limb function in multiple sclerosis using an engineered glove.* Eur J Neurol. 2020 Dec;27(12):2561-2567. doi: 10.1111/ene.14482. Epub 2020 Sep 9. PMID: 32805743.

29. Testa V, De Santis N, Scotto R, Della Giustina P, Ferro Desideri L, **Cellerino M**, Cordano C, Inglese M, Uccelli A, Vagge A, Traverso CE, Iester M. *Corneal epithelial dendritic cells in patients with multiple sclerosis: An in vivo*

confocal microscopy study. J Clin Neurosci. 2020 Nov;81:139-143. doi: 10.1016/j.jocn.2020.09.041. Epub 2020 Oct 10. PMID: 33222903.

30. **Cellerino M**, Bonavita S, Ferrero M, Inglese M, Boffa G. *Severe disease activity in MS patients treated with cladribine after fingolimod withdrawal.* J Neurol Sci. 2020 Nov 15;418:117156. doi: 10.1016/j.jns.2020.117156. Epub 2020 Sep 30. PMID: 33010653.

Articles submitted:

1. Kennedy KE, Kerlero de Rosbo N, Uccelli A, **Cellerino M**, Ivaldi F, Contini P, De Palma R, Harbo H, Berge T, Bos S, Hogestol EA, Brune-Ingebretse S, de Rodez Benavent S, Paul F, Brandt A, Baecker-Koduah P, Behrens J, Kuchling J, Asseyer S, Scheel M, Chien C, Zimmermann H, Motamedi S, Kauer-Bonin J, Saez-Rodriguez J, Rinas M, Alexopoulos L, Andorra M, Llufriu S, Saiz A, BlancoY, Martinez-Heras E, Solana E, Pulido-Valdeolivas I, Martinez-Lapiscina E, Garcia-Ojalv J, Villoslada, P. *Multiscale networks in multiple sclerosis*. Plos Computational Biology. In press.

2. Boccia, V, Boffa, G, Lapucci C, Costagli M, Bosisio L, Mancardi MM, Inglese M, **Cellerino M**. *Lesion phenotyping based on magnetic susceptibility using Magnetic Resonance Imaging in pediatric Multiple Sclerosis*. Under review.

3. Leveraro E [*], **Cellerino M[*]**, Lapucci C, Dighero M, Sirito T, Boccia D, Cavalli N, Uccelli A, Boffa G, Inglese M. Brief International Cognitive *Assessment for MS (BICAMS) and NEDA maintenance in MS patients: a 2-years follow-up longitudinal study*. Under review.

4. Lin TY, Motamedi S, Asseyer S, Chien C, Saidha S, Calabresi PA, Fitzgerald KC, Samadzadeh S, Villoslada P, Llufriu S, Green AJ, Lizrova Preiningerova J, Petzold A, Leocani L, Garcia-Martin E, Oreja-Guevara C, Outteryck O, Vermersch P, Balcer LJ, Kenney R, Albrecht P, Aktas O, Costello F, Frederiksen J, Uccelli A, **Cellerino M**, Frohman EM, Frohman TC, Bellmann-Strobl J, Schmitz-Hübsch T, Ruprecht K, Brandt A, Zimmermann H, Paul F. *Individual prognostication of disease activity and disability worsening in multiple sclerosis with retinal layer thickness z-scores*. Under review.

5. Landi D, Bartolomeo S, Bovis F, Amato MP, Bonavita S, Borriello G, Buccafusca M, Bucello S, Cavalla P, **Cellerino M**, Centonze D, Cocco E, Conte A, Cortese A, D'Amico E, Di Filippo M, Docimo R, Fantozzi R, Ferraro E, Filippi M, Foschi M, Gallo A, Granella F, Ianniello A, Lanzillo R, Lorefice L, Lucchini M, Lus G, Mataluni G, Mirabella M, Moiola L, Napoli F, Nicoletti C, Patti F, Ragonese P, Realmuto S, Schirò G, Signoriello E, Sinisi L, Stromillo ML, Tomassini V, Vecchio D, Sormani MP, Marfia G. *Maternal and fetal outcomes in an Italian multicentric cohort of women with multiple sclerosis exposed to dimethyl fumarate during pregnancy*. Under review.

6. Aprea MG, Schiavetti I, Portaccio E, Ballerini C, Bonavita S, Buscarinu MC, Calabrese M, Cavalla P, **Cellerino M**, Cordioli C, Dattola V, De Biase S, De Meo E, Fantozzi R, Gallo A, Iasevoli L, Karabudak R, Landi D, Lorefice L, Moiola L, Ragonese P, Ruscica F, Sen S, Sinisi L, Signoriello E, Toscano S, Verrengia EP, Siva A, Masciulli C, Sormani, MP, Amato MP. *Impact of COVID-19 on pregnancy and fetal outcomes in women with Multiple Sclerosis*. Under review.

7. Zanghì A, Borriello G, Bonavita S, Fantozzi R, Signoriello E, Barone S, Abbadessa G, **Cellerino M**, Ziccone V, Miele G, Lus G, Valentino P, Bucello S, Inglese M, Centonze D, D'Amico E. *Ocrelizumab and ofatumumab comparison: an Italian real-world propensity-score matched study*. Under review.

**first co-authors*

4. BIBLIOGRAPHY

1. Thompson, A. J., Baranzini, S. E., Geurts, J., Hemmer, B. & Ciccarelli, O. Multiple sclerosis. *The Lancet* vol. 391 1622–1636 Preprint at https://doi.org/10.1016/S0140-6736(18)30481-1 (2018).
2. Jakimovski, D. *et al.* Multiple sclerosis. *The Lancet* Preprint at https://doi.org/10.1016/S0140-6736(23)01473-3 (2023).
3. Kornbluh, A. B. & Kahn, I. Pediatric Multiple Sclerosis. *Semin Pediatr Neurol* **46**, (2023).
4. Hartung, D. M. Health economics of disease-modifying therapy for multiple sclerosis in the United States. *Therapeutic Advances in Neurological Disorders* vol. 14 Preprint at https://doi.org/10.1177/1756286420987031 (2021).
5. Lublin, F. D. *et al.* Defining the clinical course of multiple sclerosis : The 2013 revisions Defining the clinical course of multiple sclerosis The 2013 revisions. 1–10 (2014) doi:10.1212/WNL.0000000000000560.
6. Bommarito, G. *et al.* Composite MRI measures and short-term disability in patients with clinically isolated syndrome suggestive of MS. *Multiple Sclerosis Journal* **24**, 623–631 (2018).
7. Petzold, A. *et al.* The investigation of acute optic neuritis: A review and proposed protocol. *Nature Reviews Neurology* vol. 10 447–458 Preprint at https://doi.org/10.1038/nrneurol.2014.108 (2014).
8. Foschi, M. *et al.* Sleep-related disorders and their relationship with MRI findings in multiple sclerosis. *Sleep Medicine* vol. 56 90–97 Preprint at https://doi.org/10.1016/j.sleep.2019.01.010 (2019).
9. Hensen, H. A., Krishnan, A. V. & Eckert, D. J. Sleep-disordered breathing in people with multiple sclerosis: Prevalence, pathophysiological mechanisms, and disease consequences. *Frontiers in Neurology* vol. 8 Preprint at https://doi.org/10.3389/fneur.2017.00740 (2018).
10. Braley, T. J., Kratz, A. L., Kaplish, N. & Chervin, R. D. Sleep and cognitive function in multiple sclerosis. *Sleep* **39**, 1525–1533 (2016).
11. Grover, S. & Sharma, M. Sleep, Pain, and Neurodegeneration: A Mendelian Randomization Study. *Front Neurol* **13**, (2022).
12. Kurtzke, J. F. Rating neurologic impairment in multiple sclerosis: An expanded disability status scale (EDSS). *Neurology* **33**, 1444–1452 (1983).
13. Degenhardt, A., Ramagopalan, S. V., Scalfari, A. & Ebers, G. C. Clinical prognostic factors in multiple sclerosis: A natural history review. *Nature Reviews Neurology* vol. 5 672–682 Preprint at https://doi.org/10.1038/nrneurol.2009.178 (2009).
14. Rae-Grant, A. *et al.* Practice guideline recommendations summary: Disease-modifying therapies for adults with multiple sclerosis. *Neurology* vol. 90 777–788 Preprint at https://doi.org/10.1212/WNL.0000000000005347 (2018).
15. Montalban, X. *et al.* ECTRIMS/EAN Guideline on the pharmacological treatment of people with multiple sclerosis. *Multiple Sclerosis* **24**, 96–120 (2018).
16. Boffa, G. *et al.* Long-term clinical outcomes of hematopoietic stem cell transplantation in multiple sclerosis. *Neurology* **96**, E1215–E1226 (2021).

17. Boffa, G. *et al.* Hematopoietic Stem Cell Transplantation in People with Active Secondary Progressive Multiple Sclerosis. *Neurology* **100**, E1109–E1122 (2023).
18. Thompson, A. J., Baranzini, S. E., Geurts, J., Hemmer, B. & Ciccarelli, O. Multiple sclerosis. *The Lancet* **6736**, 1–15 (2018).
19. Hawker, K. *et al.* Rituximab in patients with primary progressive multiple sclerosis: Results of a randomized double-blind placebo-controlled multicenter trial. *Ann Neurol* **66**, 460–471 (2009).
20. Montalban, X. *et al.* Ocrelizumab versus Placebo in Primary Progressive Multiple Sclerosis. *New England Journal of Medicine* **376**, 209–220 (2017).
21. Kappos, L. *et al.* Siponimod versus placebo in secondary progressive multiple sclerosis (EXPAND): a double-blind, randomised, phase 3 study. *The Lancet* **391**, 1263–1273 (2018).
22. Ratzer, R. *et al.* Systemic Inflammation in Progressive Multiple Sclerosis Involves Follicular T-Helper , Th17- and Activated B-Cells and Correlates with Progression. **8**, 1–11 (2013).
23. Kuhlmann, T. *et al.* Multiple sclerosis progression: time for a new mechanism-driven framework. *The Lancet Neurology* vol. 22 78–88 Preprint at https://doi.org/10.1016/S1474-4422(22)00289-7 (2023).
24. Reich, D. S., Lucchinetti, C. F. & Calabresi, P. A. Multiple Sclerosis. *New England Journal of Medicine* **378**, 169–180 (2018).
25. Hemmer, B., Kerschensteiner, M. & Korn, T. Role of the innate and adaptive immune responses in the course of multiple sclerosis. *The Lancet Neurology* vol. 14 406–419 Preprint at https://doi.org/10.1016/S1474-4422(14)70305-9 (2015).
26. Magliozzi, R. *et al.* Meningeal B-cell follicles in secondary progressive multiple sclerosis associate with early onset of disease and severe cortical pathology. *Brain* **130**, 1089–1104 (2007).
27. Guerrier, T., Labalette, M., Outteryck, O., Lefèvre, G. & Vermersch, P. Proinflammatory B-cell profile in the early phases of MS predicts an active disease. **0**, 1–8 (2017).
28. Kuhlmann, T. *et al.* Multiple sclerosis progression: time for a new mechanism-driven framework. *The Lancet Neurology* vol. 22 78–88 Preprint at https://doi.org/10.1016/S1474-4422(22)00289-7 (2023).
29. Knier, B. *et al.* Association of retinal architecture, intrathecal immunity, and clinical course in multiple sclerosis. *JAMA Neurol* **74**, 847–856 (2017).
30. Koudriavtseva, T. *et al.* Coagulation/Complement Activation and Cerebral Hypoperfusion in Relapsing-Remitting Multiple Sclerosis. *Front Immunol* **11**, (2020).
31. Esmon, C. T., Xu, J. & Lupu, F. Innate immunity and coagulation. *Journal of Thrombosis and Haemostasis* vol. 9 182–188 Preprint at https://doi.org/10.1111/j.1538-7836.2011.04323.x (2011).
32. D'haeseleer, M., Cambron, M., Vanopdenbosch, L. & De Keyser, J. Vascular aspects of multiple sclerosis. *The Lancet Neurology* vol. 10 657–666 Preprint at https://doi.org/10.1016/S1474-4422(11)70105-3 (2011).
33. Koudriavtseva, T. *et al.* Coagulation/Complement Activation and Cerebral Hypoperfusion in Relapsing-Remitting Multiple Sclerosis. *Front Immunol* **11**, (2020).

34. Plantone, D., Inglese, M., Salvetti, M. & Koudriavtseva, T. A perspective of coagulation dysfunction in multiple sclerosis and in experimental allergic encephalomyelitis. *Frontiers in Neurology* vol. 10 Preprint at https://doi.org/10.3389/fneur.2018.01175 (2019).
35. Motl, R. W. *et al.* Cardiorespiratory fitness and its association with thalamic, hippocampal, and basal ganglia volumes in multiple sclerosis. *Neuroimage Clin* **7**, 661–666 (2015).
36. Plantone, D., Inglese, M., Salvetti, M. & Koudriavtseva, T. A perspective of coagulation dysfunction in multiple sclerosis and in experimental allergic encephalomyelitis. *Frontiers in Neurology* vol. 10 Preprint at https://doi.org/10.3389/fneur.2018.01175 (2019).
37. Antoniak, S. & Mackman, N. Multiple roles of the coagulation protease cascade during virus infection. (2014) doi:10.1182/blood-2013.
38. Engelmann, B. & Massberg, S. Thrombosis as an intravascular effector of innate immunity. *Nature Reviews Immunology* vol. 13 34–45 Preprint at https://doi.org/10.1038/nri3345 (2013).
39. Tarlinton, R. E., Martynova, E., Rizvanov, A. A., Khaiboullina, S. & Verma, S. Role of viruses in the pathogenesis ofmultiple sclerosis. *Viruses* vol. 12 Preprint at https://doi.org/10.3390/v12060643 (2020).
40. Lapointe, E., Li, D. K. B., Traboulsee, A. L. & Rauscher, A. What have we learned from perfusion MRI in multiple sclerosis? *American Journal of Neuroradiology* vol. 39 994–1000 Preprint at https://doi.org/10.3174/ajnr.A5504 (2018).
41. Lagana, M., Pelizzari, L. & Baglio, F. Relationship between MRI perfusion and clinical severity in multiple sclerosis. *Neural Regeneration Research* vol. 15 646–652 Preprint at https://doi.org/10.4103/1673-5374.266906 (2020).
42. Inglese, M. *et al.* Perfusion magnetic resonance imaging correlates of neuropsychological impairment in multiple sclerosis. *Journal of Cerebral Blood Flow and Metabolism* **28**, 164–171 (2008).
43. Law, M. *et al.* Microvascular abnormality in relapsing-remitting multiple sclerosis: Perfusion MR imaging findings in normal-appearing white matter. *Radiology* **231**, 645–652 (2004).
44. Ge, Y. *et al. Dynamic Susceptibility Contrast Perfusion MR Imaging of Multiple Sclerosis Lesions: Characterizing Hemodynamic Impairment and Inflammatory Activity*.
45. Inglese, M. *et al.* Perfusion magnetic resonance imaging correlates of neuropsychological impairment in multiple sclerosis. *Journal of Cerebral Blood Flow and Metabolism* **28**, 164–171 (2008).
46. Bodini, B. *et al.* Dynamic Imaging of Individual Remyelination Profiles in Multiple Sclerosis. *Ann Neurol* **79**, 726–738 (2016).
47. Patrikios, P. *et al.* Remyelination is extensive in a subset of multiple sclerosis patients. *Brain* **129**, 3165–3172 (2006).
48. Goldschmidt, T., Antel, J., König, F. B., Brück, W. & Kuhlmann, T. *Remyelination Capacity of the MS Brain Decreases with Disease Chronicity*. www.neurology.org (2009).
49. Ksiazek-Winiarek, D. J., Szpakowski, P. & Glabinski, A. Neural Plasticity in Multiple Sclerosis: The Functional and Molecular Background. *Neural Plasticity* vol. 2015 Preprint at https://doi.org/10.1155/2015/307175 (2015).

50. Albrecht, P. *et al.* Degeneration of retinal layers in multiple sclerosis subtypes quantified by optical coherence tomography. *Multiple Sclerosis Journal* **18**, 1422–1429 (2012).
51. Cagol, A. *et al.* Optical coherence tomography reflects clinically relevant gray matter damage in patients with multiple sclerosis. *J Neurol* **270**, 2139–2148 (2023).
52. Papadopoulou, A. *et al.* Damage of the lateral geniculate nucleus in MS: Assessing the missing node of the visual pathway. *Neurology* **92**, E2240–E2249 (2019).
53. Gabilondo, I. *et al.* Trans-synaptic axonal degeneration in the visual pathway in multiple sclerosis. *Ann Neurol* **75**, 98–107 (2014).
54. Cerdá-Fuertes, N. *et al.* Optical coherence tomography versus other biomarkers: Associations with physical and cognitive disability in multiple sclerosis. *Multiple Sclerosis Journal* **29**, 1540–1550 (2023).
55. Lambe, J., Saidha, S. & Bermel, R. A. Optical coherence tomography and multiple sclerosis: Update on clinical application and role in clinical trials. *Multiple Sclerosis Journal* vol. 26 624–639 Preprint at https://doi.org/10.1177/1352458519872751 (2020).
56. Petzold, A. *et al.* Retinal layer segmentation in multiple sclerosis: a systematic review and meta-analysis. *Lancet Neurol* **16**, 797–812 (2017).
57. Balk, L. J. *et al.* Disease course heterogeneity and OCT in multiple sclerosis. *Multiple Sclerosis Journal* **20**, 1198–1206 (2014).
58. Petzold, A. *et al.* Retinal asymmetry in multiple sclerosis. *Brain* **144**, 224–235 (2021).
59. de Vries-Knoppert, W. A., Baaijen, J. C. & Petzold, A. Patterns of retrograde axonal degeneration in the visual system. *Brain* **142**, 2775–2786 (2019).
60. Balk, L. J. *et al.* Retinal inner nuclear layer volume reflects inflammatory disease activity in multiple sclerosis; a longitudinal OCT study. *Mult Scler J Exp Transl Clin* **5**, (2019).
61. Gordon-Lipkin, E. *et al. Retinal Nerve Fiber Layer Is Associated with Brain Atrophy in Multiple Sclerosis*. (2007).
62. Knier, B. *et al.* Retinal inner nuclear layer volume reflects response to immunotherapy in multiple sclerosis. *Brain* **139**, 2855–2863 (2016).
63. Knier, B. *et al.* Association of retinal architecture, intrathecal immunity, and clinical course in multiple sclerosis. *JAMA Neurol* **74**, 847–856 (2017).
64. Tur, C. *et al.* Longitudinal evidence for anterograde trans-synaptic degeneration after optic neuritis. *Brain* **139**, 816–828 (2016).
65. Petracca, M. *et al.* Retinal degeneration in primary-progressive multiple sclerosis: A role for cortical lesions? *Multiple Sclerosis* **23**, 43–50 (2017).
66. Rocca, M. A. *et al.* Wallerian and trans-synaptic degeneration contribute to optic radiation damage in multiple sclerosis: A diffusion tensor MRI study. *Multiple Sclerosis Journal* **19**, 1610–1617 (2013).
67. Oberwahrenbrock, T. *et al.* Retinal Damage in Multiple Sclerosis Disease Subtypes Measured by High-Resolution Optical Coherence Tomography. *Mult Scler Int* **2012**, 1–10 (2012).
68. Cellerino, M. *et al.* Relationship Between Retinal Layer Thickness and Disability Worsening in Relapsing-Remitting and Progressive Multiple Sclerosis 2020.98828. *Journal of Neuro-Ophthalmology* **41**, (2021).

69. Saidha, S. *et al.* Visual dysfunction in multiple sclerosis correlates better with optical coherence tomography derived estimates of macular ganglion cell layer thickness than peripapillary retinal nerve fiber layer thickness. *Multiple Sclerosis Journal* **17**, 1449–1463 (2011).
70. Martinez-Lapiscina, E. H. *et al.* Retinal thickness measured with optical coherence tomography and risk of disability worsening in multiple sclerosis: A cohort study. *Lancet Neurol* **15**, 574–584 (2016).
71. Cordano, C. *et al.* PRNFL as a marker of disability worsening in the medium/long term in patients with MS. *Neurology: Neuroimmunology and NeuroInflammation* vol. 6 Preprint at https://doi.org/10.1212/NXI.0000000000000533 (2019).
72. Rothman, A. *et al.* Retinal measurements predict 10-year disability in multiple sclerosis. *Ann Clin Transl Neurol* **6**, 222–232 (2019).
73. Zimmermann, H. G. *et al.* Association of retinal ganglion cell layer thickness with future disease activity in patients with clinically isolated syndrome. *JAMA Neurol* **75**, 1071–1079 (2018).
74. Wauschkuhn, J. *et al.* Retinal ganglion cell loss is associated with future disability worsening in early relapsing–remitting multiple sclerosis. *Eur J Neurol* **30**, 982–990 (2023).
75. Pisa, M. *et al.* No evidence of disease activity is associated with reduced rate of axonal retinal atrophy in MS. *Neurology* **89**, 2469–2475 (2017).
76. Bsteh, G. *et al.* Retinal layer thinning predicts treatment failure in relapsing multiple sclerosis. *Eur J Neurol* **28**, 2037–2045 (2021).
77. Bsteh, G. *et al.* Macular ganglion cell–inner plexiform layer thinning as a biomarker of disability progression in relapsing multiple sclerosis. *Multiple Sclerosis Journal* **27**, 684–694 (2021).
78. Bsteh, G. *et al.* Peripapillary retinal nerve fibre layer thinning rate as a biomarker discriminating stable and progressing relapsing–remitting multiple sclerosis. *Eur J Neurol* **26**, 865–871 (2019).
79. Parks, N. E., Flanagan, E. P., Lucchinetti, C. F. & Wingerchuk, D. M. NEDA treatment target? No evident disease activity as an actionable outcome in practice. *Journal of the Neurological Sciences* vol. 383 31–34 Preprint at https://doi.org/10.1016/j.jns.2017.10.015 (2017).
80. Sormani, M. P., Muraro, P. A., Saccardi, R. & Mancardi, G. NEDA status in highly active MS can be more easily obtained with autologous hematopoietic stem cell transplantation than other drugs. *Multiple Sclerosis* vol. 23 201–204 Preprint at https://doi.org/10.1177/1352458516645670 (2017).
81. Cree, B. A. C. *et al.* Long-term evolution of multiple sclerosis disability in the treatment era. *Ann Neurol* **80**, 499–510 (2016).
82. Stahle, L. & Wold, S. *PARTIAL LEAST SQUARES ANALYSIS WITH A MONTE CARL0 STUDY CROSS-VALIDATION FOR THE TWO-CLASS PROBLEM*. *JOURNAL OF CHEMOMETRICS* vol. 1 (1987).
83. Abbadessa, G., Lavorgna, L., Treaba, C. A., Bonavita, S. & Mainero, C. Hemostatic factors in the pathogenesis of neuroinflammation in multiple sclerosis. *Multiple Sclerosis Journal* vol. 28 1834–1842 Preprint at https://doi.org/10.1177/13524585211039111 (2022).
84. Soldan, S. S. & Lieberman, P. M. Epstein–Barr virus and multiple sclerosis. *Nature Reviews Microbiology* Preprint at https://doi.org/10.1038/s41579-022-00770-5 (2022).

85. Bjornevik, K. *et al. MULTIPLE SCLEROSIS Longitudinal Analysis Reveals High Prevalence of Epstein-Barr Virus Associated with Multiple Sclerosis*. *Science* vol. 375 https://www.science.org (2022).
86. Stampanoni Bassi, M. *et al.* Obesity worsens central inflammation and disability in multiple sclerosis. *Multiple Sclerosis Journal* **26**, 1237–1246 (2020).
87. Thomas, M. & Augustin, H. G. The role of the angiopoietins in vascular morphogenesis. *Angiogenesis* **12**, 125–137 (2009).
88. Zhang, Y., Kontos, C. D., Annex, B. H. & Popel, A. S. Angiopoietin-Tie Signaling Pathway in Endothelial Cells: A Computational Model. *iScience* **20**, 497–511 (2019).
89. Higgins, S. J. *et al.* Tie2 protects the vasculature against thrombus formation in systemic inflammation. *Journal of Clinical Investigation* **128**, 1471–1484 (2018).
90. Law, M. *et al.* Microvascular abnormality in relapsing-remitting multiple sclerosis: Perfusion MR imaging findings in normal-appearing white matter. *Radiology* **231**, 645–652 (2004).
91. Lagana, M., Pelizzari, L. & Baglio, F. Relationship between MRI perfusion and clinical severity in multiple sclerosis. *Neural Regeneration Research* vol. 15 646–652 Preprint at https://doi.org/10.4103/1673-5374.266906 (2020).
92. de la Peña, M. J. *et al.* Early perfusion changes in multiple sclerosis patients as assessed by MRI using arterial spin labeling. *Acta Radiol Open* **8**, 205846011989421 (2019).
93. Wang, S., Reeves, B. & Pawlinski, R. Astrocyte tissue factor controls CNS hemostasis and autoimmune inflammation. *Thromb Res* **141**, S65–S67 (2016).
94. Ziliotto, N., Bernardi, F., Jakimovski, D. & Zivadinov, R. Coagulation pathways in neurological diseases: Multiple sclerosis. *Frontiers in Neurology* vol. 10 Preprint at https://doi.org/10.3389/fneur.2019.00409 (2019).
95. Griffin, J. H., Zlokovic, B. V & Mosnier, L. O. Activated protein C: biased for translation. (2015) doi:10.1182/blood-2015-02.
96. Koudriavtseva, T. & Mainero, C. Neuroinflammation, neurodegeneration and regeneration in multiple sclerosis: Intercorrelated manifestations of the immune response. *Neural Regen Res* **11**, 1727–1730 (2016).
97. Davalos, D. *et al.* Fibrinogen-induced perivascular microglial clustering is required for the development of axonal damage in neuroinflammation. *Nat Commun* **3**, (2012).
98. Antoniak, S. & Mackman, N. Multiple roles of the coagulation protease cascade during virus infection. (2014) doi:10.1182/blood-2013.
99. Nait-Oumesmar, B. *et al. Activation of the Subventricular Zone in Multiple Sclerosis: Evidence for Early Glial Progenitors*. www.pnas.orgcgidoi10.1073pnas.0606835104 (2007).
100. Wang, X. *et al.* Quantitative proteomic analysis of age-related subventricular zone proteins associated with neurodegenerative disease. *Sci Rep* **6**, (2016).
101. Nait-Oumesmar, B., Picard-Riéra, N., Kerninon, C. & Baron-Van Evercooren, A. The role of SVZ-derived neural precursors in demyelinating diseases: From animal models to multiple sclerosis. *J Neurol Sci* **265**, 26–31 (2008).

102. Sanai, N. *et al.* Corridors of migrating neurons in the human brain and their decline during infancy. *Nature* **478**, 382–386 (2011).
103. David-Bercholz, J., Kuo, C. T. & Deneen, B. Astrocyte and Oligodendrocyte Responses From the Subventricular Zone After Injury. *Frontiers in Cellular Neuroscience* vol. 15 Preprint at https://doi.org/10.3389/fncel.2021.797553 (2021).
104. Segel, M. *et al.* Niche stiffness underlies the ageing of central nervous system progenitor cells. *Nature* **573**, 130–134 (2019).
105. Butt, A. M., Rivera, A. D., Fulton, D. & Azim, K. Targeting the Subventricular Zone to Promote Myelin Repair in the Aging Brain. *Cells* **11**, 1809 (2022).
106. Etxeberria, A., Mangin, J. M., Aguirre, A. & Gallo, V. Adult-born SVZ progenitors receive transient synapses during remyelination in corpus callosum. *Nat Neurosci* **13**, 287–289 (2010).
107. Samanta, J. *et al.* Inhibition of Gli1 mobilizes endogenous neural stem cells for remyelination. *Nature* **526**, 448–452 (2015).
108. Liu, Q. *et al.* Neural stem cells sustain natural killer cells that dictate recovery from brain inflammation. *Nat Neurosci* **19**, 243–252 (2016).
109. Mosher, K. I. *et al.* Neural progenitor cells regulate microglia functions and activity. *Nat Neurosci* **15**, 1485–1487 (2012).
110. Butti, E., Cusimano, M., Bacigaluppi, M. & Martino, G. Neurogenic and non-neurogenic functions of endogenous neural stem cells. *Frontiers in Neuroscience* Preprint at https://doi.org/10.3389/fnins.2014.00092 (2014).
111. Thompson, A. J. *et al.* Diagnosis of multiple sclerosis: 2017 revisions of the McDonald criteria. *The Lancet Neurology* vol. 17 162–173 Preprint at https://doi.org/10.1016/S1474-4422(17)30470-2 (2018).
112. Cherubini, A. *et al.* A multimodal MRI investigation of the subventricular zone in mild cognitive impairment and Alzheimer's disease patients. *Neurosci Lett* **469**, 214–218 (2010).
113. Jenkinson, M., Beckmann, C. F., Behrens, T. E. J., Woolrich, M. W. & Smith, S. M. FSL. *Neuroimage* **62**, 782–790 (2012).
114. Patenaude, B., Smith, S. M., Kennedy, D. N. & Jenkinson, M. A Bayesian model of shape and appearance for subcortical brain segmentation. *Neuroimage* **56**, 907–922 (2011).
115. Veraart, J. *et al.* Denoising of diffusion MRI using random matrix theory. *Neuroimage* **142**, 394–406 (2016).
116. Tournier, J. D. *et al.* MRtrix3: A fast, flexible and open software framework for medical image processing and visualisation. *NeuroImage* vol. 202 Preprint at https://doi.org/10.1016/j.neuroimage.2019.116137 (2019).
117. Andersson, J. L. R. & Sotiropoulos, S. N. An integrated approach to correction for off-resonance effects and subject movement in diffusion MR imaging. *Neuroimage* **125**, 1063–1078 (2016).
118. Smith, S. M. *et al.* Advances in functional and structural MR image analysis and implementation as FSL. in *NeuroImage* vol. 23 (2004).
119. Andersson, J. L. R., Skare, S. & Ashburner, J. How to correct susceptibility distortions in spin-echo echo-planar images: Application to diffusion tensor imaging. *Neuroimage* **20**, 870–888 (2003).
120. Tustison, N. J. *et al.* N4ITK: Improved N3 bias correction. *IEEE Trans Med Imaging* **29**, 1310–1320 (2010).

121. Greve, D. N. & Fischl, B. Accurate and robust brain image alignment using boundary-based registration. *Neuroimage* **48**, 63–72 (2009).
122. Kaden, E., Kelm, N. D., Carson, R. P., Does, M. D. & Alexander, D. C. Multi-compartment microscopic diffusion imaging. *Neuroimage* **139**, 346–359 (2016).
123. Kaden, E., Kruggel, F. & Alexander, D. C. Quantitative mapping of the per-axon diffusion coefficients in brain white matter. *Magn Reson Med* **75**, 1752–1763 (2016).
124. Sim, F. J., Zhao, C., Penderis, J. & Franklin, R. J. M. *The Age-Related Decrease in CNS Remyelination Efficiency Is Attributable to an Impairment of Both Oligodendrocyte Progenitor Recruitment and Differentiation*. (2002).
125. Curtis, M. A., Faull, R. L. M. & Eriksson, P. S. The effect of neurodegenerative diseases on the subventricular zone. *Nature Reviews Neuroscience* vol. 8 712–723 Preprint at https://doi.org/10.1038/nrn2216 (2007).
126. Moreno-Valladares, M. *et al.* CD8+ T cells are increased in the subventricular zone with physiological and pathological aging. *Aging Cell* **19**, (2020).
127. By, S., Xu, J., Box, B. A., Bagnato, F. R. & Smith, S. A. Multi-compartmental diffusion characterization of the human cervical spinal cord in vivo using the spherical mean technique. *NMR Biomed* **31**, (2018).
128. Lakhani, D. A., Schilling, K. G., Xu, J. & Bagnato, F. Advanced multicompartment diffusion MRI models and their application in multiple sclerosis. *American Journal of Neuroradiology* vol. 41 751–757 Preprint at https://doi.org/10.3174/AJNR.A6484 (2020).
129. Bagnato, F. *et al.* Selective inversion recovery quantitative magnetization transfer imaging: Toward a 3 T clinical application in multiple sclerosis. *Multiple Sclerosis Journal* **26**, 457–467 (2020).
130. Devan, S. P., Jiang, X., Bagnato, F. & Xu, J. Optimization and numerical evaluation of multi-compartment diffusion MRI using the spherical mean technique for practical multiple sclerosis imaging. *Magn Reson Imaging* **74**, 56–63 (2020).
131. Jäkel, S. *et al.* Altered human oligodendrocyte heterogeneity in multiple sclerosis. *Nature* **566**, 543–547 (2019).
132. Nsi, A. *et al. 65 PREMYELINATING OLIGODENDROCY TES IN CHRONIC LESIONS OF MULTIPLE SCLEROSIS PREMYELINATING OLIGODENDROCYTES IN CHRONIC LESIONS OF MULTIPLE SCLEROSIS A BSTRACT Background Multiple Sclerosis Is an Inflammatory*. *N Engl J Med* vol. 346 www.nejm.org (2002).
133. Franklin, R. J. M. & Ffrench-Constant, C. Regenerating CNS myelin - From mechanisms to experimental medicines. *Nature Reviews Neuroscience* vol. 18 753–769 Preprint at https://doi.org/10.1038/nrn.2017.136 (2017).
134. Rasmussen, S. *et al.* Reversible neural stem cell niche dysfunction in a model of multiple sclerosis. *Ann Neurol* **69**, 878–891 (2011).
135. Remaud, S. *et al.* Transient hypothyroidism favors oligodendrocyte generation providing functional remyelination in the adult mouse brain. doi:10.7554/eLife.29996.001.

136. Sulehria, T. *et al.* Increasing Progenitor Cell Proliferation in the Sub-Ventricular Zone: A Therapeutic Treatment for Progressive Multiple Sclerosis? *Recent Pat Drug Deliv Formul* **14**, 233–241 (2020).
137. Hauser, S. L. *et al.* Ocrelizumab versus Interferon Beta-1a in Relapsing Multiple Sclerosis. *New England Journal of Medicine* **376**, 221–234 (2017).
138. Rush, C. A., Maclean, H. J. & Freedman, M. S. Aggressive multiple sclerosis: Proposed definition and treatment algorithm. *Nature Reviews Neurology* vol. 11 379–389 Preprint at https://doi.org/10.1038/nrneurol.2015.85 (2015).
139. Hauser, S. L. *et al.* Five years of ocrelizumab in relapsing multiple sclerosis: OPERA studies open-label extension. *Neurology* **95**, E1854–E1867 (2020).
140. Barkhof, F. *et al.* Onset of clinical and MRI efficacy of ocrelizumab in relapsing multiple sclerosis. *Neurology* **93**, e1778–e1786 (2019).
141. Signoriello, E. *et al.* Switch from sequestering to anti-CD20 depleting treatment: disease activity outcomes during wash-out and in the first 6 months of ocrelizumab therapy. *Multiple Sclerosis Journal* **28**, 93–101 (2022).
142. Gingele, S. *et al.* Ocrelizumab depletes CD20+ T cells in multiple sclerosis patients. *Cells* **8**, (2019).
143. Fernández-Velasco, J. I. *et al.* Effect of Ocrelizumab in Blood Leukocytes of Patients With Primary Progressive MS. *Neurol Neuroimmunol Neuroinflamm* **8**, (2021).
144. Capasso, N. *et al.* Ocrelizumab depletes T-lymphocytes more than rituximab in multiple sclerosis. *Mult Scler Relat Disord* **49**, (2021).
145. Buron, M. D. *et al.* Initial high-efficacy disease-modifying therapy in multiple sclerosis: A nationwide cohort study. *Neurology* **95**, E1041–E1051 (2020).
146. He, A. *et al.* Timing of high-efficacy therapy for multiple sclerosis: a retrospective observational cohort study. *Lancet Neurol* **19**, 307–316 (2020).
147. Filippi, M. *et al.* Early use of high-efficacy disease-modifying therapies makes the difference in people with multiple sclerosis: an expert opinion. *J Neurol* **269**, 5382–5394 (2022).
148. Cruz-Herranz, A. *et al. VIEWS & REVIEWS On Behalf of the IMSVISUAL Consortium Correspondence to The APOSTEL Recommendations for Reporting Quantitative Optical Coherence Tomography Studies*. http://www.imsvisual.org (2016).
149. Cellerino, M. *et al.* Relationship between retinal inner nuclear layer, age, and disease activity in progressive MS. *Neurol Neuroimmunol Neuroinflamm* **6**, (2019).
150. Schippling, S. *et al.* Quality control for retinal OCT in multiple sclerosis: Validation of the OSCAR-IB criteria. *Multiple Sclerosis Journal* **21**, 163–170 (2015).
151. Saidha, S. *et al.* Optical coherence tomography reflects brain atrophy in multiple sclerosis: A four-year study. *Ann Neurol* **78**, 801–813 (2015).
152. Button, J. *et al.* Disease-modifying therapies modulate retinal atrophy in multiple sclerosis: A retrospective study. *Neurology* **88**, 525–532 (2017).
153. Knier, B. *et al.* Retinal inner nuclear layer volume reflects response to immunotherapy in multiple sclerosis. *Brain* **139**, 2855–2863 (2016).

154. Arnold, D. L. *et al.* Ocrelizumab reduces thalamic volume loss in patients with RMS and PPMS. *Multiple Sclerosis Journal* **28**, 1927–1936 (2022).
155. Bajrami, A. *et al.* Ocrelizumab reduces cortical and deep grey matter loss compared to the S1P-receptor modulator in multiple sclerosis. *J Neurol* (2024) doi:10.1007/s00415-023-12179-y.
156. Kolind, S. *et al.* Ocrelizumab-treated patients with relapsing multiple sclerosis show volume loss rates similar to healthy aging. *Multiple Sclerosis Journal* **29**, 741–747 (2023).
157. Saidha, S. *et al.* Microcystic macular oedema, Thickness of the inner nuclear layer of the retina, and disease characteristics in multiple sclerosis: A retrospective study. *Lancet Neurol* **11**, 963–972 (2012).
158. Pisa, M. *et al.* Subclinical anterior optic pathway involvement in early multiple sclerosis and clinically isolated syndromes. *Brain* **144**, 848–862 (2021).
159. Petzold, A. Retinal glymphatic system: an explanation for transient retinal layer volume changes? *Brain* **139**, 2816–2819 (2016).